

**Identification and characterization of a 21 kDa
iron-regulated envelope protein in
*Mycobacterium smegmatis***

A thesis

Submitted for the degree of
Doctor of Philosophy

By

Naveen Kumar

Regd. No. 10LAPH03



**Department of Animal Biology
School of Life Sciences
University of Hyderabad
Hyderabad - 500 046
India**

September 2017



University of Hyderabad
(A Central University established in 1974 by an act of parliament)
Hyderabad– 500 046, INDIA

CERTIFICATE

This is to certify that the thesis entitled “**Identification and characterization of a 21 kDa iron-regulated envelope protein in *Mycobacterium smegmatis***” submitted by **Mr. Naveen Kumar** bearing registration number **10LAPH03** in partial fulfillment of the requirements for award of Doctor of philosophy in the School of Life Sciences is a bonafide work carried out by him under my supervision and guidance.

This thesis is free from plagiarism and has not been submitted previously in part or in full to this or any other university or Institution for award of any degree or diploma.

Part of this thesis have been:

A. Published in the following publication:

1. European Journal of Clinical Microbiology & Infectious Diseases, June 2014, **34**, 33-40 (ISSN: 0934-9723)

B. Presented in the following conferences

1. AMI (KIIT University, Bhubaneswar), 2012 (**International**)
2. SBCIC (University of Hyderabad), 2013 (**International**)
3. UOH-AS joint workshop (University of Hyderabad), 2016 (**International**)

Further the student has passed the following courses towards fulfillment of coursework requirement for Ph.D

Course Code	Name	Credits	Pass/Fail
1. AS 801	Seminar 1	1	Pass
2. AS 802	Research Ethics & Management	2	Pass
3. AS 803	Biostatistics	2	Pass
4. AS 804	Analytical Techniques	3	Pass
5. AS 805	Lab Work	4	Pass

Supervisor

Head of the Department

Dean of School



University of Hyderabad
(A Central University established in 1974 by an act of parliament)
Hyderabad – 500 046, INDIA

DECLARATION

I hereby declare that the results of the study incorporated in the thesis entitled “**Identification and characterization of a 21 kDa iron-regulated envelope protein in *Mycobacterium smegmatis***” has been carried out by me under the supervision of **Prof. Manjula Sritharan** at Department of Animal Biology, School of Life Sciences. The work presented in this thesis is a bonafide research work and has not been submitted for any degree or diploma in any other University or Institute.

Date:

Naveen Kumar
(10LAPH03)

Acknowledgements

- ✚ *I would like to express my deepest gratitude and sincere appreciation to my supervisor **Prof. Manjula Sritharan** for her unwavering patience, instruction, guidance and support. At many stages in the course of my graduate studies, I benefited from her advice, particularly so when exploring new ideas. Her positive outlook and confidence in my research inspired me and elevated my confidence. Her approach to supervision has allowed me to become a confident and independent scientist. Her careful editing contributed enormously to the production of this thesis.*
- ✚ *I am thankful to Prof. Naresh Babu V Sepuri and Dr. Arunasree M K for their guidance during Doctoral Committee meetings.*
- ✚ *I am thankful to Prof. P. Jagan Mohan Rao, Head, Department of Animal Biology and the former Heads, Prof. B. Senthilkumaran and Prof. Manjula Sritharan for allowing me to use departmental facilities.*
- ✚ *I am thankful to Prof. P. Reddanna, Dean, School of Life Sciences and former Deans Prof. R. P. Sharma, Prof. Aparna Dutta Gupta and Prof. M. Ramanadham for allowing me to use the school facilities.*
- ✚ *I thank Dr. Insaf Ahmed Qureshi and Mr. Fatin Khan for helping me in bioinformatics work and I also thank all the faculty members of School of Life Sciences for their valuable discussions and suggestions.*
- ✚ *I thank all my lab members Dr. Veena, Dr. Suneel, Dr. Satya Deo Pandey, Dr. Subha Dr. Mitali, Dr. Sweena, Dr. Nilesh, Sravan Kumar, Reetika, Kavya, Nagarjuna, Anjali, Mahesh and Chandram for all their help and support in the lab.*
- ✚ *I am thankful to my friends and all the research scholars in School of Life Sciences for their timely help and co-operation during my stay in the University.*
- ✚ *I take this opportunity to thank all non-teaching staff of Department of Animal Biology for their help in all the administrative works.*
- ✚ *I sincerely thank UGC for funding during my doctoral studies.*

- ✚ *I thank DBT, ICMR, UGC, UPE-II, UGC-SAP and DBT-CREBB for providing financial support to lab and for the infrastructural facility of the school.*
- ✚ *I would like to thank my besties Ashok, Kumar, Mastan, Papa Rao, Vinod, Mohan, Ravi and Lokya for making this journey beautiful and memorable.*
- ✚ *Above and beyond all, my heartfelt gratitude to my parents, Mr. Deva Nayak and Mrs. Vinodha for their unconditional love, support and encouragement made this incredible and exhilarating journey possible.*
- ✚ *I wish to thank my brothers, sister, In-law's family, relatives, friends for their support and encouragement throughout my doctoral studies.*
- ✚ *I thank my wife 'Sakku' for her unconditional love, support and encouragement and my daughter 'Praapti Chouhan' for her cute and naughty smile to drag my attention away from the study by attacking on my laptop.*

NAVEEN KUMAR

(నవీన్ కుమార్)

**Dedicated
To
My beloved Parents and Wife**

TABLE OF CONTENTS

List of abbreviations	vi
Abstract	viii
Chapter 1: Review of Literature	
1.1. Introduction	2
1.1.1. General features of mycobacteria	2
1.1.2. Classification of mycobacteria	
1.2. Unique features of mycobacterial cell envelope	3
1.3. Iron and its importance	5
1.3.1. Adaptation of mycobacteria to iron limitation	6
1.3.2. Mycobactins	6
1.3.3. Carboxymycobactins	8
1.3.4. Exochelins	19
1.4. Iron-regulated envelope proteins in mycobacteria	10
1.4.1. HupB as an iron-regulated envelope protein in <i>M. tuberculosis</i>	11
1.4.1.1. Iron levels and HupB expression	11
1.4.1.2. HupB is a multi-functional protein	11
1.4.1.3. Role of HupB in iron metabolism	12
1.4.1.4. <i>In vivo</i> expression of HupB	12
1.5. Biosynthesis of siderophores	13
1.5.1. Biosynthesis of mycobactin / carboxymycobactin	13
1.5.2. Biosynthesis of exochelin	15
1.6. Regulation of iron metabolism in mycobacteria	16
1.6.1. Iron-dependent regulator (IdeR)	16
1.6.2. Regulation of siderophore biosynthesis by IdeR and HupB in <i>M. tuberculosis</i>	17
1.6.3. FurA, FurB (ferric uptake regulator) and SirR	19
1.7. Uptake of iron in mycobacteria	20
1.7.1. Uptake of ferri-carboxymycobactin in <i>M. tuberculosis</i>	20
1.7.2. Uptake of ferri-exochelin in <i>M. smegmatis</i>	21

1.7.3. Iron uptake through porins under high iron conditions in <i>M. smegmatis</i>	22
Objectives of the study	23
Chapter 2: Materials and Methods	
2.1. Chemicals and Reagents	25
2.2. Bacterial strains and plasmids	25
2.3. Media for the growth of mycobacteria	26
2.3.1. Lowenstein-Jenson (LJ) medium	26
2.3.2. Middlebrook 7H9 liquid medium	26
2.3.3. Middlebrook 7H11 agar medium	27
2.3.4. Proskauer and Beck (P & B) medium for iron-regulated growth	27
2.3.4.1. Preparation of iron-free glassware	28
2.3.4.2. Preparation of Proskauer and Beck (P & B) medium	28
2.3.4.3. Preparation of salt solution	28
2.3.4.4. Preparation of iron solutions	28
2.3.4.4.1. Preparation of high iron solution (800 µg Fe / mL)	28
2.3.4.4.2. Preparation of low iron solution (2.0 µg Fe / mL)	28
2.4. Maintenance and growth of mycobacteria	28
2.5. Assay of siderophores	29
2.5.1. Carboxymycobactin and exochelin	29
2.5.2. Mycobactin	29
2.6. Growth of <i>M. smegmatis</i> in P & B media with varying concentrations of iron	29
2.7. Time-dependant growth of <i>M. smegmatis</i>	30
2.8. Purification of ferri-siderophores	30
2.8.1. Purification of ferri-carboxymycobactin and ferri-mycobactin by high performance liquid chromatography (HPLC)	30
2.8.2. Purification of ferri-exochelin	31

2.9. Preparation of cell wall and cell membrane proteins by differential centrifugation	31
2.10. Separation of proteins by sodium dodecyl sulfate-polyacrylamide gel electrophoresis (SDS-PAGE)	32
2.11. Western blot analysis	34
2.11.1. Electrophoretic protein transfer	34
2.11.2. Development of immunoblot	34
2.12. Preparative gel electrophoresis for the purification of iron-regulated envelope proteins	35
2.13. Characterisation of iron-regulated envelope proteins by MALDI TOF-MS / MS Analysis	35
2.14. Development of antibodies against HupB and IrpA from <i>M. smegmatis</i>	35
2.15. Molecular techniques	36
2.15.1. <i>E. coli</i> strains and vectors	36
2.15.2. Preparation of Luria-Bertani (LB) medium	36
2.15.3. Isolation of genomic DNA from <i>M. smegmatis</i>	36
2.15.4. Agarose gel electrophoresis	38
2.15.5. Cloning procedures	38
2.15.5.1. PCR amplification	39
2.15.5.2. Restriction digestion	39
2.15.5.3. Ligation	40
2.15.5.4. Transformation into <i>E.coli</i> DH5 α	40
2.15.5.4.1. Preparation of ultra-competent cells	40
2.15.5.4.2. Transformation	40
2.15.6. Isolation of plasmid DNA by alkaline lysis SDS: Miniprep method	40
2.15.7. Expression of recombinant proteins	41
2.15.7.1. Recombinant HupB	41
2.15.7.2. Recombinant IrpA	42
2.16. Radioactive iron uptake studies: uptake of ^{55}Fe -exochelin and ^{55}Fe carboxymycobactin by <i>M. smegmatis</i>	43
2.16.1. Preparation of ^{55}Fe -labelled siderophores	43

2.16.2. Uptake studies with <i>M. smegmatis</i>	44
2.16.3. Uptake studies with liposome-incorporated cell wall proteins	44
2.16.3.1. Preparation of liposomes	45
2.16.3.2. Uptake of ⁵⁵ Fe-exochelin by liposomes	46
2.17. Modeling of IrpA and docking of ferri-exochelin	46
2.17.1. Homology modeling of IrpA	46
2.17.2. Molecular docking of ferri-exochelin on <i>IrpA</i>	47
2.18. Identification of IrpA-interacting proteins by immunoprecipitation with anti-IrpA antibodies	47

Chapter 3: Results

3.1. Constitutive expression of the HupB homologue (MSMEG_2389) in <i>M. smegmatis</i>	49
3.1.1. Elevated levels of mycobactin and exochelin by iron-limited <i>M. smegmatis</i>	49
3.1.2. Constitutive expression of the HupB homologue in <i>M. smegmatis</i> : presence of the protein in organisms grown in high and low iron media	50
3.1.3. Lowering of iron in growth medium influenced production of siderophores but had no effect on HupB expression in <i>M. smegmatis</i>	51
3.1.4. Time course study: profile of the siderophores and HupB	53
3.1.5. HupB of <i>M. bovis</i> BCG was not regulated by iron	55
3.2. Identification and characterization of novel iron-regulated envelope proteins in <i>M. smegmatis</i>	56
3.2.1. Up-regulation of three proteins in the cell wall fraction of iron-limited <i>M. smegmatis</i>	56
3.2.2. Purification and identification of the three iron-regulated envelope proteins by MALDI-TOF MS / MS analysis	57
3.2.3. Characterisation and analysis of the features of the three iron-regulated envelope proteins	59

3.2.3.1. General features	59
3.2.3.2. Evolutionary relationship of the three iron-regulated envelope proteins among mycobacteria and other Gram-positive bacteria	60
3.2.3.2.1. IrpA (MSMEG_3761)	60
3.2.3.2.2. IrpB (MSMEG_1959)	64
3.2.3.2.3. IrpC (MSMEG_1707)	69
3.3. <i>In silico</i> and experimental studies on IrpA	66
3.3.1. Physical features of IrpA and functional partners identified using <i>in silico</i> tools	66
3.3.1.1. IrpA of <i>M. smegmatis</i> is absent in <i>M. tuberculosis</i>	67
3.3.1.2. Generation of polyclonal mono-specific anti-IrpA antibodies	69
3.3.2. Iron-regulated expression of IrpA	69
3.3.2.1. Presence of IdeR box in <i>irpA</i> promoter	69
3.3.2.2. Coordinated expression of IrpA and siderophores	70
3.3.2.3. Time-course expression of IrpA	71
3.3.2.4. IrpA is absent in <i>M. bovis</i> BCG Pasteur	72
3.3.3. Cloning and expression of rIrpA	73
3.4. Functional characterisation of IrpA as a putative receptor for ferri-exochelin	75
3.4.1. <i>In silico</i> analysis: modeling and docking studies	75
3.4.1.1. Homology modeling of IrpA	75
3.4.1.2. Docking of exochelin onto IrpA	77
3.4.2. Experimental studies to establish IrpA as ferri-exochelin receptor	78
3.4.2.1. Uptake of ⁵⁵ Fe-exochelin by <i>M. smegmatis</i>	78
3.4.2.2. Uptake of ⁵⁵ Fe-carboxymycobactin by <i>M. smegmatis</i>	79
3.4.2.3. Uptake of ⁵⁵ Fe-exochelin by <i>M. smegmatis</i> was inhibited by antibodies against IrpA	80
3.4.2.4. Uptake of ⁵⁵ Fe-exochelin by liposomes prepared with IrpA-containing cell wall proteins of <i>M. smegmatis</i>	83
3.4.3. Immunoprecipitation of IrpA-interacting proteins: co-precipitation of IrpA and HupB with anti-IrpA antibodies	84
Chapter 4: Discussion	87

Chapter 5: Summary	96
Chapter 6: Bibliography	100
Chapter 7: Appendix	111
7.1: Publications	111
7.2: Anti-Plagiarism report	112

LIST OF ABBREVIATIONS

ADC	Albumin-dextrose-catalase
AG	Arabinogalactan
ATP	Adenosine triphosphate
BLAST	Basic Local Alignment Search Tool
BCG	Bacille Calmette Guérin
Bp	Base pair
CMb	Carboxymycobactin
EMSA	Electrophoretic mobility shift assay
Fe-CMb	Ferri-carboxymycobactin
Fe-Mb	Ferri-mycobactin
Fur	Ferric uptake regulator
h	Hour
HI	High iron
HIV	Human immunodeficiency virus
H ₂ O ₂	Hydrogen peroxide
HPLC	High-performance liquid chromatography
IREP	Iron-regulated envelope protein
IRMP	Iron-regulated membrane protein
IdeR	Iron-dependant regulator
kDa	kilo Dalton
KO	Knock out
LI	Low iron
mAGP	Mycolyl-arabinogalactan-peptidoglycan

Mb	Mycobactin
MS	Mass spectra
MEGA	Molecular Evolutionary Genetic Analysis
μ M	Micromolar
mg	Milligram
mL	Milliliter
mM	Mill molar
NCBI	National Center for Biotechnology Information
nm	Nanometer
NTM	Nontuberculous mycobacteria
OADC	Oleate-albumin-dextrose-catalase
OD	Optical density
O / N	Overnight
PAGE	Polyacrylamide gel electrophoresis
PBS	Phosphate buffered saline
PCR	Polymerase chain reaction
PG	Peptidoglycan
SD	Standard deviation
SDS	Sodium dodecyl sulphate
TB	Tuberculosis
TBS	Tris-buffered saline
TLC	Thin-layer chromatography
TMB	Tetramethyl benzedine
WHO	World Health Organization
WT	Wild type

Abstract

Iron is an important micronutrient for all aerobic bacteria except lactobacilli and *Borrelia burgdorferi*. This metal ion that can exist in the ferrous (Fe^{2+}) and ferric (Fe^{3+}) states plays an important role in electron transport and serves as a cofactor for several enzymes involved in vital cellular functions ranging from respiration to DNA replication. However, there is limited bioavailability of this essential micronutrient, mainly due to its poor insolubility at biological pH. The concentration of free iron is often too low to support the growth of bacteria. Mycobacteria, like other bacteria, have adapted to iron limitation by elaboration of Fe^{3+} -specific iron chelating compounds called siderophores. They produce the intracellular mycobactins and secrete the extracellular carboxymycobactin / exochelin. While both pathogenic and saprophytic mycobacteria produce mycobactin, with the exception of *Mycobacterium paratuberculosis*, carboxymycobactins are the sole extracellular siderophores in pathogenic mycobacteria and form a small fraction in the non-pathogens which produce the peptidic exochelins as the predominant extracellular siderophore.

Bacteria elaborate cell surface receptors for the internalization of the ferri-siderophores. These uptake systems, identified in several bacteria are well characterized in *E. coli*. In mycobacteria, iron-regulated envelope proteins (IREPs) were reported much later and the first IREP to be demonstrated was the 29 kDa protein from *M. smegmatis*. This protein was also seen in other mycobacterial species, including in vivo derived mycobacteria. This however was not sequenced and identified. But functional studies showed that it was associated as a receptor for ferri-exochelin, since antibodies against the protein blocked uptake of the ferri-exochelin. In *M. neoaurum*, a 21 kDa protein was shown to be co-expressed with mycobactin and exochelin. Interestingly, a 21 kDa protein was also identified in the cell wall of *M. leprae*. The latter was able to acquire iron only from ferri-exochelin from *M. neoaurum* and not from other

mycobacterial siderophores, implicating it as a possible receptor for ferri-exochelin from *M. neoaurum*.

Earlier studies in our lab identified and characterized a 28 kDa iron-regulated envelope protein, called HupB as an iron-regulated cell wall-associated protein in iron-limited *M. tuberculosis*. The expression of HupB was shown to be regulated by the iron regulator IdeR. The latter, forming a complex with Fe²⁺ bound the IdeR box upstream of iron-regulated genes, thereby blocking transcription. Studies with the *hupB* KO generated by homologous recombination established the functional role of HupB as a transcriptional activator. Transcriptional profiling by microarray analysis showed that there was down-regulation of the mycobactin biosynthetic genes, which was in agreement with the low levels of both mycobactin and carboxymycobactin in the mutant strain. In addition, the transcript levels showed alterations in the expression of genes involved in other biosynthetic pathways, some of which have been addressed in previous studies, specifically lipid metabolism. Our studies also showed the role of HupB in iron transport across the mycobacterial cell envelope and experimental evidence was provided to prove our hypothesis that HupB functions as a receptor for ferri-carboxymycobactin and mediates the transfer of iron to mycobactin present near the cytoplasmic membrane. The multi-functional role of the protein probably explains the significance of this protein in the pathogen, as the KO strain is unable to survive inside macrophages.

Considering the iron-regulated expression of HupB and its significance in the pathogenic mycobacterium, the expression of the corresponding homologue in *M. smegmatis* was addressed in this study. It was however seen that the protein expression was unaffected by iron levels, as seen in cultures grown with varying concentrations of iron added to the medium of growth. It was interesting to note that constitutive expression was also seen in the vaccine strain *M. bovis* BCG. In this study, unlike previous reports in *M. smegmatis*, the organisms were grown in medium containing 0.02 µg Fe / mL (low) and 8.0 instead of 4.0 µg Fe / mL (high). Under these conditions, three IREPs were found to be up-regulated in iron-limited *M. smegmatis*. These proteins with approximate molecular masses of 21, 109 and 145 kDa

respectively and referred to as IrpA, IrpB and IrpC were purified and identified by MALDI-TOF MS / MS analysis.

The 21 kDa iron-regulated protein, henceforth referred to as IrpA was identified as Clp-protease subunit in the genome of *M. smegmatis* with the locus tag of MSMEG_3671. This protein was absent in *M. tuberculosis* that showed the presence of several other Clp proteases. This protein was therefore chosen for detailed study. IrpA was characterized using bioinformatic tools and experimental studies and shown to be a putative receptor for ferri-exochelin.

CHAPTER 1
REVIEW OF LITERATURE

1.1 Introduction

1.1.1. General features of mycobacteria

Mycobacteria are aerobic, non-motile and non-sporulated rods with a unique lipid-rich cell wall. Although mycobacteria are aerobic, some of them, for example *M. bovis* are microaerophilic and grow better at lower oxygen tensions. The genome has a high G+C content (61-71%) with approximately 4000 ORFs, 10% of which is dedicated to lipid metabolism (Cole *et al.*, 1998). These bacteria are called as acid-fast bacteria based on the fact that their lipid-rich cell wall does not allow the leaching out of carbol fuchsin upon staining. This forms the basis of the Ziehl Neelsen staining used to identify these organisms as pink rods, as they are not decolorized upon treating them with acid-alcohol (95% ethanol and 3% hydrochloric acid). These organisms are not fastidious and require simple substrates for growth, namely ammonia or amino acids as nitrogen sources, glycerol as carbon source and mineral salts.

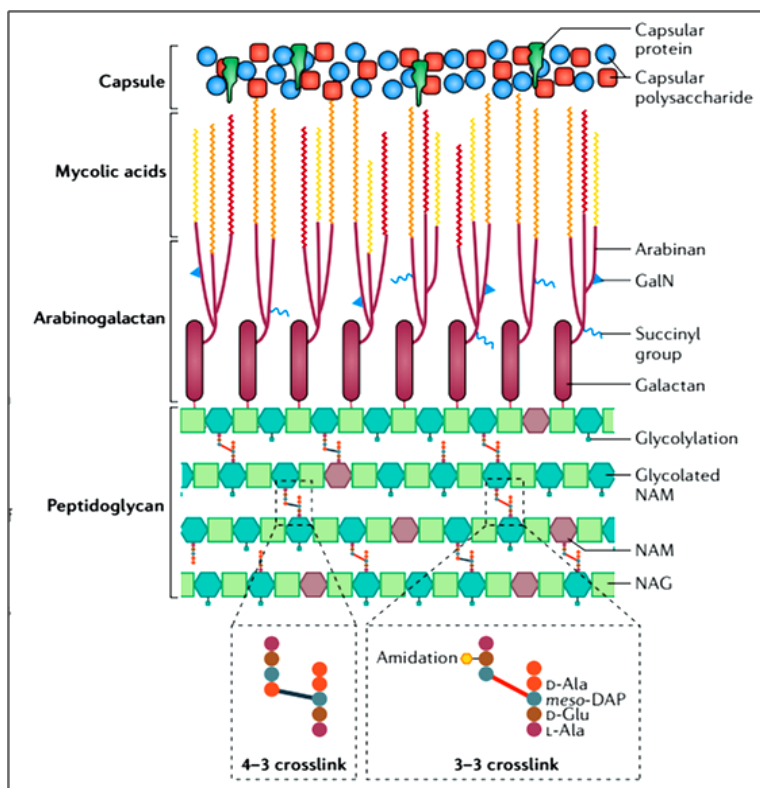
In 1882, Robert Koch discovered *Mycobacterium tuberculosis* as the causative agent of tuberculosis for which he was awarded the Nobel Prize in 1905. The generic name *Mycobacterium* was given due to its mould-like growth in liquid medium (Lehman & Neumann, 1896). The genus *Mycobacterium* consists of more than 100 species which belong to the family Mycobacteriaceae. Due to the high level of genetic relatedness, 0.01-0.03% synonymous nucleotide variation (Gutacker *et al.*, 2002 & Hughes *et al.*, 2002) (*M. tuberculosis*, *M. africanum*, *M. bovis*, *M. canetti*, *M. microti*, *M. pinnipedii* and *M. caprae* are grouped under *Mycobacterium tuberculosis* complex (MTBC). Mycobacteria, other than *M. tuberculosis*, causing clinical disease are known by various names, such as non-tuberculous mycobacteria (NTM) and atypical mycobacteria. NTM infections can be caused by *M. avium*, *M. kansasii*, *M. abscessus* etc. found in pulmonary infections, lymphadenitis, skin, soft tissue infections and others (Chan & Iseman, 2013). Mycobacteria that are not normally associated with human tuberculosis but can cause disease in immunocompromised individuals such as HIV-infected individuals are called opportunistic pathogens. They include *M. avium-intracellulare* complex and *M. kansasii* (Canueto-Quintero *et al.*, 2003)

1.1.2. Classification of mycobacteria

Taxonomically, mycobacteria belong to the Genus *Mycobacterium*, family Mycobacteriaceae and the Order Actinomycetales that include diverse bacteria. Mycobacteria and other allied taxa are distinguished by their ability to synthesize mycolic acids. Mycobacteria can be classified based on their growth rates and pigment production. On the basis of generation time, they are classified as rapid growers (generation time of 3-4 h) which include *M. smegmatis*, *M. neoaurum*, *M. kansasii* and *M. fortuitum*; slow growers (generation time of 20-24 h) are the pathogenic mycobacteria, including *M. tuberculosis*, *M. bovis* and *M. leprae*. On the basis of pigment production (Runyon classification, 1959) (Runyon, 1959), mycobacteria are classified as a) Scotochromogens, like *M. scrofulaceum*, *M. gordonae* that produce yellow pigment when incubated in the absence of light, b) Photochromogens, like *M. kansasii*, *M. marinum* that turn orange when incubated in the presence of light and the c) Achromogens, like *M. avium*, *M. intracellulare*, *M. ulcerans* that do not produce any pigment.

1.2. Unique features of mycobacterial cell envelope

Mycobacterial cell envelope is complex and unique with high content of lipids. It accounts for ~40% of the cell dry mass of the bacteria compared to less than 5% in other Gram-positive bacteria and only 10% in Gram-negative bacteria (Goren, 1972) but this percentage is dependent on the species / isolate and the growth conditions. The mycobacterial cell wall (Fig. 1.1) contains unique lipids called mycolic acids (C₆₀-C₉₀ α -alkyl β -hydroxy fatty acids) that are covalently bound to the arabinogalactan-peptidoglycan copolymer and form the mycolylarabinogalactan-peptidoglycan complex (MAPc) present in the inner layer of the outer membrane (Brennan & Crick, 2007; Brennan & Nikaido, 1995).



(Kieser & Rubin, 2014)

Fig. 1.1. Structural organization of the mycobacterial cell envelope: The mycobacterial cell envelope shows the presence of the highly lipophilic, long chain mycolic acids covalently attached to arabinogalactan. The capsule consists of various polysaccharides, proteins and lipids. The thick peptidoglycan layer, with carbohydrate residues forms a considerable part of the cell envelope. In addition, there are several non-covalently linked lipids and proteins associated with the cell envelope.

Mycolic acids form an integral component of the mAGP complex or found as free lipids esterified to trehalose or glucose in the cell wall (Fig. 1.1). Different chromatographic techniques, including high-performance liquid chromatography have identified that mycobacterial species present unique mycolic acid patterns, which can be used as taxonomic markers (Tortoli, 2003). Using established solvent systems for extraction, several lipids including trehalose dimycolates (TDMs), phthiocerol dimycocerosates (PDIM), sulfolipids (SLs), phenolic glycolipid (PGL), glycopeptidolipids (GPLs) and lipo-oligosaccharides (LOSs) characterized and shown to be species and strain-specific (Russell, 2007).

The complex organization of the mycobacterial cell envelope results in its low permeability and renders it resistant to most antibiotics, but hydrophilic nutrients pass through transmembrane channel proteins called porins. Mycobacterial porin was first detected in *M. chelonae* (Trias *et al.*, 1992) and MspA in *M. smegmatis* revealed a homo-octomeric goblet-like conformation with a single central channel by X-ray analysis (Faller, 2004). Apart from MspA, *M. smegmatis* contains MspB, MspC and MspD (Stahl *et al.*, 2001). Porins of *M. smegmatis* are responsible for iron uptake under high iron condition (Jones & Niederweis, 2010). No homologue of MspA was found in *M. tuberculosis*.

1.3. Iron and its importance

Iron is essential for the growth of aerobic bacteria, the exceptions being lactobacilli and *Borrelia burgdorferi* (Sritharan, 2016). This metal ion that can exist in the ferrous (Fe^{2+}) and ferric (Fe^{3+}) states plays an important role in electron transport and serves as a co-factor of several enzymes involved in intermediary metabolism, including biosynthesis of several essential molecules such as heme, nucleic acids and amino acids (Sritharan, 2000 & De voss *et al.*, 1999). Its requirement in *M. tuberculosis* is evident as the whole genome sequence of the pathogen indicates its role as cofactors in 40 different enzymes (Cole *et al.*, 1998) that includes oxygenases, superoxide dismutases, hydroxylases and ribonucleotide reductases.

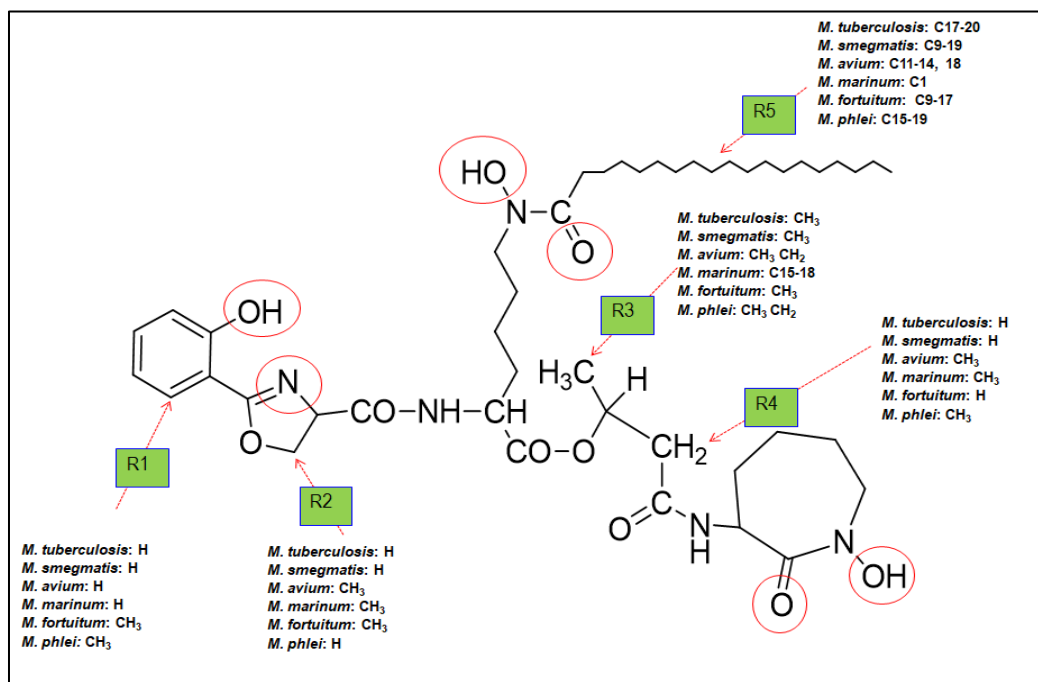
Despite the essentiality of this metal ion, its bioavailability is restricted as it can be harmful when present in excess. The limited bioavailability is due to its insolubility at biological pH, with the metal ion existing as insoluble ferric hydroxide and oxyhydroxide. At physiological pH 7.0, the major form of iron is $\text{Fe}(\text{OH})_2^+$, with a solubility of approximately 1.4×10^{-9} M (Chipperfield & Ratledge, 2000). These low levels of free iron do not support the growth of bacteria that require 10^{-7} M iron. In addition, pathogens face iron limitation as the mammalian host holds 99.9% of the metal ion as protein-bound iron in the form of transferrin (in blood circulation) and lactoferrin (in extracellular fluids) and by ferritin (in liver) (Bullen & Griffith, 1999). Restriction of the iron by the mammalian host is referred to as “nutritional immunity” (Kochan, 1976).

1.3.1. Adaptation of mycobacteria to iron limitation

Mycobacteria have adapted to iron limitation by expressing siderophores, a feature seen in several bacteria (Ratledge & Dover, 2000; Sritharan, 2000) including *E. coli*, in which it is well studied. In addition to the siderophore-mediated iron acquisition, some bacteria can acquire iron directly by elaborating specific receptors for hemin, transferrin & lactoferrin; this however, does not seem to be expressed by mycobacteria. In general, siderophores are low molecular weight (500-1000 Da) Fe^{3+} -specific high-affinity molecules with binding affinity constant K_s ranging from 10^{22} to 10^{50} that can remove iron from insoluble $\text{Fe}(\text{OH})_3$ and from host-iron binding compounds, but not from heme proteins. Mycobacteria produce two types of siderophores: cell-associated mycobactin and the secreted carboxymycobactin (by pathogens) and exochelins (by non-pathogenic mycobacteria).

1.3.2. Mycobactins

Mycobactins are intracellular hydrophobic siderophores localized in the lipid-rich cell wall. These extensively characterized molecules (Snow, 1970) consist of a core nucleus (Fig. 1.2) to which side chains with variations in their length and composition (Table 1.1) are attached.



(Sritharan, 2016)

Fig. 1.2. General structure of mycobactin: The figure shows the core nucleus of mycobactin; with varying residues in positions R1-R5 in different mycobacterial species. Usually H, CH₃ or CH₂CH₃ are present in R1-R4; R5 on the other hand carries the long chain alkyl group of C17-20 that makes mycobactin hydrophobic. Replacement of this acyl chain with a simple ester gives rise to carboxymycobactin that is hydrophilic. The red color circles indicates the iron chelating groups

The latter give species specificity to these molecules, which can be used to identify mycobacterial species (Ratledge, 2004). These molecules have high affinity for Fe³⁺ (~10³⁰) that enables them to chelate insoluble and protein-bound iron. They have low affinity for Fe²⁺ (Ratledge, 2004) that possibly must play a role in the transfer of the iron from these molecules.

The core nucleus of mycobactin is shown in Fig. 1.2. This includes the salicylate, two lysine molecules, one of which is cyclised to give a seven-membered lactam ring. The various regions indicated as R shows variations among different mycobactin molecules. For example, a methyl group may or may not be present at the 6th position of phenolic ring (R1) or at the 5th position of the oxazoline (R2). Presence of both types of oxazoline has been reported in *M. tuberculosis* (Gobin *et al.*, 1995). Various alkyl substituents of the hydroxyl acid at R3 and R4 are seen (Table 1.1) and notable is the length of the fatty acyl chain in R5, which contributes to its species-specificity (Snow, 1970; Hall & Ratledge, 1984; Sriharan, 2000).

Mycobactin is a mixed type of siderophore, using both hydroxamate and phenolate residues for chelating the metal ion. Fe³⁺ is chelated by the two hydroxamic acids of the ε-N-hydroxylysines, the nitrogen of the oxazoline ring, and the phenolate oxygen atom (Fig. 1.2).

Table 1.1: Variation in the mycobactins produced by different mycobacterial species

Organism	Mycobactin	Different substituents				
		R ₁	R ₂	R ₃	R ₄	R ₅
<i>M. aurum</i>	A	CH ₃	H	CH ₃	H	C ₁₃
<i>M. avium</i>	Av	H	CH ₃	CH ₃ CH ₂	CH ₃	C _{11-14, 18}
<i>M. fortuitum</i>	F	CH ₃ /H	CH ₃	CH ₃	H	C ₉₋₁₇
<i>M. marinum</i>	M	H	CH ₃	C ₁₅₋₁₈	CH ₃	C ₁
<i>M. marinum</i>	N	H	CH ₃	C ₁₅₋₁₈	CH ₃	C ₂
<i>M. phlei</i>	P	CH ₃	H	CH ₃ CH ₂	CH ₃	C ₁₅₋₁₉
<i>M. smegmatis</i>	S	H	H	CH ₃	H	C ₁₉
<i>M. tuberculosis</i>	T	H	H	CH ₃	H	C ₁₇₋₂₀

1.3.3. Carboxymycobactins

Carboxymycobactins are the predominant extracellular siderophores expressed by pathogenic mycobacteria (Ratledge, 2004). Their expression at low levels in the saprophytic *M. smegmatis* is unclear (Ratledge & Ewing, 1996). The core structure of these molecules is identical to the respective mycobactin in the particular species. The major difference is the absence of the long alkyl chain at R5 (Fig. 1.3) that renders them more polar. It is observed that each species produces a mixture of carboxymycobactins, with short alkyl chains at R5 that appear as mixture of closely eluting molecules when subjected to HPLC. Their structures have been elucidated in *M. avium* (Lane *et al.*, 1995), *M. tuberculosis* (Gobin *et al.*, 1995), *M. bovis* and *M. bovis* BCG (Gobin *et al.*, 1999) and in *M. smegmatis* (Lane *et al.*, 1998).

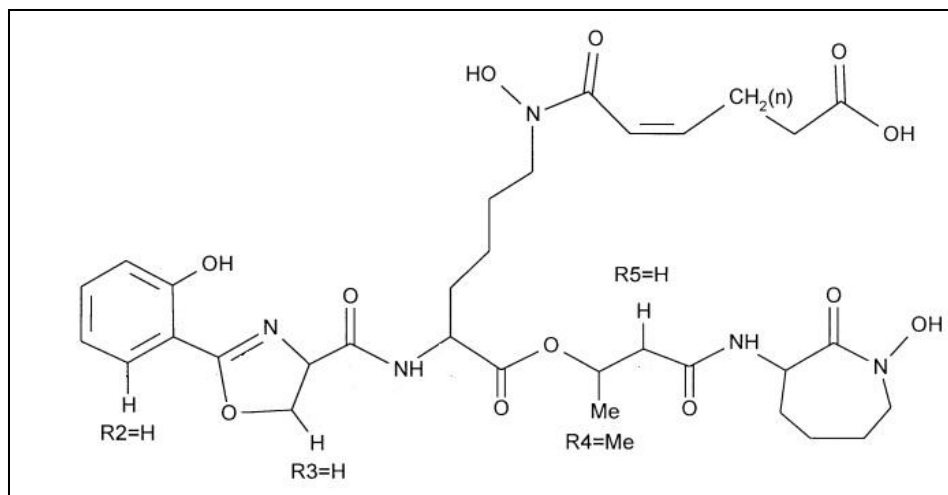
(Lane *et al.*, 1998)

Fig. 1.3. Structure of carboxymycobactin from *M. smegmatis*: The various substitutions at positions R2 – R5. R1 in mycobactin is replaced by a smaller side chain, with $n = 2-9$

1.3.4. Exochelins

Exochelins are water-soluble, peptidic siderophores produced extracellularly by non-pathogenic mycobacteria. It was first identified in *M. smegmatis* (Macham & Ratledge, 1975) and with its structural elucidation posing considerable challenges, it was unraveled twenty years later in *M. smegmatis* and *M. neoaurum* (Sharman *et al.*, 1995a & Sharman *et al.*, 1995b). The amino acids are D-amino acids with ornithine being predominant (Ratledge & Dover, 2000). The coordination center with Fe^{3+} is hexadentate, with the metal ion held in an octahedral structure involving the three-hydroxamic acid groups donated by ornithine. Exochelin MS from *M. smegmatis* is a formylated pentapeptide derived from three molecules of δ -N-hydroxyornithine, β -alanine and threonine (Fig. 1.4A). Exochelin MN from *M. neoaurum* is a hexapeptide with two δ -N-hydroxyhistidines, two β -alanine residues and an ornithine (Fig. 1.4B).

Exochelin from *M. smegmatis* was isolated from cultures grown in iron-deficient media and purified to $\geq 98\%$ purity by a combination of ion-exchange chromatography and HPLC. It is unextractable into organic solvent, is basic (pI 9.3-9.5), has a λ_{max} at 420nm and probable K_s for Fe^{3+} between 10^{25} and 10^{30} .

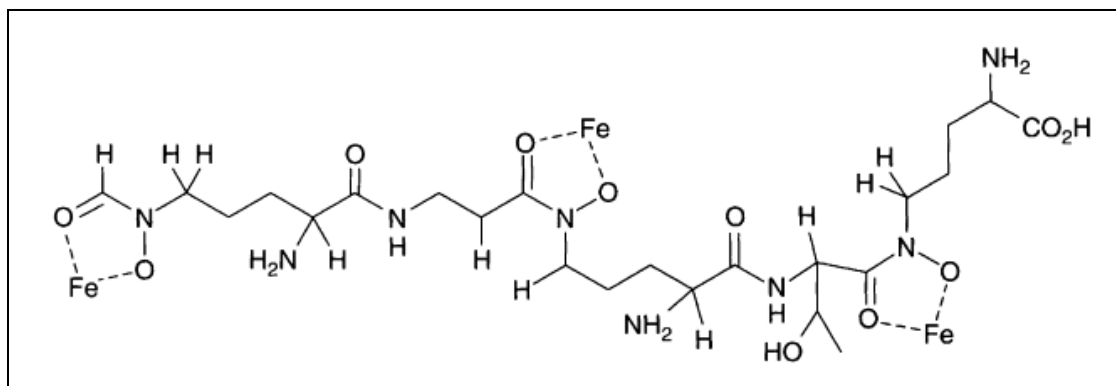
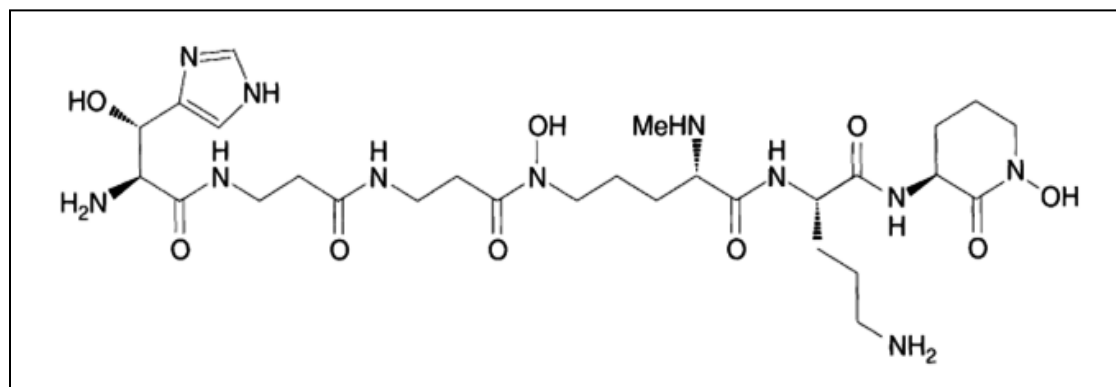
A. Exochelin MS from *M. smegmatis*B. Exochelin MN from *M. neoaurum*(Sharman *et al.*, 1995a & b)

Fig. 1.4. General structure of exochelins MS and MN: Exochelin MS and MN are the two extracellular siderophores expressed by *M. smegmatis* and *M. neoaurum* respectively. They contain usual amino acids like ornithine and substituted amino acids like N-hydroxyhistidine.

1.4. Iron-regulated envelope proteins in mycobacteria

Iron-regulated envelope proteins (IREPs) in mycobacteria were first demonstrated in *M. smegmatis* (Hall *et al.*, 1987). The organisms grown in the presence of 0.02 $\mu\text{g Fe / mL}$ (low iron) expressed a predominant 29 kDa protein in addition to several other proteins that were repressed or present in low levels in organisms grown in the presence of 4.0 $\mu\text{g Fe / mL}$ (high iron). Subsequent studies by Ratledge and his group identified iron-regulated envelope proteins in other mycobacterial species, including *M. neoaurum*, *M. avium* and *M. leprae* (Sritharan & Ratledge, 1990). These IREPs were not seen in axenic cultures but also in *in vivo* derived mycobacteria. Protein bands of approximate molecular mass of 180, 29, 21 and 14 kDa respectively were identified in *M. avium*

isolated from infected C57 black mice, while the 21 kDa IREP was shown in the cell wall fraction of *M. leprae* obtained from infected armadillo liver (Sritharan, 2000).

In *M. smegmatis*, the 29 kDa IREP was shown as a potential receptor for the exochelin MS by specifically blocking its uptake using protein specific antibodies against the 29 kDa protein. This was further substantiated by the specificity of this protein as a ferri-exochelin receptor (Dover & Ratledge, 1996). In *M. neoaurum*, the 21 kDa IREP, shown to be co-regulated with expression of mycobactin and exochelin MN (Sritharan & Ratledge, 1989) remains to be studied as an exochelin receptor. The presence of the 21 kDa IREP in *M. leprae*, possibly the homologue of the protein in *M. neoaurum* is likely to be a receptor of ferri-exochelin MN as *M. leprae* acquired iron from ferri-exochelin MN (Hall *et al.*, 1983) and not from other mycobacterial ferri-siderophores.

1.4.1. HupB as an iron-regulated envelope protein in *M. tuberculosis*

1.4.1.1. Iron levels and HupB expression.

HupB was identified as a 28 kDa protein in the cell wall fraction of *M. tuberculosis* grown in the presence of 0.02 µg Fe / mL (Yeruva *et al.*, 2006), with repression of the protein when iron levels were increased to 8 µg Fe / mL in the medium of growth. Under these conditions, HupB expression correlated with the levels of the two siderophores mycobactin and carboxymycobactin. These observations from our lab projected a different role for HupB in *M. tuberculosis* that was reported as a histone-like protein, with immunoproliferative properties based on studies in human patients with tuberculosis (Prabhakar *et al.*, 1998).

1.4.1.2. HupB is a multi-functional protein

HupB is variously called and assigned different functions in mycobacteria. In *M. tuberculosis*, it is 214 amino acid long, rich in basic amino acids arginine and lysine that gives the protein a high pI value of 12.5. The length of the protein differs among the mycobacterial species, with the mycobacterial-specific C-terminal region showing variation; the N-terminal region of 90 amino acids is conserved and is homologous to the *E. coli* histone-like DNA-binding HU class of nucleoid proteins. It is called as HLP_{Mt} in *M. tuberculosis* (Prabhakar *et al.*, 1998 & Cohavy *et al.*, 1999), MDP1 (mycobacterial

DNA-binding protein 1) in *M. bovis* BCG (Matsumoto *et al.*, 2000), Hlp in *M. smegmatis* (Lee *et al.*, 1998) and LBP (laminin binding protein) in *M. leprae* (Shimoji *et al.*, 1999). The implications of the protein in host cell immunoproliferation, protection against stress, cell wall assembly, and recombination are some of the functions demonstrated as detailed below. In *M. smegmatis*, its elevated expression during dormancy and cold shock was shown to be protective (Shires & Steyn, 2001). Mycobacterial histone-like proteins (HupB) was able to constrain DNA in negative supercoils as well as introduce negative super helical turns into relaxed DNA, and inhibit DNA strand exchange promoted by RecA in homologous recombination (Sharadamma *et al.*, 2011). MDP1, first studied by Matsumoto and his group (Matsumoto *et al.*, 2000) was also shown to negatively regulates *katG* expression, thereby influencing INH activity (Niki *et al.*, 2012). Association of HupB with iron metabolism was reported by Takatsuka and colleagues who demonstrated its direct interaction with iron and the expression of ferroxidase activity that catalyses the conversion of Fe^{2+} to Fe^{3+} . One molecule of MDP1 was shown to capture up to 81 iron (Fe^{3+}) atoms, suggesting its role in iron storage (Takatsuka *et al.*, 2011).

1.4.1.3. Role of HupB in iron metabolism

This is discussed in detail in Section 1.6.2

1.4.1.4. *In vivo* expression of HupB

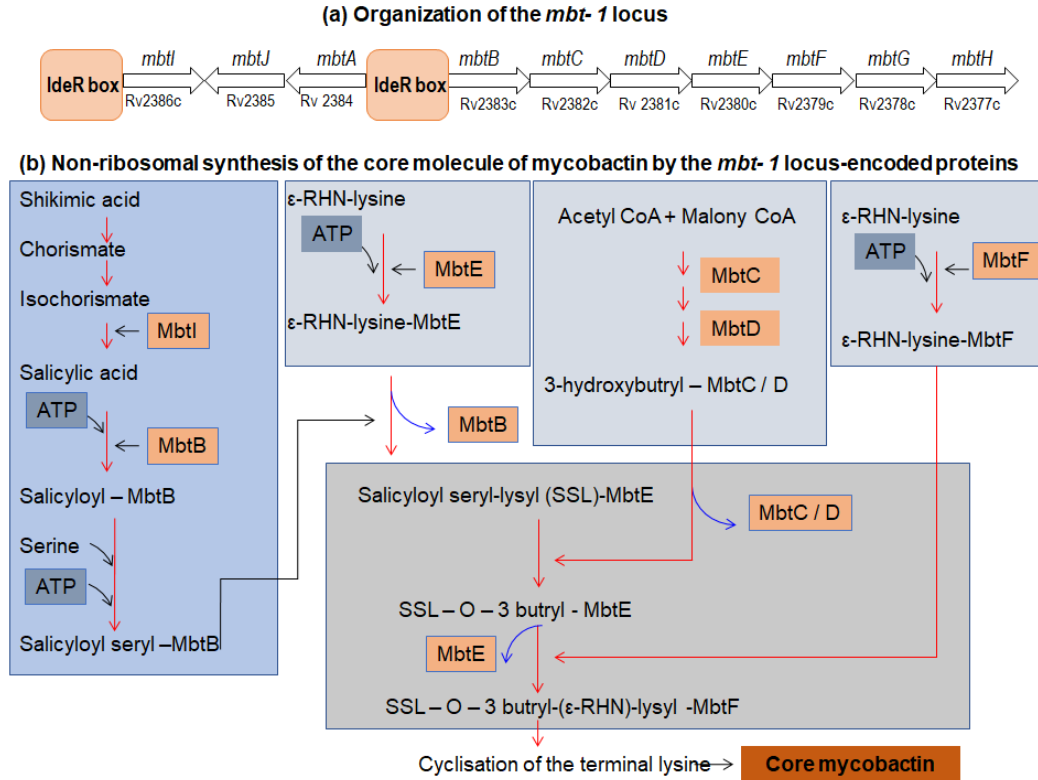
Earlier reports from our lab (Yeruva *et al.*, 2006; Sivakolundu *et al.*, 2013; Sriitharan *et al.*, 2014) and reports by others (Cohavy *et al.*, 1999; Prabhakar *et al.*, 2004; Kumar *et al.*, 2011) have unequivocally established the *in vivo* expression of HupB by demonstrating the presence of anti-HupB antibodies in tuberculosis patients. Our *in vitro* observations of the influence of iron on its expression correlated well with the finding that there was a strong negative correlation of anti-HupB antibodies with serum iron status in patients with tuberculosis, a feature not observed in household contacts of these patients and healthy controls (Sivakolundu *et al.*, 2013). Interestingly, the maximal titre of anti-HupB antibodies was seen in patients with extrapulmonary tuberculosis, a finding observed in two separate studies performed on two different study populations.

In the second study, in addition to high values in extra pulmonary cases, the highly variable C-terminal region (amino acids 63-161) cloned and expressed as HupB-F2 fragment performed well as an antigen in detecting serum antibodies from pulmonary TB and extrapulmonary TB patients (Sritharan *et al.*, 2014).

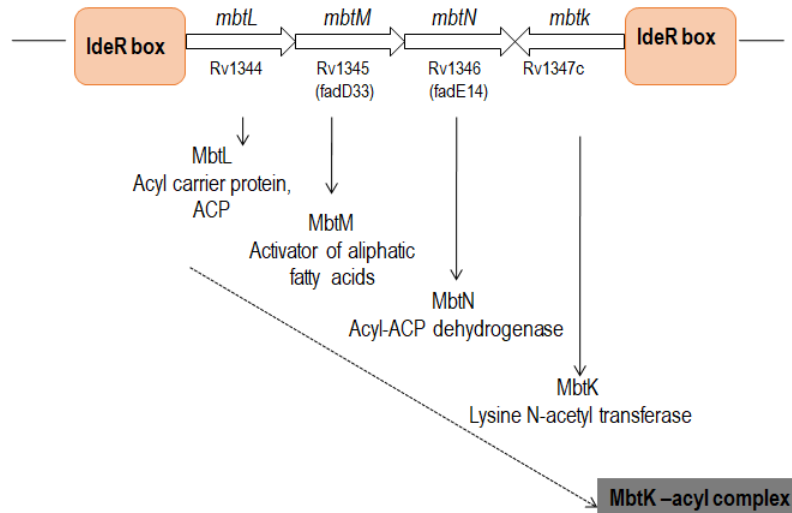
1.5. Biosynthesis of siderophores

1.5.1. Biosynthesis of mycobactin / carboxymycobactin

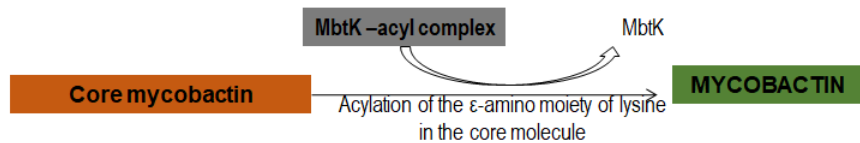
Mycobactins are synthesized by polyketide synthase / non-ribosomal peptide synthetases (NRPs) pathway. The mycobactin biosynthetic machinery was first identified by Quadri and his group (Quadri *et al.*, 1998). They identified the *mbt-1* operon, with the subsequent identification of the *mbt-2* cluster (Krithika *et al.*, 2006). *mbt-1* cluster consists of ten genes *mbtA-J* responsible for synthesizing the core structure of mycobactin (Fig. 1.5a) The *mbt-2* cluster consists of the four genes *mbtK-N*, whose translated products were shown to assemble the lipophilic aliphatic side chain onto the mycobactin backbone (Fig. 1.5c). The functionality of eight of the genes in the *mbt-1* cluster was established by systematic mutational approach in *M. smegmatis* (Chavadi *et al.*, 2011).



(c) Synthesis of the long chain acyl moiety by the four proteins encoded in the *mbt-2* locus



(d) Acylation of the core mycobactin to form mycobactin



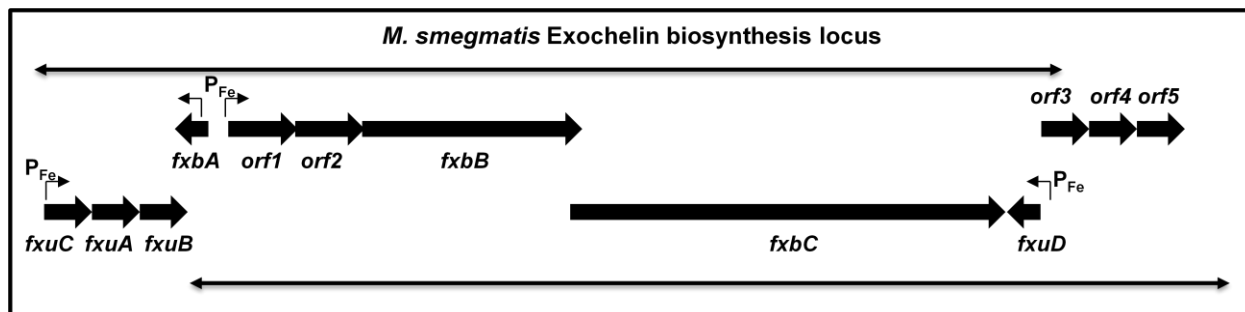
(Sritharan, 2016)

Fig. 1.5. Schematic representation of biosynthesis of mycobactin: Panel (a) shows the organization of *mbt-1* genes in the genomes of *M. tuberculosis* and IdeR boxes. Panel (b) shows the biosynthetic pathway for the synthesis of core mycobactin molecule by the non-ribosomal machinery. Panel c shows the *mbt-2* cluster whose translated products catalyse the formation of the synthesis of the long alkyl chain, with acylation of the core mycobactin forming mycobactin represented in Panel (d).

Fig. 1.5 represents the non-ribosomal synthesis of core molecule of mycobactin by *mbt-1* locus. In the biosynthesis of mycobactin, involves synthesis of salicylate by MbtI from isochorismic acid and hydroxylation of lysine by MbtG N⁶-hydroxy lysine. Mycobactin backbone is synthesized by mega synthase complex containing three nonribosomal peptide synthases (NRPs; MbtB, MbtE and MbtF) and two polyketide synthase (PKS; MbtC and MbtD). MbtH and MbtJ roles yet to identify in the mycobactin synthesis (Fig. 1.5). Acetylation of core mycobactin molecule by a long-chain fatty acyl group to form mycobactin and this reaction mediated by *mbt-2* locus containing MbtL, MbtM, MbtN and MbtK (Fig 1.5). Long fatty acyl chain transferred to core mycobactin molecule by MbtK-fatty acyl complex for forming the functional mycobactin (Fig. 1.5) (Krithika *et al.*, 2006).

1.5.2. Biosynthesis of exochelin

The first report on the genes associated with biosynthesis of exochelin in *M. smegmatis* (Fiss *et al.*, 1994) identified *fxbA* (ferri exochelin biosynthesis) encoding N-formyltransferase and the operon containing genes *fxuA*, *fxuB* and *fxuC* (Fig. 1.6). Subsequently, two genes *fxbB* and *fxbC* were identified (Yu *et al.*, 1998). The corresponding homologues are not present in the genome of *M. tuberculosis* (Cole *et al.*, 1998), explaining its absence in cultures of the pathogen.



(Yu *et al.*, 1998)

Fig. 1.6. Exochelin biosynthetic locus: The figure shows the organization of the different genes associated with exochelin synthesis and transport, with the arrows showing the direction of transcription. P_{Fe} refers to the putative iron box in the respective promoter region.

In the biosynthesis of exochelin, the non-ribosomal peptide synthetases include FxbB and FxbC that contains six activation modules, namely FxbB1, FxbB2, FxbC1, FxbC2, FxbC3 and FxbC4. Each module contains an ATP-binding motif, an ATPase motif and pantetheine attachment motif (Yu *et al.*, 1998 & Zhu *et al.*, 1998). Three epimerase domains within the C-terminal motifs of FxbB1, FxbC1 and FxbC2 convert the *S*- to *R*-amino acid. The linear formylated pentapeptide exochelin is organized with six unusual amino acids: β -alanine, (*R*)-allo-threonine, two molecules of (*R*)- δ -*N*-hydroxyornithines and (*S*)- δ -*N*-hydroxyornithine. The FxbB1 and its C-terminal that contains an epimerase domain upload the first (*R*)- δ -*N*-hydroxyornithines which follows the attachment of β -alanine and (*S*)- δ -*N*-hydroxyornithine to the backbone by FxbB2 and FxbC3 (or FxbC4) (Yu *et al.*, 1998). The third and fourth *R*-amino acids, (*R*)- δ -*N*-hydroxyornithines and (*R*)-allo-threonine are packed by the FxbC1 and FxbC2 respectively. The FxbA transfers a formyl group to the first (*R*) δ -*N*-hydroxyornithine.

The ORFs are associated with transport and ORF1, ORF2, ORF3 are so named based on the homology with other ABC transporters; ORF4 and ORF5 are putative membrane proteins of *M. tuberculosis* and *M. leprae* respectively (Yu *et al.*, 1998). It was suggested that *fxuD* encoded a putative membrane-related receptor for exochelin and *exiT*, an ABC transporter involved in the secretion of exochelin (Zhu *et al.*, 1998).

1.6. Regulation of iron metabolism in mycobacteria

There is extensive information on mycobacterial siderophores and iron as an intracellular sensor molecule regulating the expression of these siderophores via its interaction with the iron regulator IdeR. Compared to other bacteria, an event occurring at the molecular level was slow due to the difficulty in the generation of mutants in mycobacteria. But, now with the advancement in mycobacterial genetics, considerable information is available that however has not been sufficient to completely understand iron acquisition and regulation in pathogenic and saprophytic mycobacteria that show

considerable differences in the siderophore machinery as seen above. The different players in mycobacterial iron acquisition and regulation are detailed below.

1.6.1. Iron-dependent regulator (IdeR)

Fur is the global iron regulator present in Gram-negative bacteria. Similarly, DtxR of *Corynebacterium diphtheriae* was seen to be present in several Gram-positive bacteria. The mycobacterial iron regulator IdeR was first identified based on its homology with DtxR. In addition, mycobacteria express FurA that acts in association with iron in regulating oxidative stress machinery. IdeR is the key regulator of mycobactin biosynthesis in *M. tuberculosis* and exochelin biosynthesis in *M. smegmatis*. It is a 230-amino acid protein showing 59% overall amino acid identity with DtxR from *C. diphtheriae* with 78% similarity in the N-terminal 140 amino acid region (Schmitt *et al.*, 1995). Crystal structure of IdeR shows the association of four monomeric units forming two functional dimers (Feese *et al.*, 2001). Each monomer has three functional domains with two metal-binding sites. In the presence of iron, IdeR forms IdeR-Fe²⁺ complex and binds to the 19 bp IdeR box or iron box (5'-TTAGGTTAGGCTAACCTAA-3') and regulates the expression of the genes associated with iron acquisition; it represses the transcription of the *mbt* genes in *M. tuberculosis* and *fxb* genes in *M. smegmatis*. In addition to iron (the natural cofactor and optimal metal for IdeR function), IdeR can also bind other divalent metal ions such as Mn²⁺, Zn²⁺, Co²⁺, Ni²⁺, and Cd²⁺ (Schmitt *et al.*, 1995). IdeR, in addition to functioning as a repressor of mycobactin biosynthesis can function as a positive regulator of the iron storage genes *bfrA* and *bfrB* (Gold *et al.*, 2001).

1.6.2. Regulation of siderophore biosynthesis by IdeR and HupB in *M. tuberculosis*

In the presence of iron; the IdeR-Fe²⁺ complex is formed that binds specifically to a 19 bp consensus sequence called the 'iron box or IdeR box' in the *mbtB* promoter DNA (located at -32 position from the predicted start point of *mbtB*) that blocks the transcription of the first gene in the biosynthetic pathway of mycobactin (Gold *et al.*, 2001). When the intracellular iron concentration becomes low, transcription initiation

requires binding of HupB to a 10 bp sequence (5'-CACTAAAATT-3') called the HupB box, located immediately upstream of the IdeR box (-40 bp from the transcriptional start point of *mbtB*) although IdeR-Fe²⁺ complex is absent (Pandey *et al.*, 2014b & Sritharan, 2016). HupB box has also been identified in the promoter region of *hupB* showing that HupB regulates its own synthesis (Pandey *et al.*, 2014a). Under high iron conditions ($\geq 200 \mu\text{M}$) IdeR-Fe²⁺ complex binds the IdeR box and represses the transcription of siderophore biosynthetic genes by RNA polymerase. When there is a drop in the intracellular iron level, IdeR can no longer form IdeR-Fe²⁺ complex and HupB can bind the *mbtB* promoter DNA as HupB-iron complex; therefore, transcription by RNA polymerase can start and mycobactin is synthesized. It was shown that, HupB can bind the *mbtB* promoter DNA even in the presence of very low level of iron ($\leq 25 \mu\text{M}$).

In silico analysis revealed two IdeR and one HupB boxes upstream of *hupB* promoter DNA (Fig. 1.7a). First IdeR box is at -127 bp upstream of the start point of *hupB*, second IdeR box at -5 bp and the HupB box was at -99 bp upstream of the start point of *hupB* (Fig. 1.7b) (Pandey *et al.*, 2014a). This was further experimentally proved by DNA foot printing and EMSA (Electrophoretic mobility shift assay). When the intracellular iron concentration is $\geq 200 \mu\text{M}$, IdeR exists as IdeR-Fe²⁺ complex, occupies both IdeR boxes and completely represses the synthesis of *hupB*. When iron levels fall, the HupB-iron complex can bind to HupB box located in -99 bp upstream of *hupB* start point and positively regulate its own expression.

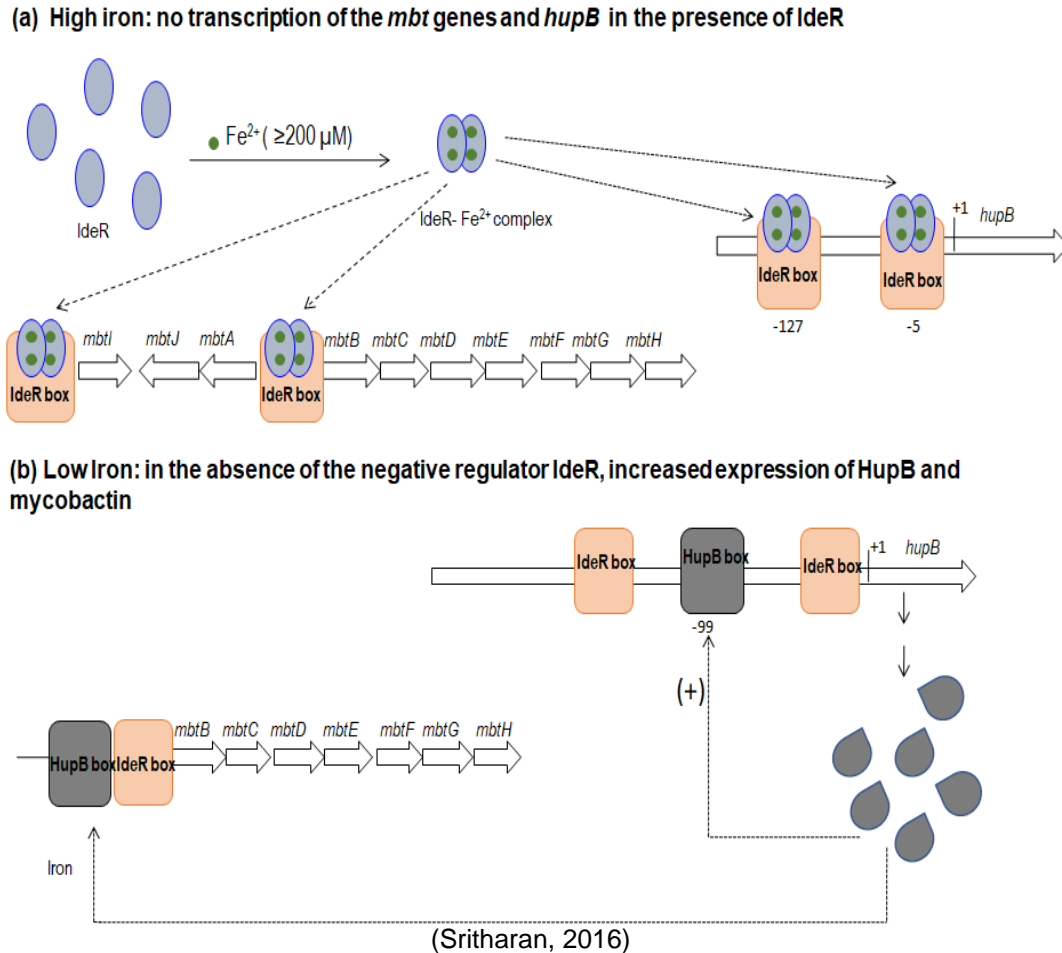


Fig. 1.7. Transcriptional regulation of mycobactin biosynthesis—a schematic model: Panel A shows the repression of the *mbt* genes and *hupB* by IdeR-Fe²⁺ complex. Panel B shows the positive regulation of mycobactin and autoregulation of HupB

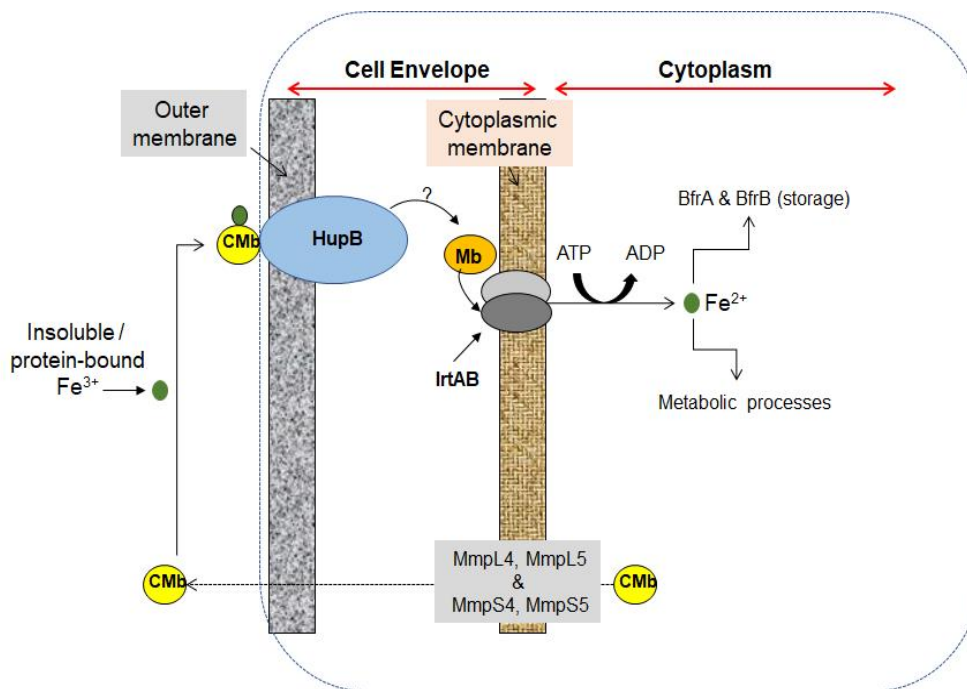
1.6.3. FurA, FurB (ferric uptake regulator) and SirR

Though studies with *ideR* mutants confirmed the role of the IdeR in iron homeostasis, it is not the sole iron regulator (Dussurget *et al.*, 1999). FurA is an additional iron regulator and studies in *M. tuberculosis* and *M. smegmatis* showed that FurA negatively regulates the expression of KatG, thereby playing a role in oxidative stress (Pym *et al.*, 2001) (Zahrt *et al.*, 2001). The *furA-katG* is expressed as an operon, with FurA auto regulating its own expression (Sala *et al.*, 2003). FurB belongs to the Fur family and has been demonstrated to function as a Zinc uptake regulator (Zur) in *M. tuberculosis*. SirR (Rv2788), annotated as an iron-dependent regulator belonging to the DtxR family in the *M. tuberculosis* genome is yet to be characterized as an iron regulator.

1.7. Uptake of iron in mycobacteria

1.7.1. Uptake of ferri-carboxymycobactin in *M. tuberculosis*

Siderophore-mediated iron uptake by *M. tuberculosis* has been extensively reviewed recently by (Sritharan, 2016) (Fig. 1.8). *M. tuberculosis* synthesizes siderophores when iron levels were low and which are exported across the membrane by membrane transport proteins MmpL4 / MmpS4 and MmpL5 / MmpS5 (Wells *et al.*, 2013). The extracellular desferri-CMb chelates Fe^{3+} from insoluble or protein-bound iron forming Fe-CMb. Iron from ferri-carboxymycobactin is transferred to mycobactin in the cell envelope of *M. tuberculosis*, where HupB (cell wall-associated protein) functions as the iron transporter. The ABC transporters IrtAB present on the cytoplasmic membrane mediates the internalization of iron, possibly from the Fe-Mb by reduction of Fe^{3+} to Fe^{2+} catalysed by the FAD dependent reductase associated with IrtA (Ryndak *et al.*, 2010). The metal ion, as Fe^{2+} , is transported into the cytoplasm by an energy-dependent process, and once inside, it is utilized for various metabolic processes, and the excess iron is stored in BfrA and BfrB.



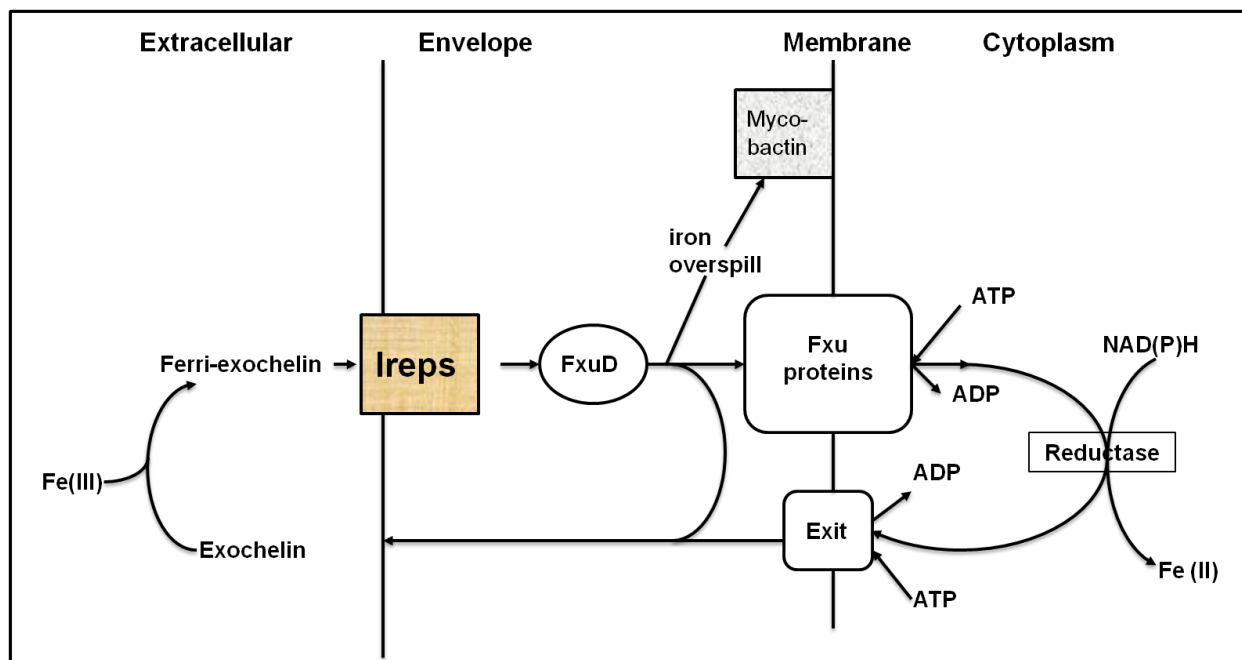
(Sritharan, 2016)

Fig. 1.8. Mechanism of iron the transport of in *M. tuberculosis*: Desferri-CMb produced by *M. tuberculosis* upon iron deficient condition is exported to the outside, process by the MmpL4 &

MmpS4 and MmpL5 & MmpS5 proteins. It chelates Fe^{3+} present as insoluble or protein-bound iron and forms ferri-carboxymycobactin. HupB present in the cell envelope is hypothesized to mediate the transfer of iron to mycobactin. The IrtAB present on the plasma membrane transports the Fe^{3+} into the cytoplasm after reducing it to Fe^{2+} utilising the reductase activity of the bound NAD.

1.7.2. Uptake of ferri-exochelin in *M. smegmatis*

Uptake of ferri-exochelin in *M. smegmatis* (Ratledge, 2004) has been proposed to occur as an active transport process as it was found to be inhibited by energy poisons and uncouplers of oxidative phosphorylation (Macham *et al.*, 1975). Ratledge proposed that ferri-exochelin is transferred across the cell envelope by the FxuD protein and then internalized into the cytoplasm by the cytoplasmic membrane proteins FxuA, FxuB and FxuC, proposed based on their homology with the corresponding proteins FepG, FepC and FepD in *E. coli* (Ratledge, 2004). Excess iron is thought to be moved into mycobactin. In the cytoplasm, the iron is presumed to be released as Fe^{2+} that is used for biological processes. Exochelin, after releasing its iron into the cytoplasm is exported to the outside by ExiT (Zhu *et al.*, 1998) that operates in conjunction with other proteins and involves the input of energy.



(Ratledge, 2004)

Fig. 1.9. Iron uptake mechanism in *M. smegmatis* via ferri-exochelin: Exochelin produced by *M. smegmatis* in iron deficient conditions was able to chelates iron from protein bound and it is recognized by cell surface receptor (iron-regulated envelope proteins). The complete molecule of ferri-exochelin is taken across by envelope with association of FxuD and across the membrane via Fxu permease system. The intracellular reductase release the Fe (III) to Fe (II), the deferrated siderophore transferred back to extracellular environment by Exit protein.

1.7.3. Iron uptake through porins under high iron conditions in *M. smegmatis*

As explained detailed ferri-exochelin uptake in iron deficient conditions in Section 1.7.2. However under high iron condition Msp (porins) are responsible for iron uptake in *M. smegmatis* (Jones & Niederweis, 2010). A triple mutant of porin (*mspA mspC mspD*) accumulated approximately 40% less iron than wild type *M. smegmatis* which clearly demonstrates that the reduced uptake of iron was due to loss of Msp porins only. Under high-iron conditions the iron requirements of the cells are met by diffusion of ferric citrate complexes through porins in *M. smegmatis*, when the iron concentration decreases below a certain threshold, or the number of porins is reduced, *M. smegmatis* compensates by up regulating iron acquisition genes.

Siderophores expressed by pathogenic and non-pathogenic mycobacteria differing in the extracellular siderophores and intracellular cell-associated mycobactin present in both the organisms, but the non-pathogenic *M. smegmatis* express predominantly as exochelins which are structurally different from carboxymycobactin and mycobactin as detailed mentioned in Section 1.3.4. Both the siderophores exochelin and carboxymycobactin from non-pathogenic and pathogenic mycobacteria appear to have different mechanisms for iron transport into the cell (Ratledge, 2004). Uptake of carboxymycobactin from pathogens is taken up by a process which is not energy dependent and it is not affected by poisons and uncouplers of ATP biosynthesis and it's a facilitated diffusion process (Stephenson & Ratledge, 1980). However ferri-exochelin is taken by an active transport mechanism which is energy dependent and it is effected by uncouplers of oxidative phosphorylation (Stephenson & Ratledge, 1979).

Objectives of the study

The main objective of this study was to understand iron acquisition in the non-pathogenic *M. smegmatis* and compare with that seen in the pathogenic *M. tuberculosis*.

Specific objectives include

- I. Influence of iron levels on the expression of the HupB homologue in *M. smegmatis*.
- II. Identification of novel iron-regulated envelope protein(s) that is coordinately regulated with the siderophores.
- III. Characterisation of a 21 kDa iron-regulated protein IrpA as a putative ferri-exochelin receptor

CHAPTER 2
MATERIALS AND METHODS

2.1. Chemicals and Reagents

Bacterial grade media components were purchased from HiMedia (Mumbai, India). Routine analytical reagents and solvents were purchased from Qualigens (Qualigens Fine Chemicals Pvt. Ltd, India). Fine chemicals (molecular biology grade) were purchased from Sigma-Aldrich Pvt. Ltd. (MO, USA). Culture media Middlebrook 7H9 / 7H10 and 7H11 were purchased from Difco (MD, USA), supplements oleic acid-albumin-dextrose-catalase (OADC) / albumin-dextrose-catalase (ADC) from Becton and Dickinson (BD) (MD, USA), Lowenstein-Jensen base from HiMedia (Mumbai, India) and iron-free chemicals ($ZnSO_4 \cdot XH_2O$, $MnSO_4 \cdot XH_2O$ and $MgSO_4 \cdot 7H_2O$) from Puratronic Alfa AESAR (Massachusetts, United States). All molecular biology chemicals were purchased from Thermo Fisher Scientific Corporation (MA, USA) and Ni-Sepharose resin from GE Healthcare (Little Chalfont, United Kingdom). TLC Silica gel 60 F254 plates, nitrocellulose membrane, and syringe filters were purchased from Merck (NJ, USA). Anti-IgG antibodies (ALP and HRP conjugated) were obtained from Bangalore Genei (India). Oligonucleotide primers were synthesized by Biosquare Technologies (India). $^{55}FeCl_3$ was purchased from American Radiolabeled Chemicals (MO, USA).

2.2. Bacterial strains and plasmids

Table 2.1: List of bacterial strains and plasmids

a) Bacterial strains

Strain	Source
<i>M. smegmatis</i> ATCC19420	ATCC
BCG strains Connaught, Phipps, Brazil, Sweden and Pasteur	Kind gift by Dr. Peter Small, Stanford University, USA
<i>E. coli</i> DH5 α , BL21(DE3) and BL21(DE3) pLysS	Novagen, USA
<i>Pichia pastoris</i>	Invitrogen, USA

b) Plasmids

Plasmids	Source
pET22b (+) & pET23b (+)	Novagen, USA
pGEX-4T-1	GE Healthcare, UK
pPICZα A	Invitrogen, USA
pMS201	MSMEG_2389 (<i>hupB</i>) cloned into pET22b (+)
pMS202	MSMEG_2389 (<i>hupB</i>) cloned into pPICZα A
pMS203	MSMEG_3761 (<i>irpA</i>) cloned into pGEX-4T-1
pMS204	MSMEG_3761 (<i>irpA</i>) cloned into pET23b (+)

2.3. Media for the growth of mycobacteria**2.3.1. Lowenstein-Jenson (LJ) medium**

5.8 g LJ base, 2 mL glycerol and 1.8 mL of Tween-80 were dissolved in a final volume of 90 mL of double-distilled water and autoclaved at 121°C, 15 lbs / sq. inch pressure for 20 min. 100 mL of egg white (3 eggs) were homogenized in a sterile 500 mL conical flask with glass beads by shaking vigorously to form a uniform homogenate. Egg homogenate and 1 mL of 2% malachite green solution were added into the autoclaved LJ base medium and mixed thoroughly. The medium was filtered, and 8 mL was aliquoted into 30 mL McCartney glass bottles. The slants were subjected to inspissation at 80°C for 90 min each for three successive days.

Inoculation: 100 µL of liquid culture was dropped onto the slant, allowed to be absorbed into the LJ media and incubated at 37°C for 3-4 weeks. After colonies appeared the slants were stored at 4°C for 2-3 months.

2.3.2. Middlebrook 7H9 liquid medium

0.47 g of Middlebrook 7H9 base, 0.1 g of bactocasitone and 0.2 mL of glycerol was dissolved in 90 mL of autoclaved double-distilled water in a 250 mL conical flask and autoclaved at 121°C, 15 lbs / sq. inch pressure for 20 min and the medium was allowed to cool. 10 mL of ADC (albumin-dextrose-catalase) enrichment was then added under aseptic conditions and stirred well, then stored at 4°C.

Inoculation: A colony from LJ slant was picked, or 100 μ L from glycerol stock was inoculated in Middlebrook 7H9 liquid medium and allowed to grow at 37°C and 150 rpm in an orbital shaker.

2.3.3. Middlebrook 7H11 agar medium

2.1 g of Middlebrook 7H11 base and 0.5 mL of glycerol was added to 90 mL of autoclaved double-distilled water in a 250 mL conical flask and autoclaved at 121°C, 15 lbs / sq. inch pressure for 20 min and the medium was allowed to cool. 10 mL of OADC (oleic acid-albumin-dextrose-catalase) enrichment was then added under aseptic conditions and stirred well. Slants were made using 8 mL of medium in iron-free McCartney glass bottles and stored at 4°C.

Inoculation: The mycobacterial cultures were spread on 7H11 plates and incubated at 37°C for 3-4 weeks till the appearance of colonies. The plates were stored at 4°C after growth by sealing them with parafilm.

2.3.4. Proskauer and Beck (P & B) medium for iron-regulated growth

2.3.4.1. Preparation of iron-free glassware

All glassware was made iron-free by first soaking in 2% methanolic KOH. They were rinsed with running water and then soaked overnight in 8 N HNO₃, and the glassware washed with glass double-distilled water.

2.3.4.2. Preparation of Proskauer and Beck (P & B) medium

5 g of L-asparagine and 5 g of potassium dihydrogen orthophosphate (KH₂PO₄) were dissolved in 900 mL of glass double-distilled water. 20 mL glycerol was added, the pH adjusted to 6.8 with 10 N NaOH and the volume was made up to 1 L. 6 g alumina was added and autoclaved at 121°C, 15 lbs / sq. inch pressure for 20 min. The medium was cooled and filtered using Whatman Grade 541 filters to remove the alumina. After filtration, the medium was aliquoted as 100 mL volume in 250 mL conical flasks and re-autoclaved at 121°C, 15 lbs / sq. inch pressure for 20 min.

2.3.4.3. Preparation of salt solution

567.75 mg $\text{ZnSO}_4 \cdot \text{XH}_2\text{O}$, 137.8 mg $\text{MnSO}_4 \cdot \text{XH}_2\text{O}$ and 20.5 g $\text{MgSO}_4 \cdot 7\text{H}_2\text{O}$ were dissolved in 200 mL of glass double-distilled water in a 500 mL iron-free volumetric flask. The volume was made up to 500 mL and pipetted as 10 mL aliquots into McCartney bottles and autoclaved.

2.3.4.4. Preparation of iron solutions

Stock solution containing 1 mg Fe / mL was prepared by dissolving 497.8 mg of $\text{FeSO}_4 \cdot 7\text{H}_2\text{O}$ (Merck, NJ, USA) in 5 mL of 1 N H_2SO_4 and making up to 100 mL with glass double-distilled water in a volumetric flask.

2.3.4.4.1. Preparation of high iron solution (800 μg Fe / mL): 80 mL of the above stock solution was made up to 100 mL with 0.01 N H_2SO_4 in a 100 mL volumetric flask. This was pipetted as 10 mL aliquots in McCartney bottles and autoclaved. 1 mL of this solution added to 99 mL of culture medium gives a final concentration of 8.0 μg Fe / mL.

2.3.4.4.2. Preparation of low iron solution (2.0 μg Fe / mL): 0.25 mL of high iron solution was made up to 100 mL with 0.01 N H_2SO_4 in a 100 mL volumetric flask, aliquoted as 10 mL in McCartney bottles and autoclaved. 1 mL of this solution added to 99 mL of culture medium gives a final concentration of 0.02 μg Fe / mL.

2.4. Maintenance and growth of mycobacteria

Glycerol stocks of *Mycobacterium smegmatis* ATCC19420 and *M. bovis* BCG strains were inoculated in Middlebrook 7H9 medium supplemented with ADC. After two days of growth, the cells were transferred to a tube with glass beads, vortexed and iron-free medium was added to obtain a cell suspension equivalent to McFarland #1; this was further adjusted to obtain a cell suspension with $\text{OD}_{600 \text{ nm}}$ of 0.15. 50 μL of this suspension was inoculated into 100 mL of Proskauer and Beck medium supplemented with 1 mL of salt solution, 8 μg Fe / mL (144 μM Fe) and 0.02 μg Fe / mL (0.36 μM Fe) iron. The organisms were grown at 37°C with shaking at 150 rpm for 5 days for *M.*

smegmatis and 12 days for *M. bovis* BCG strains. The cells were harvested by centrifugation at 6000 rpm for 15 minutes.

2.5. Assay of siderophores

The siderophores carboxymycobactin & exochelin were extracted from the spent growth medium, while mycobactin was extracted from the cell pellet.

2.5.1. Carboxymycobactin and exochelin (Lane *et al.*, 1998)

To 100 mL spent medium, 1 mL of aqueous saturated FeCl_3 was added drop wise, left to stand at room temperature for 30 min. It was centrifuged at 12000 rpm for 15 min. The supernatant contained both ferri-exochelin and ferri-carboxymycobactin. The carboxymycobactin from this was extracted by adding one and a half volumes of chloroform. This extract was transferred to a separating funnel and washed thrice with double-distilled water. The chloroform extract was dried down and the siderophore was dissolved in 1 mL of ethanol and the concentration determined from its absorbance at $A_{450 \text{ nm}}$ ($A_{450 \text{ nm}}^{1\%} = 48$).

The ferri-exochelin in the aqueous solution after extraction of carboxymycobactin was determined from its absorbance at $A_{420 \text{ nm}}$ ($A_{420 \text{ nm}}^{1\%} = 15.8$).

2.5.2. Mycobactin (Ratledge & Ewing, 1996)

10 mL of absolute ethanol was added to the cell pellet; left at room temperature overnight and centrifuged at 6000 rpm for 15 min. 1 mL of ethanolic saturated FeCl_3 was added to supernatant and left for 30 min at room temperature. The ferri-mycobactin was extracted with 10 mL of chloroform, washed thrice with double-distilled water and the concentration was determined by reading at $A_{450 \text{ nm}}$ using chloroform as blank ($A_{450 \text{ nm}}^{1\%} = 43$).

2.6. Growth of *M. smegmatis* in P & B media with varying concentrations of iron

M. smegmatis was grown in 100 mL P & B medium supplemented with iron at 0.02, 0.05, 0.1, 0.5, 1.0, 2.0, 4.0, 8.0 and 12.0 $\mu\text{g Fe / mL}$ respectively and grown for 5 days as mentioned above.

2.7. Time-dependant growth of *M. smegmatis*

M. smegmatis was inoculated separately into 5 sets of flasks, with each set consisting of high (8 µg of Fe / mL) and low (0.02 µg Fe / mL) iron media respectively. They were grown with shaking as mentioned above and the organisms were harvested on days 2, 4, 6, 8 and 10 respectively.

2.8. Purification of ferri-siderophores

2.8.1. Purification of ferri-carboxymycobactin and ferri-mycobactin by high performance liquid chromatography (HPLC)

Purification of both ferri-carboxymycobactin and ferri-mycobactin was done from 500 mL culture of *M. smegmatis* grown under low iron media by HPLC using published protocols (Lane *et al.*, 1998 & Barclay *et al.*, 1985). The chloroform extracts of both the siderophores were taken in a separating funnel, washed thrice with double-distilled water to remove the excess ferric chloride. The sample was air dried, and the residue was dissolved in the minimal quantity of chloroform and filtered through Nylon membrane filter (Pall Corporation, India) to remove any insoluble material. Both the siderophores were separated by reverse phase HPLC on a C18 column at a flow rate of 1 mL / min for 50 min and observed continuously at 450 nm. The hydrophobic ferri-mycobactin was separated using a gradient of 0 to 100% with buffer A (0.09% formic acid and 90% acetonitrile) and buffer B (0.1% formic acid in 60% acetonitrile) and 40% methanol. Ferri-carboxymycobactin was separated using a gradient of 0 to 100% with buffer A (0.1% formic acid) and buffer B (0.09% formic acid in 90% acetonitrile). In each run, 20 µL of sample was injected using Hamilton syringe, and the sample was collected. Eluates with maximum $A_{450\text{ nm}}$ were collected.

Table 2.2: HPLC gradient for purification of Fe-Mb and Fe-CMb

Time (min)	Buffer A %	Buffer B%
2	100	0
32	0	100
33	0	100
35	100	0
50	100	0
51	STOP	STOP

2.8.2. Purification of ferri-exochelin

The aqueous clear supernatant, after extraction of the ferri-carboxymycobactin was passed through Sephadex G-50, and the orange color band of exochelin was collected and concentration was determined by measuring the absorbance at 420 nm.

2.9. Preparation of cell wall and cell membrane proteins by differential centrifugation

Reagents

1. Tris-HCl Buffer: 0.05 M Tris-HCl pH 7.8
2. Solubilization buffer (10 mL): 2.5 mL of stacking gel buffer pH 6.8, 6% SDS (0.6 g) and 7.5 mL of double-distilled water

Protocol: This was done as per published protocol (Yeruva *et al.*, 2006). Mycobacteria grown in high and low iron media were harvested at 6,000 rpm for 15 min, washed cell pellet twice with 0.05 M Tris-HCl pH 7.8 and resuspended in 6 mL of 0.05 M Tris-HCl pH 7.8. The cell pellet was sonicated for 20 min (30 s pulse with 30 s interval at amplitude of 40 Hz at 4°C in Vibra Cell sonicator). The sonicate was centrifuged at 6,000 rpm at 4°C for 15 min to remove cell debris and the supernatant was centrifuged at 18,000 rpm for 40 min at 4°C to pellet the cell wall. The supernatant was subjected to ultracentrifugation at 45,000 rpm for 2 h 30 min to pellet the cell membrane. Both the cell wall and cell membrane pellets were washed twice with 0.05 M Tris-HCl pH 7.8 and solubilized in 50 µL solubilization buffer by incubating at 37°C overnight. The solubilized sample was centrifuged at 13,500 rpm for 15 min. Protein estimation was done by Bicinchoninic acid (BCA) method (Protein assay kit, Sigma-Aldrich, USA).

2.10. Separation of proteins by sodium dodecyl sulfate-polyacrylamide gel electrophoresis (SDS-PAGE) (Laemmli, 1970)

Reagents

- a) Acrylamide and N, N'-bisacrylamide mix (30:0.8): 30 g of Acrylamide and 0.8 g of bisacrylamide were dissolved in 60 mL of double-distilled water and made up to 100 mL
- b) Resolving gel buffer: Tris-HCl (1.5 M, pH 8.8) with 0.4% SDS; 36.3 g of Tris base and 0.8 g of SDS were dissolved in 150 mL of double-distilled water and made up to 200 mL. The pH was adjusted to 8.8 with HCl
- c) Stacking gel buffer: Tris-HCl (0.5 M, pH 6.8) with 0.4% SDS; 12.0 g of Tris base and 0.8 g of SDS were dissolved in 150 mL of double-distilled water and made up to 200 mL. The pH was adjusted to 6.8 with HCl
- d) Ammonium persulfate (APS) 10%: 0.1 g of APS was dissolved in 1 mL of double-distilled water
- e) Tetramethyl ethylene diamine (TEMED): this was used as obtained commercially
- f) Sample buffer (2X): 0.125 M Tris-HCl (pH 6.8) containing 4% SDS, 20% glycerol and 0.002% bromophenol blue.
- g) Running buffer: 24.75 g of Tris base and 108 g of glycine was dissolved in 900 mL of double-distilled water. 7.5 g of SDS was dissolved in this solution, made up to 1 L and stored at 4°C
- h) Coomassie blue stain: 0.25 g of Coomassie Brilliant Blue was dissolved in 30 mL of methanol and made up to 100 mL with methanol: glacial acetic acid: water (5:2:5)
- i) De-staining solution: This was prepared by mixing methanol, glacial acetic acid, water in the ratio of 1:1:8.

Preparation of 5-20% gel: 5-20% resolving gel was prepared using the recipe given in Table 2.3 and allowed to polymerize for 40 min. 10 mL of the stacking gel, prepared as shown in Table 2.4 was poured over it after positioning the comb. 50 µg of total protein was mixed with 2X sample buffer (1:1 v / v), boiled for 10 min, centrifuged at 13,000 rpm for 10 min to remove any insoluble material and the clear supernatant was loaded onto the gel (Hoefer electrophoresis unit, Amersham Pharmacia Biotech AB, CA, USA). Electrophoresis was

carried out initially at 90 V till the bromophenol blue dye entered the resolving gel and then at 200-250 V maintaining a constant current of 25 mA. When the tracking dye migrated off the gel, an additional run for 30 min done for optimal resolution. The gel was stained with Coomassie Blue for 1-3 h and then de-stained overnight.

Preparation of 10% gel: 10% resolving gel was prepared as per recipe in Table. 2.3, with the remaining procedures performed as described above. 30 µg total proteins was loaded and electrophoresis was carried out initially at a voltage of 70 V and then at 100 V. Gel was run till the dye migrated off the gel.

Table 2.3: Preparation of resolving gel

Ingredients	Volume (mL)		
	Gradient gel		Mini gel
	5%	20%	10%
Acrylamide: Bisacrylamide mix	2.75	10.6	10.6
Resolving gel buffer	4.0	4.0	8.0
Double-distilled water	9.3	1.4	13.4
Ammonium persulfate	0.08	0.08	0.16
TEMED	0.008	0.008	0.008

Table 2.4: Preparation of stacking gel

Reagent	Volume (mL)
Acrylamide: Bisacrylamide mix	1.5
Stacking gel buffer	2.5
Double-distilled water	6.0
Ammonium persulfate	0.030
TEMED	0.010

2.11. Western blot analysis

Reagents

- a) 10X Transblot buffer (250 mM Tris and 1.3M glycine): Dissolved 15.17 g of Tris base and 48.8 g of glycine in 400 mL of double-distilled water. Working solution was prepared by mixing 200 mL of 10X stock solution, 400 mL of methanol and 1.4 L of double-distilled water.
- b) Tris-buffered saline (TBS, pH 7.4) (50 mM Tris and 150 mM NaCl): Dissolved 6.05 g of Tris base and 8.7 g of NaCl in 800 mL of double-distilled water and made up to 1 L. The pH was adjusted to 7.4 with HCl.
- c) TBST: TBS containing 0.05% Tween 20
- d) Ponceau S stain: Ponceau S, trichloroacetic acid, and sulfosalicylic acid were mixed in 2:30:30 (w / v) ratio and the final volume was made up to 100 mL with double-distilled water. Working solution was prepared by 1:10 dilution

2.11.1. Electrophoretic protein transfer (Towbin *et al.*, 1979)

Proteins separated on polyacrylamide gels were electrophoretically transferred to a nitrocellulose membrane at 30 V constant voltage overnight or 60 V for 2½ h using a 1X transblot buffer in Broviga transfer apparatus (Balaji Scientific Services, Chennai, India).

2.11.2. Development of immunoblot

The membrane was first stained with Ponceau S stain to visualize the transferred proteins and the position of the protein molecular weight marker bands were marked with a pencil. The membrane was blocked for 2 h using 5% non-fat milk solution (NFM) dissolved in TBS/T. The membrane was washed thrice with TBS/T and incubated overnight with appropriate dilutions of primary antibodies (1:2500 dilutions for anti-HupB antibodies and 1:500 for anti-IrpA antibodies). The membrane was washed 4 times with TBS/T and incubated with appropriate enzyme-conjugated secondary antibody at room temperature for 1½ h. Then, the blot was washed thoroughly with TBS/T. A ready-to-use 5-bromo-4-chloro-3-indolyl phosphate and nitroblue tetrazolium solution (BCIP-NBT; Sigma) was used as the substrate for alkaline phosphatase (ALP)-conjugated secondary antibodies and DAB (diaminobenzidine)-H₂O₂ (10

mg DAB in 15 mL TBS with 0.08% H₂O₂) was used as substrate for peroxidase-conjugated secondary antibodies.

2.12. Preparative gel electrophoresis for the purification of iron-regulated envelope proteins

Reagents

Gel elution buffer: 25 mM Tris-HCl (pH 8.8) buffer containing 5% glycerol, 1% SDS and 0.24 mM glycine

Protocol: Cell wall proteins were prepared from *M. smegmatis* grown under high and low iron media. Protein bands up-regulated in low iron cell wall preparations were cut out, crushed after adding 3 mL of gel elution buffer, kept overnight at 37°C with shaking and centrifuged at 4,000 rpm for 10 min. The clear supernatant was transferred to a new tube and 2 mL of gel elution buffer was added to the pellet to extract any protein in the gel pieces. This was repeated three times till the gel slices became colorless. To the pooled eluates added five volumes of chilled acetone and kept at -20°C overnight. It was centrifuged at 6,000 rpm for 20 min and the protein pellet, after washing with fresh acetone was dried and solubilized in 0.5 mL of 10 mM Tris-HCl pH 7.8 with 0.6% SDS. It was centrifuged at 12,000 rpm for 5 min to remove any insoluble material and the soluble protein was subjected to protein estimation by BCA method and stored at -80°C.

2.13. Characterisation of iron-regulated envelope proteins by MALDI-TOF-MS / MS analysis

5 µg of the purified protein(s) were subjected to MALDI-TOF-MS analysis at Sandor Lifesciences Pvt. Ltd. Hyderabad. Using the peptide sequences obtained by MALDI-TOF-MS, the protein was identified by subjecting the peptide sequences to BLAST analysis (<https://blast.ncbi.nlm.nih.gov/Blast.cgi>).

2.14. Development of antibodies against HupB and IrpA from *M. smegmatis*

Purified HupB and the 21 kDa iron-regulated protein (IrpA) were re-run on 10% gel and the gel slice containing 200 µg was crushed using a syringe and emulsified in Freund's

incomplete adjuvant (Sigma-Aldrich, USA). The emulsions were injected subcutaneously at multiple sites on the ventral side of the abdominal region in two New Zealand white rabbits. Before immunization, 10 mL blood was drawn from the respective rabbits to separate serum that was used as pre-immune serum. After three weeks, the first booster containing 100 µg of the respective antigen in incomplete Freund's adjuvant was administered intramuscularly. After 2 days, test bleed was done and the antibody titre was determined. Subsequently, additional boosters were given and high titre antibody-containing serum was collected. All the protocols were approved by Institutional Animal Ethics Committee.

2.15. Molecular techniques

2.15.1. *E. coli* strains and vectors

pET22b (+), pET23b (+) plasmids (Novagen, Madison, USA), pGEX-4T-1 (GE Healthcare, UK) and pPICZα A (Invitrogen CA, USA) were used for cloning. *E. coli* DH5α was used for high-efficiency transformation and *E. coli* BL21 (DE3), *E. coli* BL21 (DE3) pLysS and *Pichia pastoris* were used as expression hosts.

2.15.2. Preparation of Luria-Bertani (LB) medium

10 g of tryptone, 5 g of yeast extract and 10 g of NaCl were dissolved in double-distilled water, pH adjusted to 7.0 with 1N NaOH and made up to 1 L using double-distilled water. The media was sterilized by autoclaving at 121°C at 15 lbs / sq. inch pressure for 20 min. For the preparation of solid medium, added 15 gm of agar (1.5% agar) to 1 L liquid medium. If antibiotic containing plates are required, the media was allowed to cool to 50°C, the respective antibiotic added and poured into sterile 90 mm Petri plates, allowed to solidify and stored at 4°C for future use.

2.15.3. Isolation of genomic DNA from *M. smegmatis*

Reagents

- a) Tris-HCl (1M): 121.1 g of Tris base was dissolved in 800 mL of double-distilled water, followed by addition of 42 mL of concentrated HCl. The pH was adjusted to 8.0 with HCl and made up to 1L with double-distilled water and autoclaved.

- b) 0.5 M EDTA (Ethylenediaminetetraacetic acid): 186.1 g of disodium EDTA.2H₂O was dissolved in 800 mL of double-distilled water, dissolved with stirring on a magnetic stirrer by addition of sodium hydroxide pellets till the pH was 8.0 (~20 g of NaOH pellets). The volume was made up to 1 L with double-distilled water and autoclaved.
- c) TE buffer, pH 8.0 (10 mM Tris-HCl and 1 mM EDTA): 1 mL of 1 M Tris-HCl buffer and 0.2 mL of 0.5 M EDTA were mixed and made up to 100 mL with double-distilled water.
- d) Lysozyme (Bangalore Genei, India): 10 mg of lysozyme was dissolved in 1 mL of double-distilled water and stored at -20°C
- e) Proteinase K (Bangalore Genei, India) (10 mg / mL): 10 mg of Proteinase K was dissolved in 1 mL of double-distilled water and stored at -20°C
- f) 10% SDS: 10 g of SDS was dissolved in 100 mL of double-distilled water
- g) 5M NaCl: 29.2 g of NaCl was dissolved in 100 mL of double-distilled water
- h) Cetyltrimethylammonium bromide (CTAB) / NaCl (10% CTAB in 0.73 M NaCl): 4.1 g of NaCl was dissolved in 80 mL of double-distilled water. Added 10 g CTAB and dissolved by heating to 65°C. Volume adjusted to 100 mL with double-distilled water
- i) Chloroform / Isoamyl alcohol (24:1): 24 volumes of chloroform with 1 volume of isoamyl alcohol were mixed and stored at room temperature

Protocol: Genomic DNA from *M. smegmatis* was isolated as per published protocol (van Soolingen *et al.*, 1994). Two loopful of mycobacterial cells were washed thrice with TE buffer and resuspended in 600 µL of the same buffer. The cells were treated with 50 µL of lysozyme (10 mg / mL) for 1 h at 37°C, followed by incubation at 50°C after the addition of 70 µL of 10% SDS and 60 µL of Proteinase K (10 mg / mL). 100 µL of 5 M NaCl and CTAB / NaCl was added and mixed till the liquid turned into milky white color, followed by incubation at 65°C for 10 min. All contents were transferred into Phase lock gel tube (Eppendorf, Germany) and 750 µL of chloroform: isoamyl alcohol mixture (24:1 v / v) was added, centrifuged at 13,000 rpm for 5 min and the upper aqueous layer was transferred to a fresh tube. The genomic DNA was precipitated by the addition of an equal volume of isopropanol, allowed to stand for 30 min at room temperature, followed by centrifugation at 12,000 rpm for 15 min. The DNA pellet was washed with 1 mL of 70% ethanol, dried and resuspended in DNase-free water. The concentration of the genomic DNA was determined using the Nano Drop spectrophotometer (Nano Drop Technologies, Inc, USA) and stored at -20°C till use.

2.15.4. Agarose gel electrophoresis

Reagents

- a) Tris-acetate-EDTA (TAE) buffer: 4.84 g Tris base, 1.14 mL glacial acetic acid and 20 mL 0.5 M EDTA was dissolved in a final volume of 1 L of double-distilled water. The pH was adjusted to 8.0
- b) Ethidium bromide (SRL, India): 1 mg of ethidium bromide dissolved in 1 mL of double-distilled water
- c) 1 kb DNA ladder (MBI Fermentas, USA)
- d) 6X loading dye (MBI Fermentas, USA): 10 mM Tris-HCl (pH 7.6) 0.03% bromophenol blue, 0.03% xylene cyanol FF, 60% glycerol 60 mM EDTA

Protocol: Genomic DNA and PCR amplified products were subjected to electrophoretic separation using 0.8% and 1% agarose gels respectively. 0.5 g agarose was added to 50 mL of TAE buffer for 1% gel, dissolved by heating and after addition of ethidium bromide (0.1 µg / mL) poured on the trough and allowed to set. The DNA samples were prepared by adding 6X loading dye and loaded onto the gel. The molecular weight DNA marker loaded onto gel included 1 µL of 1 kb ladder. Electrophoresis was carried out in a horizontal agarose gel unit (Balaji Scientific Services, Chennai, India) at 100 V and the DNA fragments were visualized in a UV transilluminator (UVP GelDoc, Cambridge, UK).

2.15.5 Cloning procedures

All the cloning techniques were essentially followed as per standard protocols (Sambrook *et al.*, 1989). The full length 627 bp *hupB* gene (MSMEG_2389) from *M. smegmatis* was cloned into pET22b (+) and since the protein could not be expressed in *E. coli* as host, it was attempted to express it in yeast using the vector pPICZα A. The 567 bp gene (MSMEG_3761) encoding IrpA was cloned into pET23b (+) and expressed in *E. coli*; in addition, efforts were made to express the protein in a soluble form by cloning it into pGEX-4T-1 vector. Routinely used procedures were used for cloning these two genes, as detailed below.

2.15.5.1. PCR amplification

The respective primers for the amplification of these two genes is listed in Table 2.5. The reaction mix, containing 100 ng of *M. smegmatis* genomic DNA, 200 μ M dNTP mix, 10 pmoles of the respective set of primers and 0.5 U Taq DNA polymerase (Fermentas, Thermo Scientific, Pittsburgh PA, USA) in a total volume of 20 μ L of the commercially supplied enzyme-compatible buffer, was subjected to PCR in Master cycler (Eppendorf, CA, USA) using the following program: initial denaturation for 5 min at 95°C, 30 cycles of amplification for 4 min at 68°C (annealing and extension) and denaturation for 1 min at 95°C, followed by a final extension for 10 min at 72°C. A negative control without template DNA was included. The PCR products were subjected to agarose gel electrophoresis using 1% gel. Both the amplicons were purified by PCR purification kit (Invitrogen, USA) as per manufacturer's instructions.

Table 2.5: List of primers specific for *hupB* and MSMEG_3761

Gene	Vector & Host	Sequence (5' to 3')
<i>hupB</i>	pET22b (+)	For (<i>Bam</i> HI): ACGTGGATCCTATGAACAAAGCGGAGCTCA
		Rev (<i>Hind</i> III): ACGTAAGCTTCCTGCGGCCCTTCTTGCCG
	pPICZ α A	For (<i>Eco</i> RI): GCATGAATTCAACAAAGCGGAGCTCA
		Rev (<i>Xba</i> I): ATGCTTCTAGAATCCTGCGGCCCTTCTTG
<i>irpA</i>	pGEX-4T-1	For (<i>Eco</i> RI):AGCAGAATTCCAGAAGTACAACCG
		Rev (<i>Not</i> I): ATCGCGGCCGCGTCCGGTGGGAAGAC
	pET23b (+)	For (<i>Nde</i> I):ATGCATCATATGATGTTTCGAGCGGTTTCAGCCGGCATG
		Rev (<i>Hind</i> III): CATATGCAAGCTTGGCGGCCGACTCCAGCAGGC CGATAATGT

2.15.5.2. Restriction digestion

1 μ g of the respective vector DNA and the purified amplicons of the two genes were individually subjected to double digestion at 37°C overnight with 10 units of the respective restriction enzymes. After heat inactivation at 65°C for 10 min, the amplicons were purified using clean-up kit (Invitrogen, USA) as per manufacturer's instructions.

2.15.5.3. Ligation

Ligation was done using vector and insert DNA in the molar ratio of 1:3 (100 ng of vector DNA and 300 ng of insert DNA) in 20 μ L of ligation mixture containing 1 μ L of T4 DNA ligase (5 U / μ L), 2 μ L of 10X ligation buffer and Milli - Q water. The ligation mixture was incubated at 4°C overnight.

2.15.5.4. Transformation into *E.coli* DH5 α

2.15.5.4.1. Preparation of ultra-competent cells

Ultracompetent cells were prepared as per standard procedure (Inoue *et al.*, 1990). 1% overnight *E. coli* DH5 α was inoculated into 100 mL of LB broth in 500 mL flask and allowed to grow at 18°C till cell density reached OD_{600 nm} of 0.4-0.5. It was kept on ice for 10 min and harvested by centrifuging at 6,000 rpm for 10 min at 4°C. The cell pellet was suspended in 80 mL of ice-cold Inoue transformation buffer (55 mM MnCl₂.4H₂O, 15 mM CaCl₂.2H₂O, 250 mM KCl, 10 mM PIPES pH 6.7) and centrifuged at 3,000 rpm for 10 min at 4°C. The pellet was then re-suspended in 20 mL of ice cold Inoue buffer and incubated on ice for 10 min after adding 1.5 mL of DMSO. The cells were quickly dispensed into sterile micro centrifuge tubes as 100 μ L aliquots and then frozen in liquid nitrogen. The tubes were stored at -80°C until further use.

2.15.5.4.2. Transformation

10 μ L of the respective ligation mixture was added to 100 μ L of ultra competent *E. coli* DH5 α cells and incubated on ice for 30 min. After 30 min, the cells were subjected to heat shock at 42°C for 90 s and immediately chilled on ice for 2 min. 900 μ L of LB broth was added and incubated at 37°C for 45 min. The cells were plated on LB agar-ampicillin plates and incubated at 37°C overnight.

2.15.6. Isolation of plasmid DNA by alkaline lysis SDS: Miniprep method (Birnboim & Doly, 1979)

Reagents

- a) Solution I: 50 mM glucose in 25 mM Tris-HCl (pH 8.0) containing 10 mM EDTA.
- b) Solution II: freshly prepared 0.2 N NaOH solution containing 1.5% SDS.

- c) Solution III: Prepared by mixing 5 M potassium acetate (pH 5.2), glacial acetic acid and double-distilled water in the ratio of 60:11.5:28.5 (v / v).

Protocol: A single colony was inoculated into 5 mL of LB medium with 100 µg / mL of ampicillin and incubated at 37°C overnight. 1.5 mL of the culture was centrifuged at 6,000 rpm for 5 min at 4°C. The pellet was re-suspended in 100 µL of Solution I by vortexing and incubated on ice for 5 min. 200 µL of freshly prepared Solution II was added, and the contents were mixed well and incubated on ice for 5 min. The solution was neutralized by adding 150 µL of ice-cold Solution III, mixed by inversion for five times and incubated on ice for 5 min. The mixture was centrifuged at 13,000 rpm for 10 min at 4°C, and the supernatant was carefully transferred to a fresh tube. DNase-free RNase was added to a final concentration of 10 µg / mL and incubated at 37°C for 30 min. The plasmid DNA was extracted into the aqueous phase by the addition of equal volume of phenol-chloroform (1:1 v / v) followed by centrifugation at 12,000 rpm for 10 min. The plasmid DNA was precipitated with 2 volumes of isopropanol at room temperature for 10 min and centrifuged at 12,000 rpm for 15 min. The pellet was washed with 70% ethanol, dried and dissolved in 20 µL of autoclaved Milli-Q water and stored at -20°C.

2.15.7. Expression of recombinant proteins

2.15.7.1: Recombinant HupB

The recombinant pET22b, carrying the *hupB* gene was transformed into the expression host *E. coli* BL21 (DE3) as per the procedures mentioned above. A single colony was taken, inoculated into LB medium containing 100 µg / mL ampicillin at 37°C, incubated with shaking for 3-4 hours till it reached mid-log phase ($OD_{600\text{ nm}}$ of 0.5-0.6). 1 mM IPTG was added and incubated for 3h. An identical control culture, allowed to grow without addition of IPTG was used as control. Both uninduced and induced cells were harvested by centrifugation at 6000 rpm for 15 min at 4°C. The cells were subjected to sonication for 5 min (20 sec pulse with 20 s interval for total 5 min in Vibra Cell sonicator, USA), centrifuged at 13,000 rpm for 20 min in Eppendorf mini centrifuge and both the pellet and supernatant were analyzed by SDS-PAGE.

The above procedure was repeated using varying concentrations of IPTG (0.1 - 1.0 mM) and incubating at 18°C / 37°C.

The recombinant yeast vector pPICZα A with *hupB* cloned into it was transformed into the yeast expression host *Pichia pastoris* (Invitrogen, USA). It was first grown in the

commercially available medium BMGY (Buffered complex medium containing glycerol; Invitrogen, USA) for 16 h and then transferred to BMMY (Buffered complex medium containing methanol; Invitrogen, USA) for 48 h. The culture was grown at 30°C with shaking in an orbital shaker at 180 rpm and 1% (v / v) methanol was added for every 24 h to induce the expression of the recombinant protein.

2.14.7.2: Recombinant IrpA

The above procedure was done for the recombinant plasmid bearing the gene encoding IrpA and expression in *E. coli* as a host was done. The rIrpA was obtained as insoluble protein. In order to obtain it as a soluble protein, it was expressed as a GST-fusion protein and purified by affinity chromatography on Glutathione Superflow resin (Qiagen, Germany)

Reagents

- a) Equilibration buffer: 0.1 M PBS pH 7.3 (140 mM NaCl, 2.7 mM KCl, 10 mM Na₂HPO₄ and 1.8 mM KH₂PO₄)
- b) Elution buffer: 50 mM Tris-HCl pH 8.0 and 10 mM reduced glutathione (Sigma, USA)

Protocol: Glutathione Superflow resin was washed two times with two-bed volumes of double-distilled water, followed by two-bed volumes of equilibration buffer. Cell-free whole-cell sonicates (3 mL) was loaded onto the column and incubated for 30 min at room temperature. The column was washed with three-bed volumes of equilibration buffer. The bound protein was then eluted with elution buffer. The eluates were collected as 1 mL fractions, analyzed by SDS-PAGE and immunoblot analysis was performed with anti-GST and anti-IrpA antibodies.

The purified GST-fusion protein was subjected to cleavage with thrombin as per published protocol (Walls & Loughran, 2011). 1:1000 (units of enzyme per µg of fusion protein) ratio was incubated at 4°C 2 h. SDS sample buffer was immediately added to the digested fusion protein and analyzed by SDS-PAGE. Re-chromatography was performed to separate individual protein of interest and glutathione S-transferase.

2.16. Radioactive iron uptake studies: uptake of ^{55}Fe -exochelin and ^{55}Fe carboxymycobactin by *M. smegmatis*

Reagents

1. $^{55}\text{FeCl}_3$ (Specific activity 44.66 mCi / mg, 2mCi / 74MBq; American Radiolabelled Chemicals, Inc. MO, USA)
2. 50 mM EDTA: Added 1.86 g of disodium EDTA.2H₂O to 80 mL of double-distilled water, adjusted pH to 4 with glacial acetic acid and volume made up to 100 mL
3. 0.1 M Lithium acetate: Dissolved 0.65 g of Lithium acetate in 100 mL double-distilled water
4. 100% Ethanol
5. Cocktail 'O' Scintillation fluid: Ready-to-use scintillation fluid contains 6 g PPO and 0.2 g POPOP dissolved in 1 L toluene (Sisco Research Laboratories, India)

2.16.1. Preparation of ^{55}Fe -labelled siderophores

To the purified ferri-carboxymycobactin dissolved in acetonitrile, an equal volume of 50 mM EDTA, pH 4.0 was added and incubated for 18 h at room temperature (Ryndak *et al.*, 2010). The desferri-carboxymycobactin thus obtained, was extracted into chloroform, dried and the residue was re-suspended in 50% ethanol, prepared with iron-free water. Titration of an aliquot of the purified desferri-siderophore was done to determine the amount of ^{55}Fe required to completely saturate it. This was done by titrating with 0.5 M FeCl_3 by adding aliquots of the ferric chloride solution to the siderophore and determining the absorbance at 450 nm. When the OD values reached a constant value, the amount the ferric chloride needed to reach the maximal absorbance was noted and used to determine the amount of the radiolabeled iron to be added. Appropriate amount of $^{55}\text{FeCl}_3$ was added, incubated for 10 min at room temperature and the ^{55}Fe -CMb was extracted into chloroform, washed twice with iron-free water to remove excess ^{55}Fe . The chloroform extract was dried, solubilized in minimal volume of 50% ethanol and stored as aliquots at -20°C .

^{55}Fe -exochelin was prepared by obtaining the desferri form using 8-hydroxyquinoline as per published protocols (Macham *et al.*, 1977). Ferri-exochelin in water was mixed vigorously with 8-hydroxyquinoline in methanol and allowed to stand at

22°C for 2h for the complete formation of green ferri-8-hydroxyquinoline. Chloroform was added to remove the ferri-8-hydroxyquinoline. This was done thrice to remove residual ferri-8-hydroxyquinoline. The aqueous desferri-exochelin was titrated as done for carboxymycobactin and the appropriate amount of $^{55}\text{FeCl}_3$ was added and allowed for stand at 22°C for 2 h. Excess of $^{55}\text{FeCl}_3$ was removed from ^{55}Fe -exochelin by passing through Sephadex G-10 column.

2.16.2. Uptake studies with *M. smegmatis*

M. smegmatis was grown in high (8.0 µg Fe / mL) and low (0.02 µg Fe / mL) iron media for 3 days. The cultures were harvested, washed twice with iron-free P & B media, re-suspended to get a cell suspension of 3×10^8 cells / mL. The experiment was performed using the following reaction set-up:

- a) Cell suspension (3×10^8 cells / mL) of *M. smegmatis* grown in high and low iron media
- b) Cell suspension (3×10^8 cells / mL) of *M. smegmatis* grown in high and low iron media pre-incubated with i) Anti-HupB antibodies (1:100 dilution), ii) Anti-IrpA antibodies (1:100 dilution) and iii) Pre-immune serum (1:100 dilution). The respective cells were incubated for 1 h 30 min with shaking and the unbound antibodies were removed by washing.

The above reaction set-up was established a) separately for uptake of ^{55}Fe -exochelin and ^{55}Fe -carboxymycobactin in duplicates and b) extraction of mycobactin and determination of the label in the mycobactin. The procedures for both the uptake studies were similar. 1×10^5 cpm of ^{55}Fe -exochelin / ^{55}Fe -carboxymycobactin was added to each reaction mixture and incubated at 37°C for 2 h with gentle shaking at 150 rpm. The cells were harvested, washed with 0.1 M Lithium acetate once and twice with cold iron-free P & B medium. After removing all liquid from the cells, the latter was transferred into 5 mL of the scintillation cocktail and the radioactivity determined in the liquid scintillation counter (TriCarb 2910 TR, Packard).

Mycobactin from the cells was extracted with 100% ethanol overnight, dried, dissolved in 20 µL chloroform, added to scintillation fluid and the radioactivity counted as above.

2.16.3. Uptake studies with liposome-incorporated cell wall proteins

Liposomes were prepared with cell wall proteins isolated from iron-limited and iron replete *M. smegmatis* and uptake of ^{55}Fe -exochelin was done essentially as per reported protocol (Dover & Ratledge, 1996)

2.16.3.1. Preparation of liposomes

Reagents

1. 1 M CHAPS {3-[(3-Cholamidopropyl) dimethylammonio]-1-propanesulfonate}:
Dissolved 6.15 g CHAPS in 10 mL double-distilled water
2. 50 mM KH_2PO_4 / NaOH, pH 7.1: Dissolved 6.8 g KH_2PO_4 in 800 mL double-distilled water, adjusted pH to 7.1 with 10 N NaOH and volume made up to 1L
3. Solubilising buffer: 8 mM CHAPS in 50 mM KH_2PO_4 , pH 7.1

Protocol: The cell wall from iron-limited and iron replete *M. smegmatis* was prepared by differential centrifugation as described above. CHAPS-based solubilising buffer was added to the cell wall pellet and incubated with shaking at 4°C overnight. It was centrifuged at 18,000 rpm for 30 min at 4°C and the supernatant containing the CHAPS-solubilised envelope proteins was transferred into another tube. The CHAPS-solubilised envelope proteins were dialyzed against 50 mM KH_2PO_4 pH 7.1 overnight at 4°C to remove the detergent.

In order to study if the iron from the ferri-exochelin was transferred to mycobactin, test liposomes were prepared by including desferri-mycobactin. Iron was removed from the mycobactin by gently shaking the chloroform suspension with 1 mL of methanol and 1 mL of 6 M HCl. The wine red colour of the ferri-mycobactin was replaced with the colourless desferri-mycobactin in the chloroform layer. Suitable aliquots were transferred to tubes and dried before using them for preparing liposomes.

Liposomes were prepared using a total amount of 300 µg of Phosphatidylcholine and cholesterol (Sigma, USA) taken in the molar ratio of 1:1. They were taken along with 100 nM desferri-Mb, dissolved in chloroform and dried as a thin film in an inert atmosphere using nitrogen gas were dried onto the walls of a test-tube. The following liposomes were prepared based as described (Dover & Ratledge, 1996)

1. Empty liposomes - these served as controls and were prepared by adding 1 mL of phosphate buffer to the dried lipid film and shaking vigorously for 30 s to get the milky suspension.
2. Cell wall proteins incorporated liposomes: 100 µg of the CHAPS-solubilized cell wall proteins prepared from iron-limited and iron replete organisms was added to the dried lipid film.

2.16.3.2. Uptake of ⁵⁵Fe-exochelin by liposomes

To liposome sets 1 and 2 prepared as above, 1×10^5 cpm of ⁵⁵Fe-exochelin was added and incubated for 30 min at 37°C. The reaction mixtures were filtered through 0.22 µ pore size GVWP filters (Millipore Corporation, MA, USA), washed twice with 2 mL of buffer to remove free ⁵⁵Fe-exochelin. The filters, with the liposomes were dried and the associated radioactivity was measured by transferring it into 5 mL scintillation fluid and reading the radioactivity as mentioned above.

In order to establish if IrpA, present in the cell wall proteins of iron-limited organisms played a role in the uptake of ⁵⁵Fe-exochelin, anti-IrpA antibodies were added to the set 2 liposomes and incubated for 2 hours before the addition of ⁵⁵Fe-exochelin; serum control included incubation of an identical set of liposomes with the pre-immune rabbit serum.

2.17. Modeling of IrpA and docking of ferri-exochelin

2.17.1. Homology modeling of IrpA

Using Smegmalist online database, IrpA (locus tag - MSMEG_3761) was identified as a protein of 188 amino acid residues. From the Protein Data Bank (PDB), this protein was observed to share 34% identity and 97% query coverage with the N-terminal domain of *M. tuberculosis* Clpc1 protein (PDB ID: 3WDB) that was therefore used as a suitable template for predicting the folding of IrpA. Using Modeller 9.17v (Eswar *et al.*, 2006), homology modelling was done to predict the folding of IrpA. The generated 3D structure of the protein was validated through PROCHECK tool (Laskowski *et al.*, 1993) and the loops were further optimized by using ModLoop server (Fiser & Sali, 2003). Optimized model was energy-minimized on molecular dynamic simulations (MSD) software

Gromacs 5.0v (Abraham *et al.*, 2015), and the model was validated on PROCHECK to access the stereochemical quality of the model, reliability and its agreement with template coordinates.

2.17.2. Molecular docking of ferri-exochelin on IrpA

The three-dimensional structure of ferri-exochelin MS was developed by using the ChemDraw 3D ultra (version 10.0) (Mendelsohn, 2004) software. Energy minimized protein structure of IrpA was subjected for docking with ferri-exochelin MS using Autodock-Vina V-1.5.6 (Trott & Olson, 2010). The docked model with least binding energy was selected to study the binding patterns between IrpA and ferri-exochelin MS. PyMOL software was used to visualize and analyze the interaction.

2.18. Identification of IrpA-interacting proteins by immunoprecipitation with anti-IrpA antibodies

With the objective of identifying proteins interacting with IrpA, published protocol (Huang & He, 2010) was followed.

Reagents

- a) Protein A agarose beads (Santa Cruz Biotechnology, Texas, USA)
- b) 0.1 M PBS pH 7.3 (140 mM NaCl, 2.7 mM KCl, 10 mM Na₂HPO₄ and 1.8 mM KH₂PO₄)
- c) Solubilising buffer: 8 mM CHAPS in 50 mM KH₂PO₄, pH 7.1

Protocol: 60 µL of anti-IrpA antibodies was added to 20 µL of Protein A beads, incubated at 4°C for 3 hours and the beads were washed three times with PBST (Tween 80) to remove unbound antibodies. Then added 50 µg of CHAPS-solubilized low iron cell wall proteins and incubated overnight at 4°C. After washing with PBST to remove unbound proteins, the beads were re-suspended in 25 µL of buffer, added an equal volume of 2X SDS sample buffer, boiled and loaded onto a 5-20% gradient gel of polyacrylamide and subjected to SDS-PAGE. The proteins were transferred onto nitrocellulose membranes and probed with anti-HupB and anti-IrpA antibodies.

CHAPTER 3
RESULTS

3.1. Constitutive expression of the HupB homologue (MSMEG_2389) in *M. smegmatis*

3.1.1. Elevated levels of mycobactin and exochelin by iron-limited *M. smegmatis*

M. smegmatis, grown in low iron (0.02 $\mu\text{g Fe / mL}$) Proskauer and Beck growth medium showed a marked increase in the amount of the intracellular mycobactin; there was a 74-fold increase when compared with organisms grown in high (8.0 $\mu\text{g Fe / mL}$) iron medium (Fig. 3.1a). Exochelin, the major extracellular siderophore was found to be 5-fold higher (Fig. 3.1b) than carboxymycobactin, reported as an additional extracellular siderophore several years after the establishment of exochelin as the major siderophore secreted into the spent growth medium (Ratledge & Ewing, 1996). Each of these siderophores were expressed in greater amounts upon iron limitation relative to iron sufficient conditions.

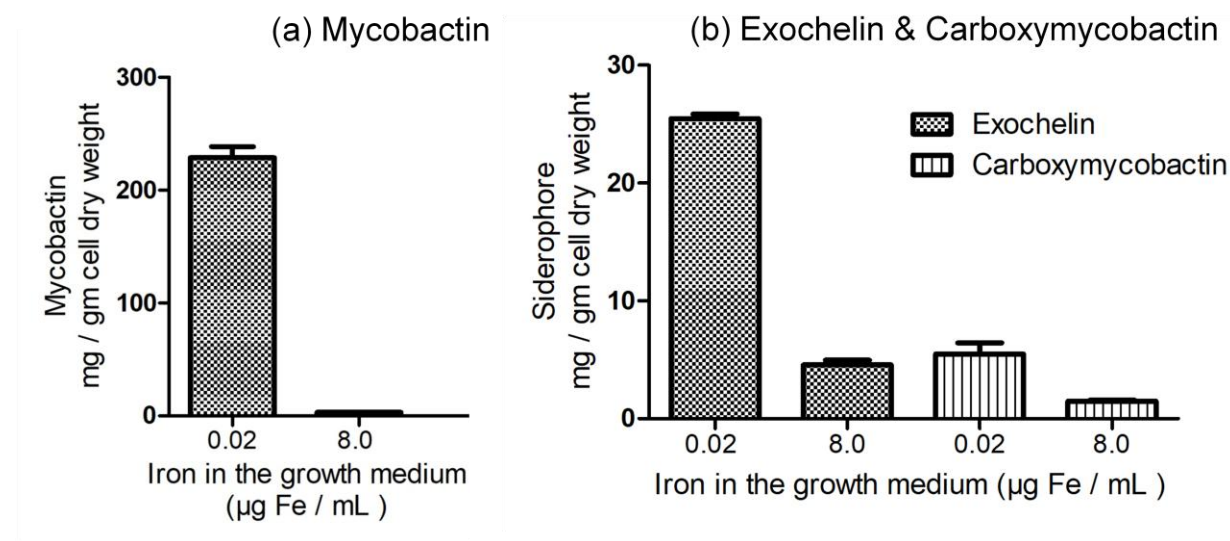


Fig. 3.1. Iron levels and siderophore expression in *M. smegmatis*: Panel (a) shows high production of mycobactin by *M. smegmatis* when grown in low iron (0.02 $\mu\text{g Fe / mL}$) medium. Panel (b) shows the relative amounts of the two extracellular siderophores exochelin and carboxymycobactin, the latter being produced at much lower levels than exochelin. The error bars represent the standard deviation of the mean from four independent experiments.

3.1.2. Constitutive expression of the HupB homologue in *M. smegmatis*: presence of the protein in organisms grown in high and low iron media

As described in the methods, the cell wall was obtained by differential centrifugation and solubilized in SDS-containing buffer. The expression of a 29 kDa *protein* was detected in immunoblot analysis with anti-HupB antibodies raised against the antigen of *M. tuberculosis*, and the expression of HupB was remained similar in both low and high iron media (Fig. 3.2). The homology of HupB proteins between *M. tuberculosis* and *M. smegmatis* was 98% (Pandey *et al.*, 2014b); this could be one of the reasons that the anti-HupB antibodies from *M. tuberculosis* were reacting at 29 kDa protein in *M. smegmatis*. Further, all immunoblot analyses were performed with anti-HupB antibodies from *M. tuberculosis*.

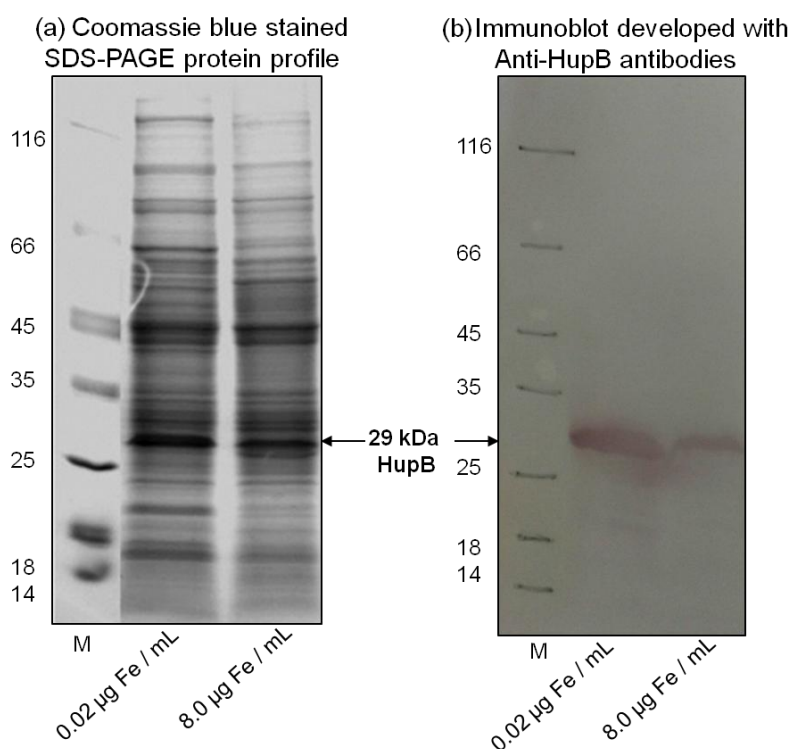


Fig.3.2. SDS-PAGE and immunoblot analysis of the cell wall proteins of *M. smegmatis*:

Panel (a) shows the Coomassie-stained profile of 50 µg of cell wall proteins of *M. smegmatis* grown under low and high iron conditions. Panel (b) shows the immunoblot of cell wall proteins in Panel (a) developed with antibodies raised against HupB from *M. tuberculosis*. Lane M represents the protein molecular weight marker.

3.1.3. Lowering of iron in growth medium influenced production of siderophores but had no effect on HupB expression in *M. smegmatis*

M. smegmatis was grown in media with iron added at 0.02, 0.05, 0.1, 0.5, 1.0, 2.0, 4.0, 8.0 and 12.0 $\mu\text{g Fe / mL}$ respectively. The level of all the three siderophores under these conditions is represented in Fig. 3.3.

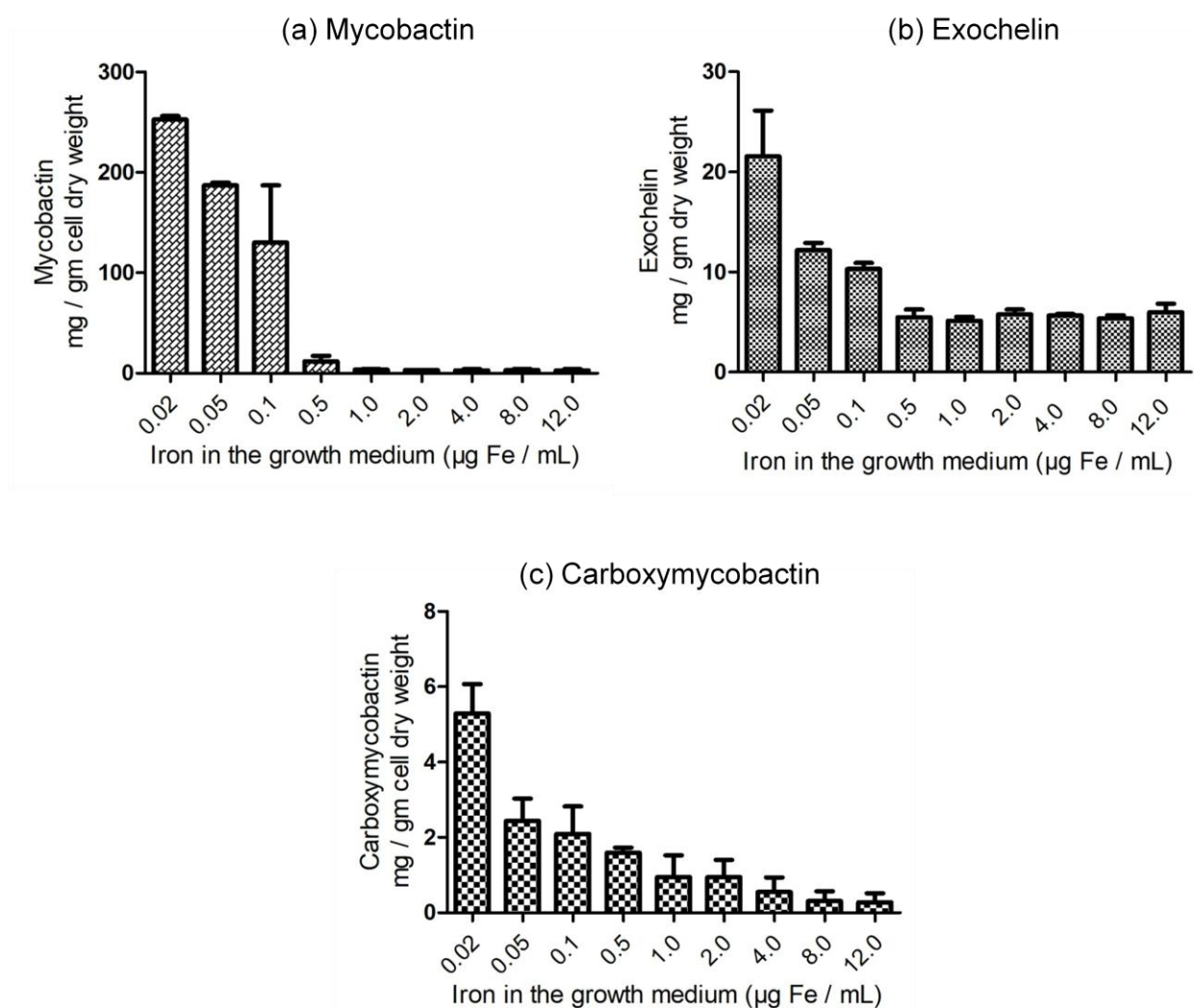


Fig. 3.3. Siderophore production by *M. smegmatis* with varying iron levels in the growth medium: *M. smegmatis* was grown in P & B medium with iron added at concentrations ranging from 0.02 to 12.0 $\mu\text{g Fe / mL}$ for 5 days. Panel (a) shows the intracellular mycobactin while Panels b and c represent the extracellular siderophores exochelin and carboxymycobactin

respectively. The error bars represent the standard deviation of the mean from three independent experiments.

As expected, the highest concentrations of all the three siderophores were seen at 0.02 $\mu\text{g Fe / mL}$. With increase in the iron levels, the mycobactin levels (Fig. 3.3a) showed a marked reduction at 0.5 $\mu\text{g Fe / mL}$. Among the two extracellular siderophores, exochelin expression was reduced to half when iron was marginally increased to 0.05 $\mu\text{g Fe / mL}$. Notable reduction was seen at 0.5 $\mu\text{g Fe / mL}$ (Fig. 3.3b) with no further decrease seen with increasing iron in the medium of growth. Carboxymycobactin expression (Fig. 3.3c), like exochelin was reduced by more than 50% at 0.05 $\mu\text{g Fe / mL}$ but unlike exochelin showed a gradual decrease with increase in iron levels and was almost negligible at 12 $\mu\text{g Fe / mL}$.

From Fig. 3.4, representing the complete protein profile of the cell wall proteins and the corresponding immunoblot developed with anti-HupB antibodies, it is evident that HupB is expressed at equal concentrations by the organism, irrespective of the amount of iron in the medium of growth.

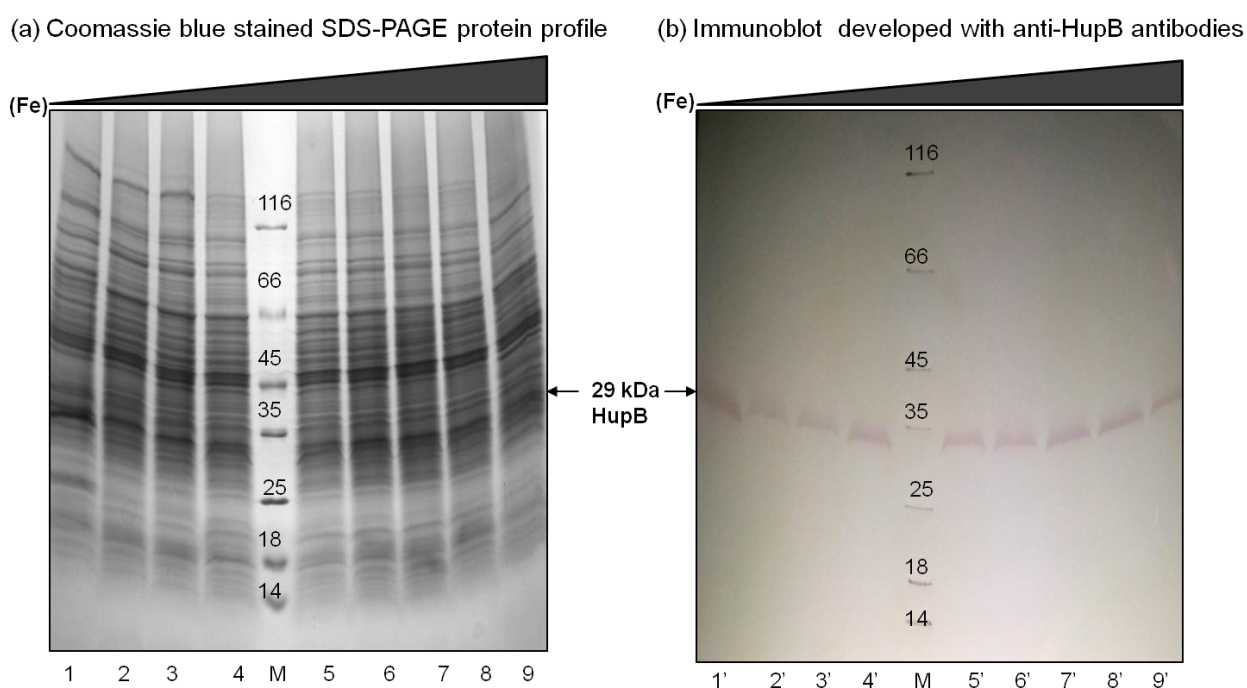


Fig. 3.4. Expression of HupB by *M. smegmatis* unaffected by iron in the medium of growth: *M. smegmatis* was grown in the presence of 0.02, 0.05, 0.1, 0.5, 1.0, 2.0, 4.0, 8.0 and

12.0 $\mu\text{g Fe / mL}$ (lanes 1-9 respectively). Panel (a) shows the profile of the cell wall proteins of *M. smegmatis* separated by SDS-PAGE and stained with Coomassie blue. Panel (b) shows the corresponding immunoblot showing the unaltered expression of HupB, as detected with antibodies against HupB from *M. tuberculosis*. Lane M represents the protein molecular weight marker.

3.1.4. Time course study: profile of the siderophores and HupB

Fig. 3.5 shows that HupB was expressed at equal amounts in the cell wall fraction of *M. smegmatis* harvested on different days, irrespective of the iron levels in the growth medium.

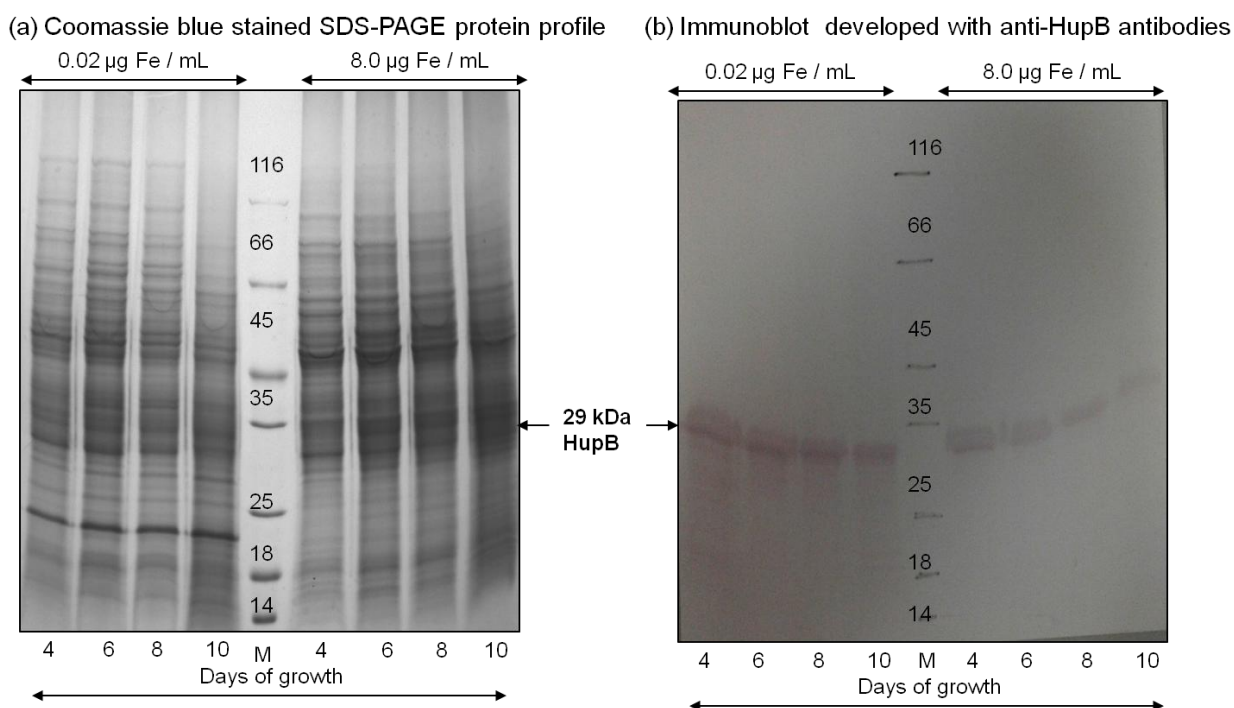


Fig. 3.5. HupB in the cell wall fraction of *M. smegmatis* harvested on different days: *M. smegmatis*, grown in low (0.02 $\mu\text{g Fe / mL}$) and high (8.0 $\mu\text{g Fe / mL}$) iron media were harvested on days 2, 4, 6, 8 and 10 respectively. 50 μg of cell wall proteins from the organisms were electrophoretically separated on 5-20% SDS-PAGE (Panel a), transferred onto nitrocellulose membrane and developed with anti-HupB antibodies from *M. tuberculosis* diluted 1:2500 (Panel b). M: Molecular weight marker.

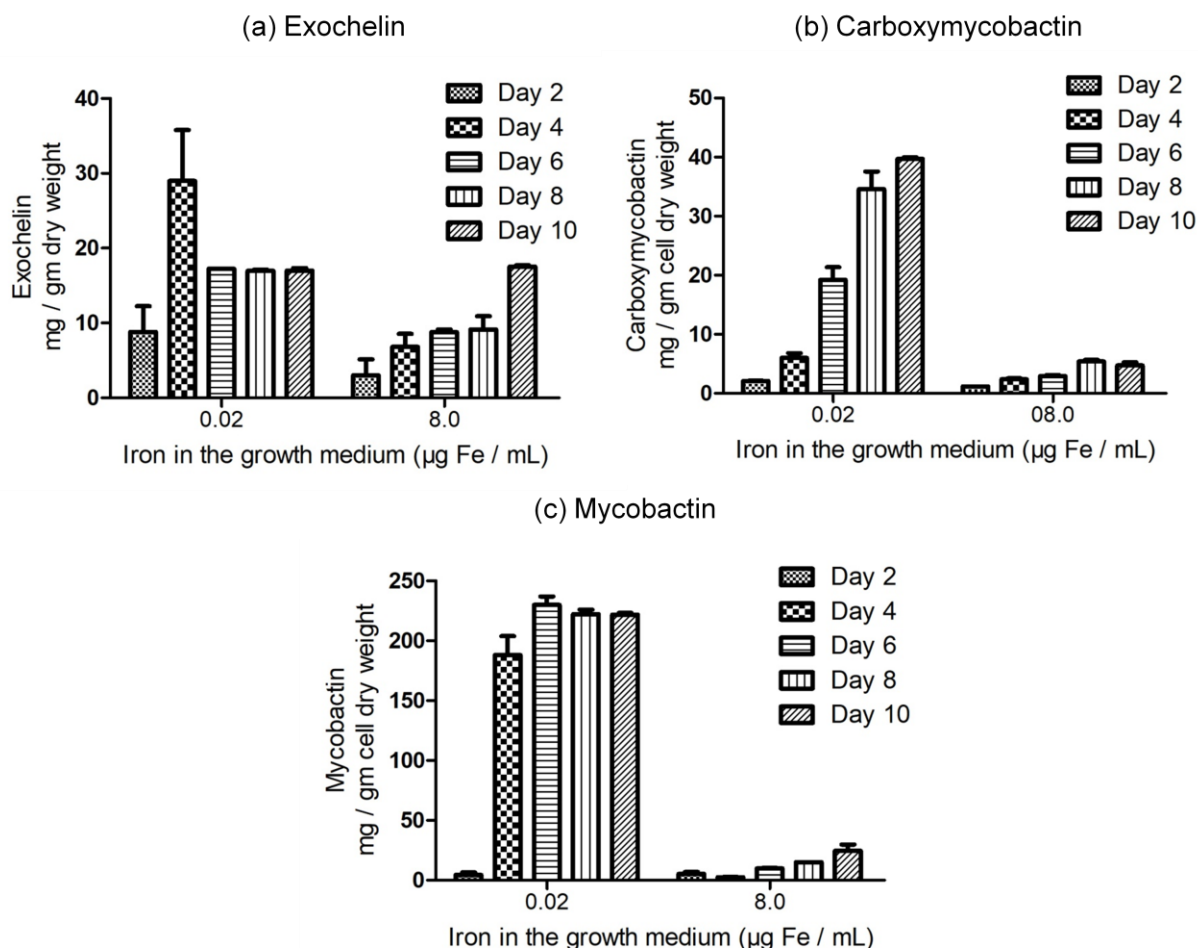


Fig. 3.6. Time-course expression of exochelin, carboxymycobactin and mycobactin in *M. smegmatis*: *M. smegmatis* was grown in high (8.0 $\mu\text{g Fe} / \text{mL}$) and low (0.02 $\mu\text{g Fe} / \text{mL}$) iron media over a period of 10 days. Panels a, b and c represent exochelin, carboxymycobactin and mycobactin respectively. The error bars represent the standard deviation of the mean from three independent experiments.

Considering iron-limited organisms, exochelin appeared to be the first siderophore to increase (Fig. 3.6a), with almost negligible values seen with the other two siderophores. Exochelin reached maximal levels on day 4, followed by a steep decrease that was however maintained till day 10. The other extracellular siderophore carboxymycobactin (Fig. 3.6b) showed a steady increase that reached maximal value on day 10. Mycobactin, almost negligible on day 2 was highly expressed from days 4-10 (Fig. 3.6c). Interestingly, organisms in high iron medium secrete increasing amounts of exochelin with time; there is a steady increase in this siderophore from days 4-10,

though the actual amount in these cultures is low even on day 10. This increase could reflect the onset of iron limitation with time of growth and exochelin is the first extracellular siderophore to rise. The levels of the other two siderophores were relatively low even on day 10 of growth.

3.1.5. HupB of *M. bovis* BCG was not regulated by iron

HupB is regulated by iron in *M. tuberculosis*. Since the above studies with the non-pathogenic *M. smegmatis* showed that the expression of the protein was not under the control of iron levels, it was proposed to study the protein profile in the attenuated mycobacterium *M. bovis* BCG. The five *M. bovis* BCG strains viz, Connaught, Phipps, Brazil, Sweden, and Pasteur used in the study responded to iron-limitation by producing high amounts of carboxymycobactin and mycobactin (Fig. 3.7); exochelin is not produced by these organisms. The fold increase in carboxymycobactin was about 12-15 fold in Brazil, Connaught and Pasteur strains and was lower (~7 fold) in Phipps and Sweden strains. Mycobactin was high in Connaught and Sweden strains (23-27 fold), with a smaller increase in Phipps, Brazil and Pasteur (10-13 fold).

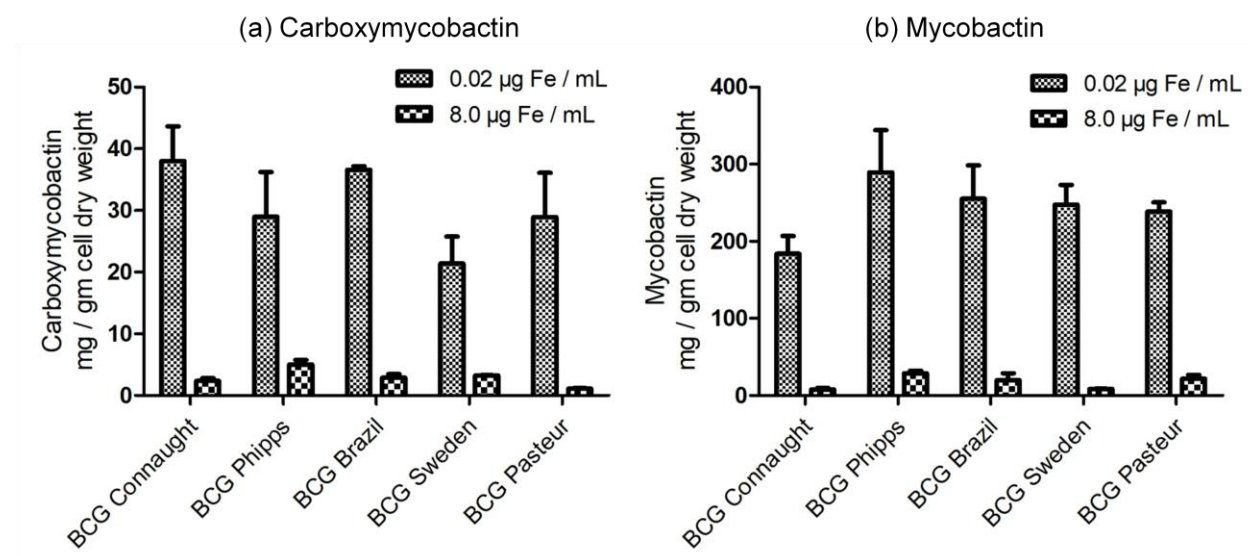


Fig. 3.7 Iron levels and expression of carboxymycobactin and mycobactin in iron-limited *M. bovis* BCG: All the five BCG strains produced high levels of carboxymycobactin (Panel a) and mycobactin (Panel b) when grown in low (0.02 µg Fe / mL) iron medium. The error bars represent the standard deviation of the mean from three independent experiments.

While these BCG strains responded to iron limitation by production of siderophores, there was no variation in the expression of HupB, as seen in Fig. 3.8. The greater mobility of the protein from iron-limited organisms seen in all the five strains is notable and could reflect changes in the protein due to post-translational acetylation or methylation of the lysine residues reported in this protein.

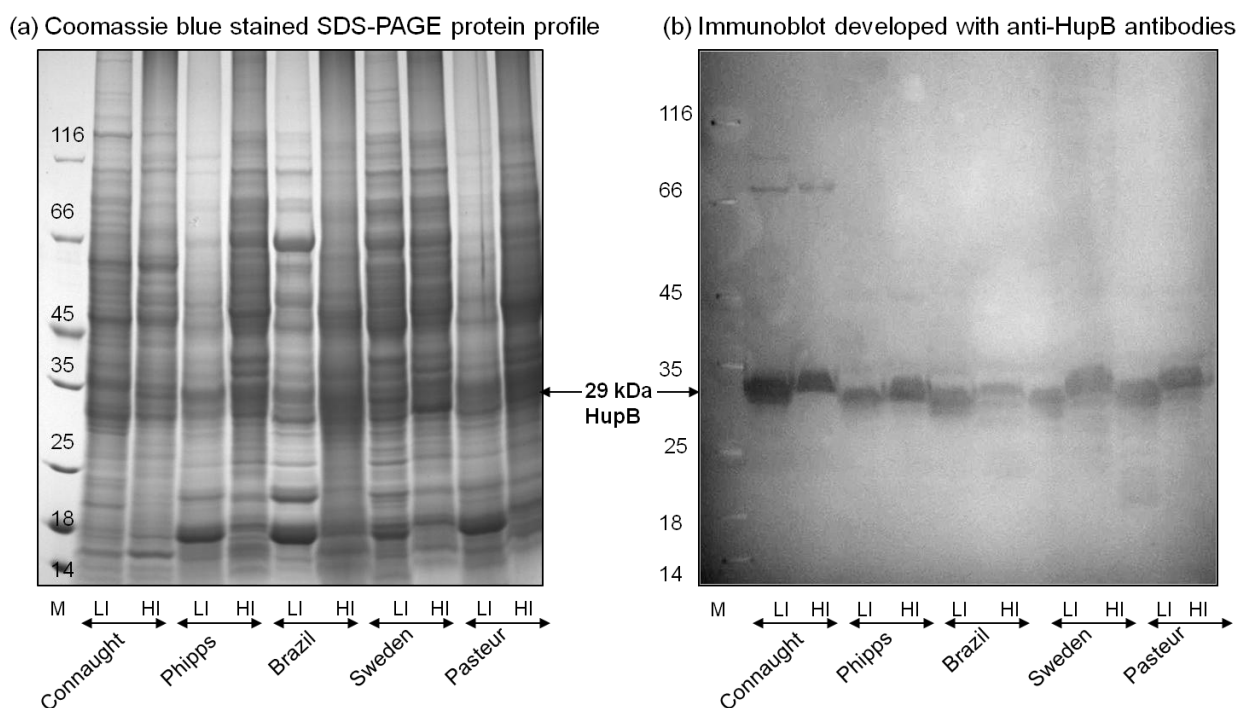


Fig. 3.8. Iron levels and expression of HupB in *M. bovis* BCG strains: 50 μ g of cell wall proteins from the five BCG strains were electrophoretically separated on 5-20% SDS-PAGE (Panel a), transferred onto nitrocellulose membrane and probed with anti-HupB antibodies from *M. tuberculosis* diluted 1:2500 (Panel b). M represents the molecular weight marker.

3.2. Identification and characterization of novel iron-regulated envelope proteins in *M. smegmatis*

3.2.1. Up-regulation of three proteins in the cell wall fraction of iron-limited *M. smegmatis*

Fig. 3.9 shows the up-regulation of three proteins in the cell wall fraction of iron-limited *M. smegmatis*; these proteins were repressed in iron replete organisms. The

approximate molecular masses of these proteins, determined by UVP GelDoc were 21, 109 and 145 kDa respectively. These proteins are henceforth referred to as IrpA, IrpB, and IrpC respectively.

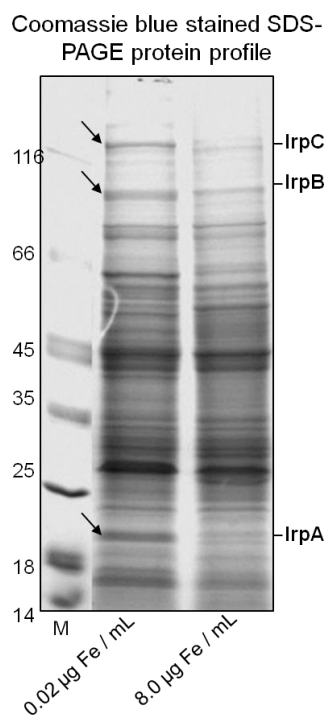


Fig. 3.9. Identification of three iron-regulated envelope proteins in *M. smegmatis*: Cell wall proteins from *M. smegmatis* grown under high and low iron media were subjected to SDS-PAGE and visualized with Coomassie Blue. The arrows indicate the three iron-regulated envelope proteins expressed by iron-limited organisms. M represents molecular weight marker.

3.2.2. Purification and identification of the three iron-regulated envelope proteins by MALDI-TOF MS / MS analysis

As detailed in Methods, the three IRPs were purified by preparative gel electrophoresis. Fig. 3.10 shows the purity of the gel-eluted proteins corresponding to IrpA, IrpB and IrpC. The purified IRPs, subjected to MALDI-TOF-MS / MS analysis showed characteristic peptide mass fingerprints (Fig. 3.11) that were used to identify the proteins.

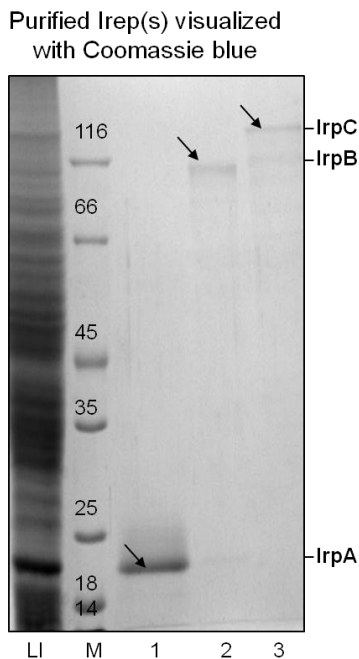
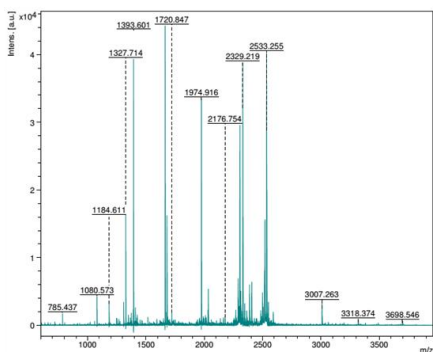
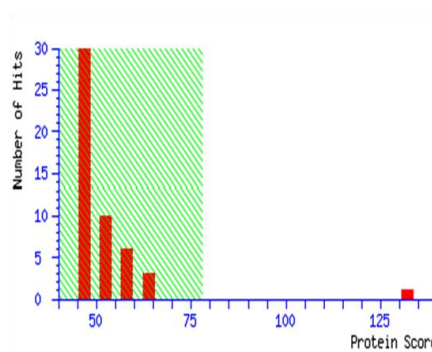


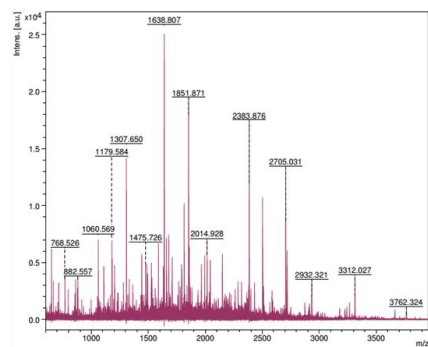
Fig. 3.10. SDS-PAGE of the gel purified IRPs: The three gel-purified proteins were subjected to SDS-PAGE and stained with Coomassie Blue. Lanes 1-3 represents IrpA, IrpB and IrpC respectively and M represents the protein molecular weight marker. The cell wall protein of iron-limited *M. smegmatis* was loaded as a control for confirmation of the IRPs.



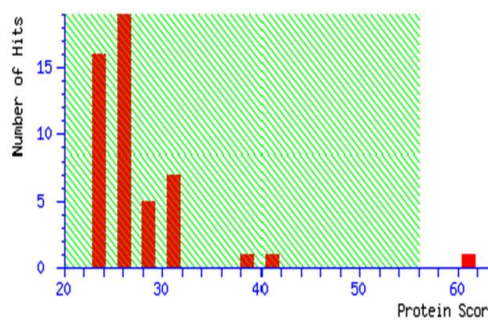
(a) Spectrum of IrpA generated by MALDI-TOF-MS



(b) MASCOT results showing the significance of IrpA identification



(a) Spectrum of IrpB generated by MALDI-TOF-MS



(b) MASCOT results showing the significance of IrpB identification

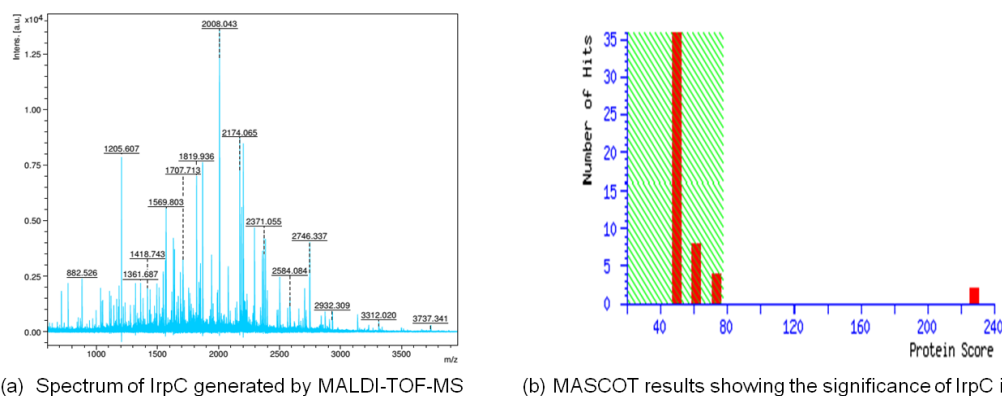


Fig. 3.11. Identification of iron-regulated envelope proteins by MALDI-TOF-MS / MS: The three iron-regulated envelope proteins were subjected to MALDI-TOF-MS / MS. Panel (a) shows the peptide mass fingerprint of each of these proteins and Panel (b) shows the MASCOT score.

The MASCOT scores of 132 and 228 for IrpA and IrpC were found to be satisfactory and the peptide sequences obtained by MALDI-TOF-MS, subjected to BLAST analysis in the NCBI nr database identified them as Clp protease subunit and FtsK/SpoIIIE family protein (ESX conserved component eccC3) respectively. SwissProt identified IrpB (with a Mascot score of 61) as a putative membrane protein.

3.2.3 Characterisation and analysis of the features of the three iron-regulated envelope proteins

3.2.3.1. General features

Table 3.1 lists the features of the three proteins as annotated in the respective databases.

Table 3.1: Features of IrpA, IrpB and IrpC identified by MALDI-TOF-MS analysis

IREP	Protein annotation	Accession number	Locus tag	Molecular mass (kDa)
IrpA	Clp protease subunit	gi 118470816	MSMSEG_3761	21
IrpB	Putative membrane protein	gi 500047325	MSMEG_1959	109
IrpC	FtsK/SpoIIIE family protein (ESX conserved component eccC3)	gi 118468237	MSMEG_1707	144.7

3.2.3.2. Evolutionary relationship of the three iron-regulated envelope proteins among mycobacteria and other Gram-positive bacteria

3.2.3.2.1 IrpA (MSMEG_3761)

IrpA is present only in non-pathogenic mycobacteria and is absent in pathogenic members including *M. tuberculosis*. It is also seen in the related Gram-positive *Nocardia*, *Rhodococcus*, and *Streptomyces*. Fig. 3.12a shows that the protein shows about 70% similarity among the non-pathogenic mycobacteria, with about 40% similarity when compared with the other related Gram-positive bacteria (Fig. 3.12b).

(a)

```

M.neoaureum      MFERFGRHARVAVVLAQEEAKDLGATVIGPEHLVAGIVQSASSELSGELAAVGMTVDSVR
M.abscessus      MFEKFKSAKVAVVLSQEEAREMDDTRIGAEHVLVGVLDLSAGAPLSELMGGYGLTADGVR
M.chelonae       MFEKFKSAKVAVVLSQEEAREMDDTRIGAEHVLVGVLDLSAGAPLSELMGGYGLTADGVR
M.phlei          MFERFARNARIAVWLAQEEAHELGAEEIRPEHLLVGVLVQVAGRDLARVLDHGLTVTAVR
M.vulneris       MFERFSRHARVAVVLAQEEARELEANDIRPEHLLVGVLVQSSGRELSALLAGFGLTSDAVR
M.fortuitum      MFERFSRHARIAVWLAQEEARELGANEIRPEHLLVGVLVQSSGRELSALVAGFGLTSDVVR
M.hassiacum      MFERFTRHARIAVILAQEEAAL ELDDDEIRPSHLLVGVLVQSSGRELSRVLAGYGLTADTVR
M.thermoresistibile MFERFSRHARVAVVLAQEEARELQCDEIRPEHLLVGVLVQSSGRELSRVLAGYGLTADTVR
M.smegmatis(IrpA) MFERFSRHARVAVVLAQEEARELQCDEIRPEHLLVGVLVQSSGRELSRVLAGYGLTADTVR
M.goodii         MFERFSRQARISVWLAQEEARELQCDEIRPEHLLVGVLVQSSGRELSRVLAGYGLTADTVR
***:* : *::*:**:* * :: * .*:.*::: :: * . : ** **

M.neoaureum      EQLGANA--SGASFESDADALQSIGIDLHRVREINHTFGAGTFDDAVSDAGRRPQ----
M.abscessus      DRLRAGSE-QPPTDDEDAEALRAIGIDLSQLVRESVSKVFGPQAFDEAFKSGRRKGRMRG
M.chelonae       DRLRAGSE-QP-----
M.phlei          ADLESRESPD-DLFEEDAESLRRIGIDLVAIRDVRRNLGPDANDTA--RPPARRRR---
M.vulneris       AELVQADAPGDESFDQDAEALQSIGIDLRAVRTNVDRTFGDGFADNLRSTGRRRRR---
M.fortuitum      TELAAADAPGDESFDQDAEALRSIGIDLRAVRANVDRTFGDGFADNLRSTGRRRRR---
M.hassiacum      ERLAAG-EDDDPGFADDAEALRAIGIDLHAVRDRVVRAFGADANDAAAGRPPRR-RR---
M.thermoresistibile GRIASADNPDETFERDAEALRAIGIDLHAVRDSVARSFGPDANDGALRRSGRRRR---
M.smegmatis(IrpA) AGLGAVATPEDETFERDADALRSIGIDLHAVRDSVRSFSGADANDGALQRSRRRRR---
M.goodii         ARLESATPEDETFERDADALRSLGIDLHAVRDSVRSFSGADANDGALRRSGRRRRR---
:

M.neoaureum      ---RGNLAFSKPAKEALKLALREAVAHHESTIDSEHLLLVLRGGDPVACALITAHVEED
M.abscessus      WRPFGMIPFNSSAKKCLELALREIAHKDNWIGCEHMLVGLIRGGDPVALAVITERVSDV
M.chelonae       -----
M.phlei          ---RTHIPFTRAAKKALQALREAVAHRDSTIDCEHLLGILRGGDSATTELITAHVDPA
M.vulneris       ---RGHLPFTKAARKVLELALRESLAHKDGFICGEHILLGILRGGDRAVALITEHVAG
M.fortuitum      ---RGHLPFTKSAKKVLELALRESLAHKDGCIGCEHILLGILRGGDARAVALITEHVAG
M.hassiacum      ---RKHLPFTKSAKKALELALREALAHKDNIGCEHLLGILRGADEPTLELIADHVPA
M.thermoresistibile ---RRHLPFTKPAKKTLELALREATAHKDSVTDSEHMLGTLRGGDHTLELITEHVDP
M.smegmatis(IrpA) ---RGHLPFTKPAKKALELALREALAHKDSVIESEHMLGILRGGDHTLSLITEYVDVA
M.goodii         ---RGHLPFTKPAKKALELALREIAHKDSEIGSEYVLLGILRGGDYTLSLITAHVDIA

M.neoaureum      VLRSNIIALLDRAA
M.abscessus      ELRQAVVGLLDQAA
M.chelonae       -----
M.phlei          RLRADVALLDRAA
M.vulneris       ELRAGIVGLLDQAA
M.fortuitum      ELRTGIVGLLDQAA
M.hassiacum      RLRADIDGLLAAAA
M.thermoresistibile RLRADIDGLLDAAA
M.smegmatis(IrpA) RLRADIIGLLESAA
M.goodii         RLRSIDDDLEAAA

```

(b)

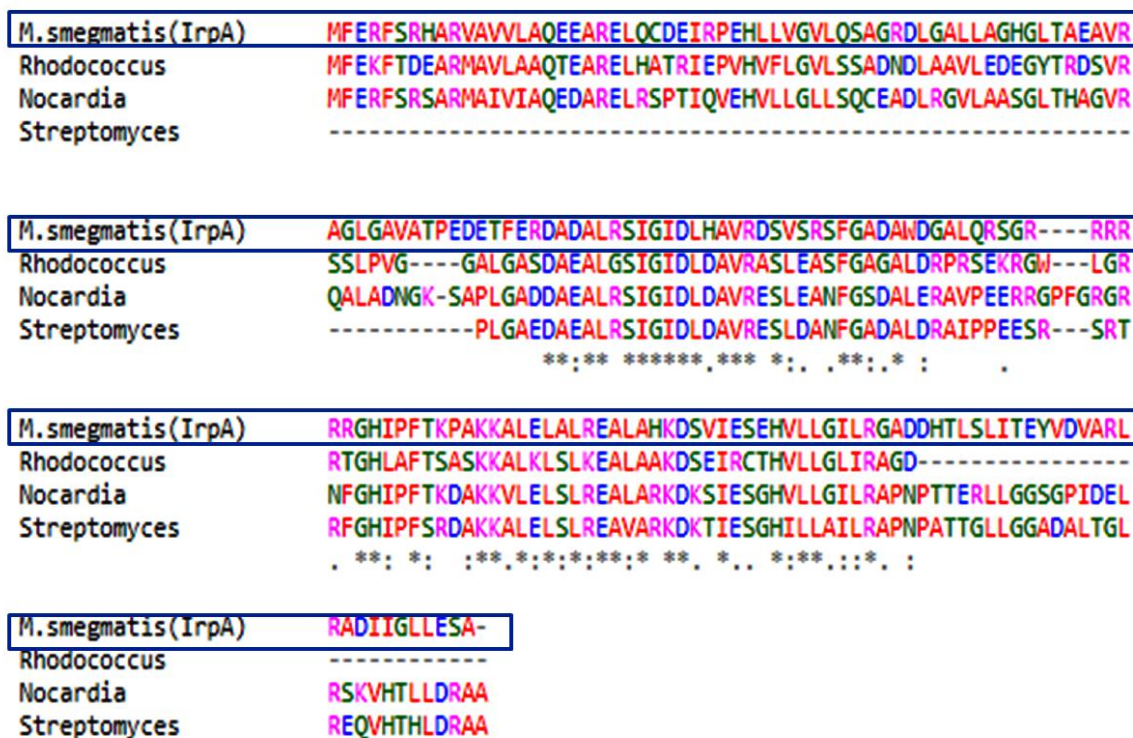


Fig. 3.12. Homology of IrpA among non-pathogenic mycobacteria and related Gram-positive bacteria. Panel a shows the sequence alignment of IrpA from non-pathogenic mycobacteria and Panel b shows the homology of IrpA among related Gram-positive bacteria, as analysed by T-Coffee. The symbols (*), (:), and (.) represents identical sequences, conserved substitutions and partially conserved amino acid residues

Fig. 3.13 shows six clusters generated when analyzing the evolutionary relationship of IrpA among non-pathogenic mycobacteria and gram-positive bacterial species. IrpA from *M. smegmatis* formed a separate cluster with *M. goodii* and *M. thermoresistibile* with more than 90% bootstrap value whereas *M. phlei*, *M. hassiacum*, *M. abscessus*, *M. chelonae* and *M. neoaurum* formed individual clusters with 40-50% bootstrap value. *Rhodococcus*, *Nocardia* and *Streptomyces* grouped together with 50% bootstrap value.

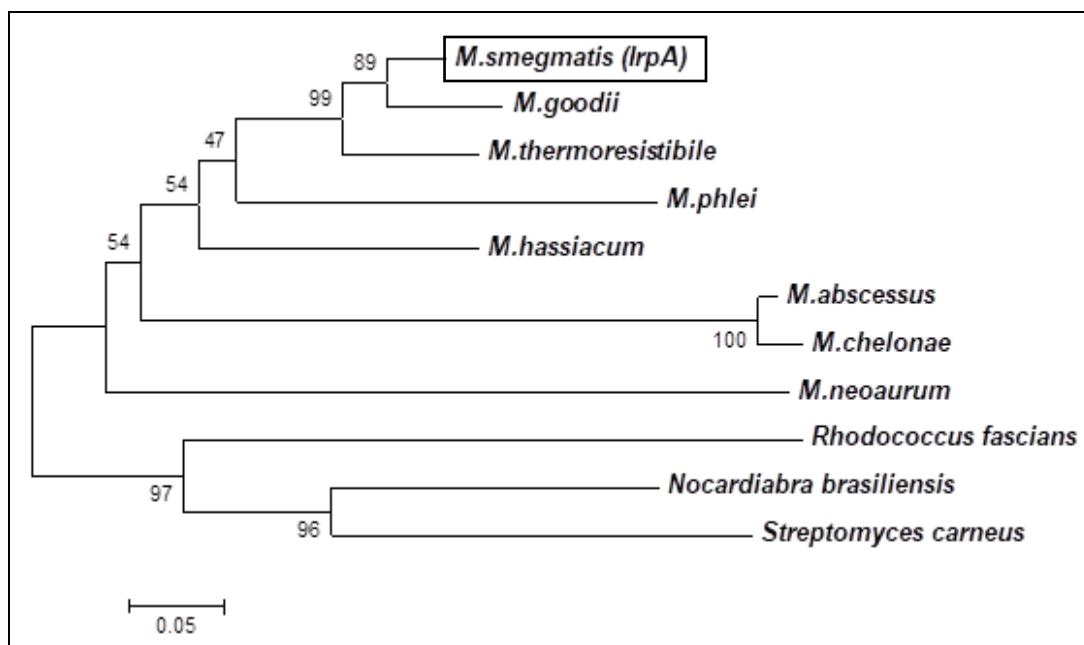


Fig. 3.13. Phylogenetic tree depicting the genetic relatedness of IrpA among non-pathogenic mycobacterial species and gram-positive bacterial species: The MEGA software tool was used to construct the phylogenetic tree based on the amino acid sequence of IrpA from *M. smegmatis* (WP_003895204.1), *M. goodii* (WP_049746430.1), *M. thermoresistibile* (WP_003925769.1), *M. phlei* (WP_003887208.1), *M. neoaurum* (WP_030132919.1), *M. hassiacum* (WP_005625052.1), *M. abscessus* (WP_005071001.1), *Rhodococcus fascians* (WP_037110590.1), *Streptomyces carneus* (WP_030113467.1) and *Nocardia brasiliensis* (WP_014988535.1).

3.2.3.2.2. IrpB (MSMEG_1959)

IrpB, annotated as a putative membrane protein is conserved in all mycobacterial species. Phylogenetic analysis revealed five distinct clusters, one of which included IrpB with the corresponding homologue from *M. neoaurum* with 100% bootstrap value (Fig. 3.14). Close to this cluster was the cluster including *M. fortuitum*, *M. rufum*, *M. gilvum* and *M. vaccae*. The pathogenic members including *M. tuberculosis* complex, *Mycobacterium avium* complex (MAC), *M. kansasii*, *M. marinum*, *M. ulcerans* and *M. xenopi* were well separated. Several other non-pathogenic mycobacteria and related *Rhodococcus*, *Streptomyces*, and *Nocardia* grouped together with lower bootstrap values.

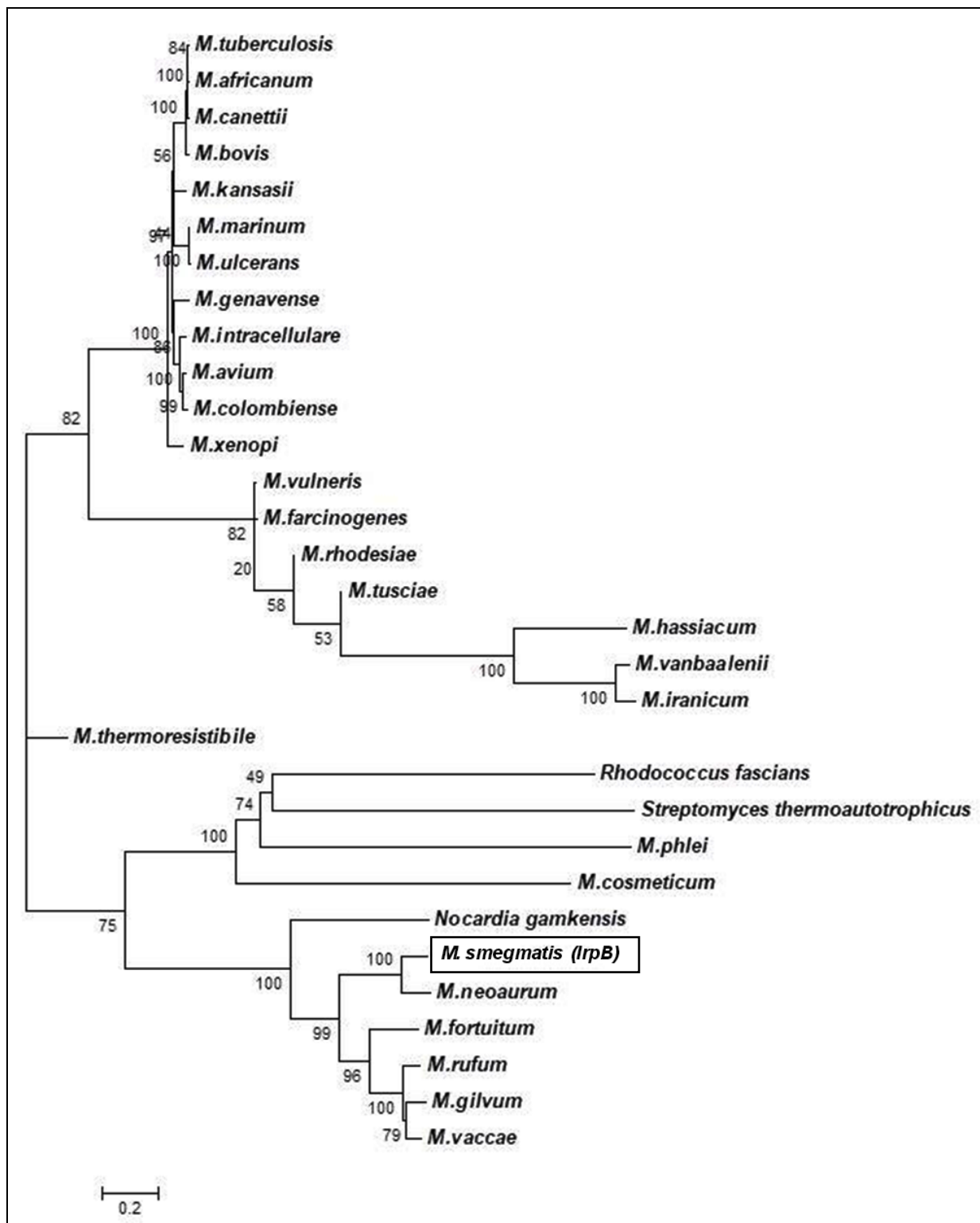


Fig. 3.14. Phylogenetic tree depicting the genetic relatedness of IrpB among mycobacteria and related Gram-positive bacteria: The MEGA6 software tool was used to construct the Phylogenetic tree based on the amino acid sequence of IrpB present in *M. smegmatis* (WP_011728043.1), *M. fortuitum* (WP_00388268.1), *M. farcinogenes* (CDP84269.1), *M. vulneris* (CDO27584.1), *M. rhodesiae* (WP_014208791.1), *M. tusciae* (WP_006245900.1), *M. xenopi* (WP_003920806.1), *M. neoaurum* (WP_023985464.1), *M. kansasii* (WP_023372773.1), *M. gilvum* (WP_011895490.1), *M. rufum* (KGI67404.1), *M. vanbaalenii* (WP_011779054.1), *M. vaccae* (WP_003929184.1), *M. avium* (WP_011725903.1), *M. cosmeticum* (CDO1055.1), *M. genavense* (WP_025735717.1), *M. thermoresistibile* (WP_003927921.1), *M. colombiense* (WP_007773012.1), *M. marinum* (WP_020732198.1), *M. ulcerans* (WP_011740463.1), *M. tuberculosis* (WP_009938015.1), *M. intracellulare* (WP_026071234.1), *M. canetti* (WP_015291267.1), *M. bovis* (WP_019283731.1), *M. africanum* (WP_031701648.1), *M. hassiacum* (WP_005625954.1), *Rhodococcus fascians* (WP_032378153.1), *Streptomyces thermoautotrophicus* (WP_066891253.1), *Nocardia gamkensis* (WP_06297551.1). IrpB indicted in the rectangle.

3.2.3.2.3. IrpC (MSMEG_1707)

IrpC is a 145 kDa protein present in all mycobacterial species and the closely related *Rhodococci*, *Streptomyces* and *Nocardia* spp. Phylogenetic tree built with IrpC clearly segregated the non-pathogens from the pathogens (Fig. 3.15). *M. tuberculosis* complex and gram-positive bacterial species have formed separate clusters. Other non-pathogenic mycobacterial species includes *M. gilvum*, *M. iranicum*, *M. vanbaalenii*, *M. vaccae*, *M. hassiacum*, *M. tusciae* and *M. phlei* have formed single cluster from IrpC with 40% bootstrap value. IrpC forms a cluster with *M. thermoresistibile*, *M. mageritense*, *M. fortuitum*, *M. farcinogenes*, *M. vulneris* with 70-100% bootstrap value and other non-pathogenic mycobacterial species forms a separate cluster with 50-60% bootstrap value.

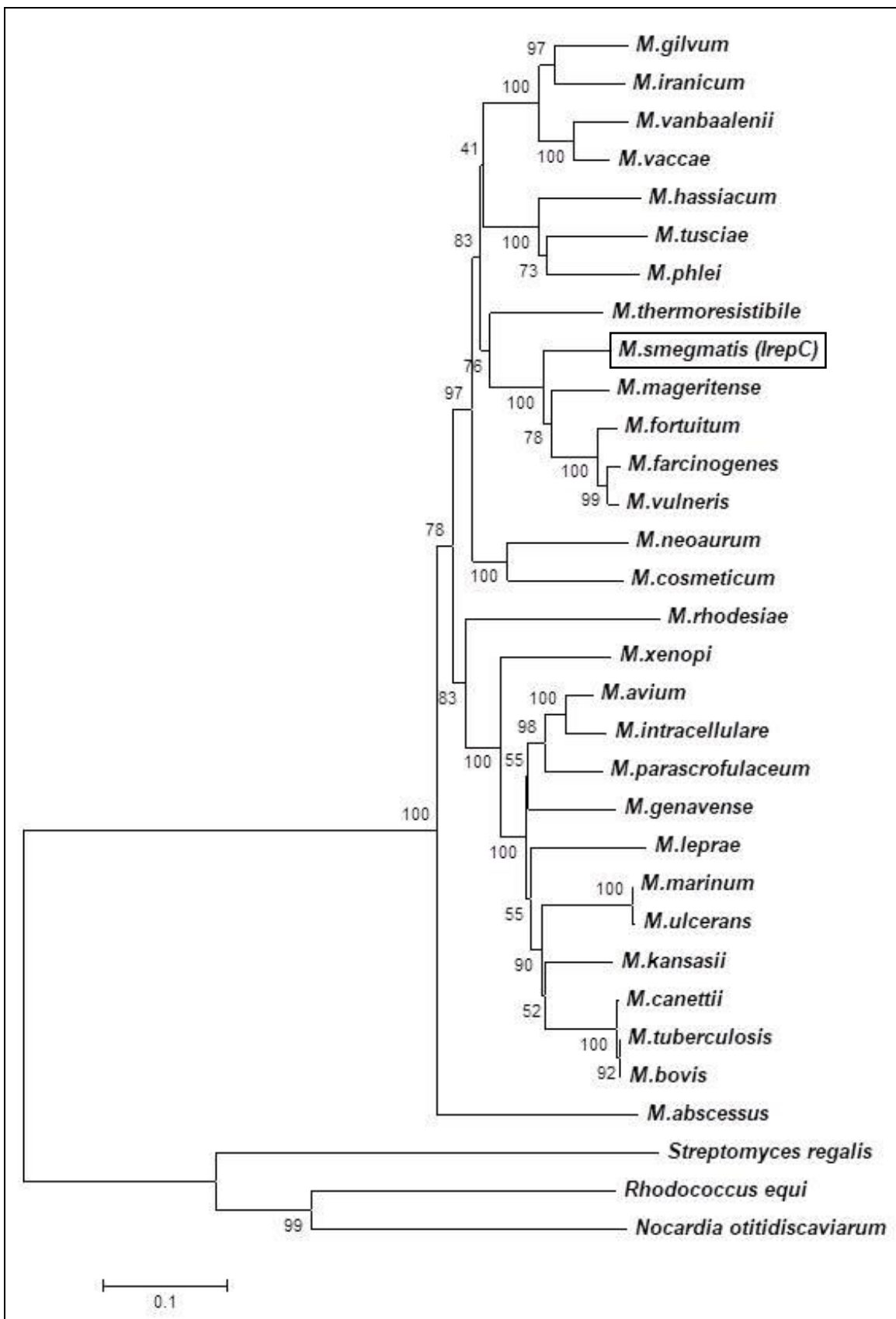
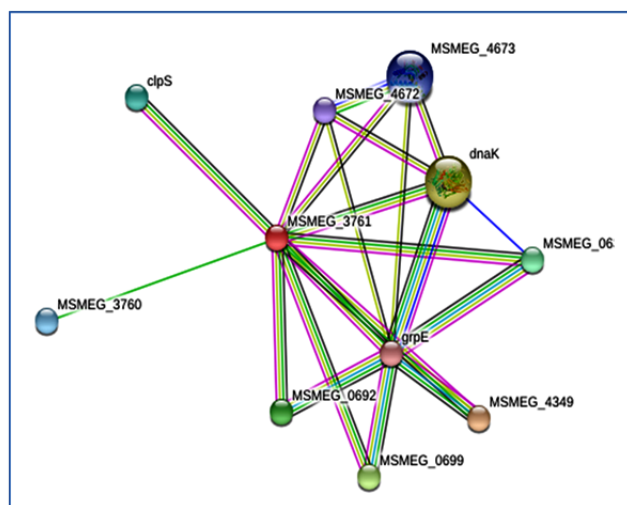


Fig. 3.15. Phylogenetic tree depicting the genetic relatedness of IrpC (FtsK/SpoIIIE family protein (ESX conserved component eccC3) among non-pathogenic mycobacterial species and gram-positive bacterial species: The MEGA6 software tool was used to construct the Phylogenetic tree based on the amino acid sequence of IrpC (FtsK/SpoIIIE family protein (ESX conserved component eccC3) protein from mycobacteria and gram-positive bacterial spp. *Mycobacterium smegmatis* (WP_003892037.1), *Mycobacterium fortuitum* (CDO31467.1), *Mycobacterium farcinogenes* (CDP8061.1), *Mycobacterium vulneris* (CDO31467.1), *Mycobacterium mageritense* (CDI23249.1), *M. neoaurum*(WP_030137393.1), *M. intracellulare* (WP_009952517.1), *M. abscessus* (WP_024571177.1), *M. phlei* (WP_003887308.1), *M. hassiacum* (WP_005624126.1), *M. tusciae* (WP_006241695.1), *M. vaccae* (WP_003933738.1), *Mycobacterium iranicum* (WP_024448874.1), *M. thermoresistibile* (WP_003924389.1), *M. gilvum* (WP_011891328.1), *M. vanbaalenii* (WP_11777734.1), *M. rhodesiae* (WP_014209851.1), *M. leprae* (WP_010908946.1), *M. marinum* (WP_012392510.1), *M. ulcerans* (WP_011739403.1), *M. kansasii* (WP_023369878.1), *M. avium* (WP_023869947.1), *M. porascrofulaceum* (WP_007167385.1), *M. gevanavense* (WP_025736519.1), *M. tuberculosis* (WP_031663040.1), *M. cannetti* (WP_015302496.1), *M. xenopi* (WP_003922936.1), *M. cosmeticum* (WP_019737496.1), *M. bovis* (WP_03705179.1), *Nocardia otitidiscaviarum* (WP_029923708.1), *Streptomyces regalis* (WP_062701901.1) and *Rhodococcus equi* (WP_064057810.1). IrpC indicted in the rectangle.

3.3. *In silico* and experimental studies on IrpA

3.3.1. Physical features of IrpA and functional partners identified using *in silico* tools

IrpA is a 21 kDa protein consisting of 188 amino acids with a pI of 6.5. It is annotated as Clp protease subunit in the genome of *M. smegmatis* strain MC² 155 (Accession No. gi|118470816; locus tag MSMEG_3761). Using STRING software, the neighborhood genes (Fig. 3.16) were found to encode several hypothetical proteins, ClpS (ATP-dependent Clp protease adaptor protein), ATP-dependent Clp protease proteolytic subunits and molecular chaperones, the roles of which are not known.



Your Input:									
●	MSMEG_3761 Clp protease subunit (188 aa) (<i>Mycobacterium smegmatis</i>)								
Predicted Functional Partners:		Neighborhood	Gene Fusion	Cooccurrence	Coexpression	Experiments	Databases	Textmining	Score
●	MSMEG_4349 hypothetical protein (592 aa)	●	●	●	●	●	●	●	0.925
●	dnaK molecular chaperone DnaK; Acts as a chaperone (By similarity) (622 aa)	●	●	●	●	●	●	●	0.925
●	MSMEG_0699 hypothetical protein (616 aa)	●	●	●	●	●	●	●	0.925
●	MSMEG_0692 hypothetical protein (595 aa)	●	●	●	●	●	●	●	0.925
●	MSMEG_0638 hypothetical protein (643 aa)	●	●	●	●	●	●	●	0.925
●	clpS ATP-dependent Clp protease adaptor protein ClpS; Involved in the modulation of the specificity [...] (100 aa)	●	●	●	●	●	●	●	0.904
●	MSMEG_3760 hypothetical protein (69 aa)	●	●	●	●	●	●	●	0.893
●	MSMEG_4673 ATP-dependent Clp protease proteolytic subunit; Cleaves peptides in various proteins in a proce [...] (203 aa)	●	●	●	●	●	●	●	0.888
●	MSMEG_4672 ATP-dependent Clp protease proteolytic subunit; Cleaves peptides in various proteins in a proce [...] (218 aa)	●	●	●	●	●	●	●	0.888
●	grpE co-chaperone GrpE; Participates actively in the response to hyperosmotic and heat shock by prev [...] (216 aa)	●	●	●	●	●	●	●	0.838

Fig. 3.16. Functional partners of Clp protease subunit, as identified by STRING software:

Colored lines between the proteins indicate the various types of interaction evidence and protein nodes which are enlarged indicate the availability of 3D protein structure information. Green line indicates neighborhood evidence; red line indicates fusion evidence; purple line indicates experimental evidence; light blue line indicates database evidence; black line indicates coexpression evidence; blue line indicates co-occurrence evidence; and yellow line indicates text-mining evidence

3.3.1.1. IrpA of *M. smegmatis* is absent in *M. tuberculosis*

IrpA is annotated as Clp protease subunit and since there are several mycobacterial Clp proteases, the genomes of *M. smegmatis* and *M. tuberculosis* were compared for the presence of Clp proteases. Table 3.2 shows seven Clp proteins in *M. smegmatis* with the corresponding orthologs seen in *M. tuberculosis*. Notably, IrpA is present only in *M. smegmatis* and the corresponding homologue is absent in the pathogen. It was also absent in the genome of the vaccine strain *M. bovis* BCG Pasteur.

Table 3.2: IrpA is an additional Clp protease subunit present in *M. smegmatis*

<i>M. smegmatis</i>			<i>M. tuberculosis</i>		
Locus tag	Annotated as	Assigned function	Locus tag	Annotated as	Assigned function
MSMEG_3761 (IrpA)	Putative Clp protease subunit	Unknown	Absent	NA	NA
MSMEG_0732	ClpB	Unknown	Rv0384c	ClpB	ATPase subunit of ATP-dependent protease
MSMEG_2792	Clp amino terminal domain protein	Unknown	Rv2667	ClpC2	Unknown
MSMEG_4671	ClpX	Unknown	Rv2457c	ClpX	ATP-dependent specificity component of the Clp protease
MSMEG_4672	ClpP	Unknown	Rv2460c	ClpP2	ATP-dependent protease activity
MSMEG_4673	ClpP	Unknown	Rv2461c	ClpP1	
MSMEG_4910	ClpS	Unknown	Rv1331	Conserved hypothetical protein	Unknown
MSMEG_6091	ClpC	Unknown	Rv3596c	ClpC1	ATP-dependent protease activity

The amino acid sequence obtained from tuberculist (<http://tuberculist.epfl.ch/>) and smegmalist (<http://mycobrowser.epfl.ch/smegmalist.html>) of genome databases for *M. tuberculosis* and *M. smegmatis*

3.3.1.2. Generation of polyclonal mono-specific anti-IrpA antibodies

The 21 kDa IrpA was excised from a preparative gel loaded with the cell wall proteins of *M. smegmatis* grown in low iron medium. The purified protein was re-run to check the purity and used for immunizing rabbit. Fig. 3.17 shows the immunoblot showing the specificity of interaction of the rabbit anti-IrpA antibodies with IrpA present in the mixture of cell wall proteins.

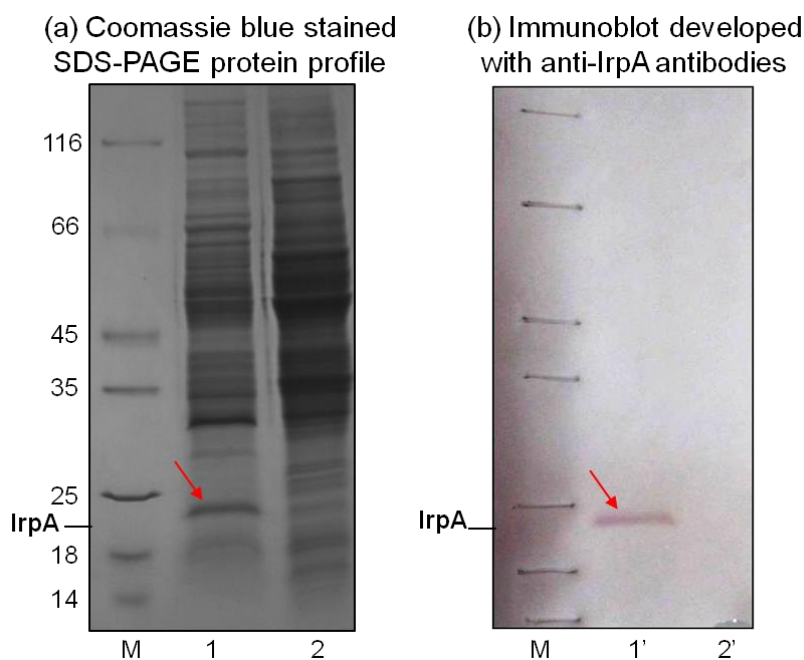


Fig. 3.17. Specificity of rabbit anti-IrpA antibodies with the 21 kDa IrpA: Panel (a) shows the SDS-PAGE profile of 50 μ g of cell wall proteins grown in low from *M. smegmatis* (0.02 μ g Fe / mL; lane 1) and high (8.0 μ g Fe / mL; lane 2) iron medium respectively. Panel (b) shows the corresponding immunoblot (lanes 1' and 2') developed with anti-IrpA antibodies diluted 1:500. M represents the protein molecular weight marker

3.3.2. Iron-regulated expression of IrpA

3.3.2.1. Presence of IdeR box upstream of *irpA*

In silico analysis of the promoter region of *irpA* for the identification of IdeR box was done with a region overlapping +20 to -250 bp of *irpA*. Compared to the 19 bp (5'-TTAGGACAGCCTGTGCTAA-3') consensus IdeR box, an IdeR box with the sequence

TCGCGAATGCCCGCGCACA was identified at position -103 bp relative to the start point.

3.3.2.2. Coordinated expression of *IrpA* and siderophores

IrpA is expressed maximally by *M. smegmatis* grown in medium containing 0.02 $\mu\text{g Fe / mL}$ with the levels showing a relative decrease upon increasing to 0.05 $\mu\text{g Fe / mL}$, with complete repression at 8.0 $\mu\text{g Fe / mL}$ (Fig. 3.18).

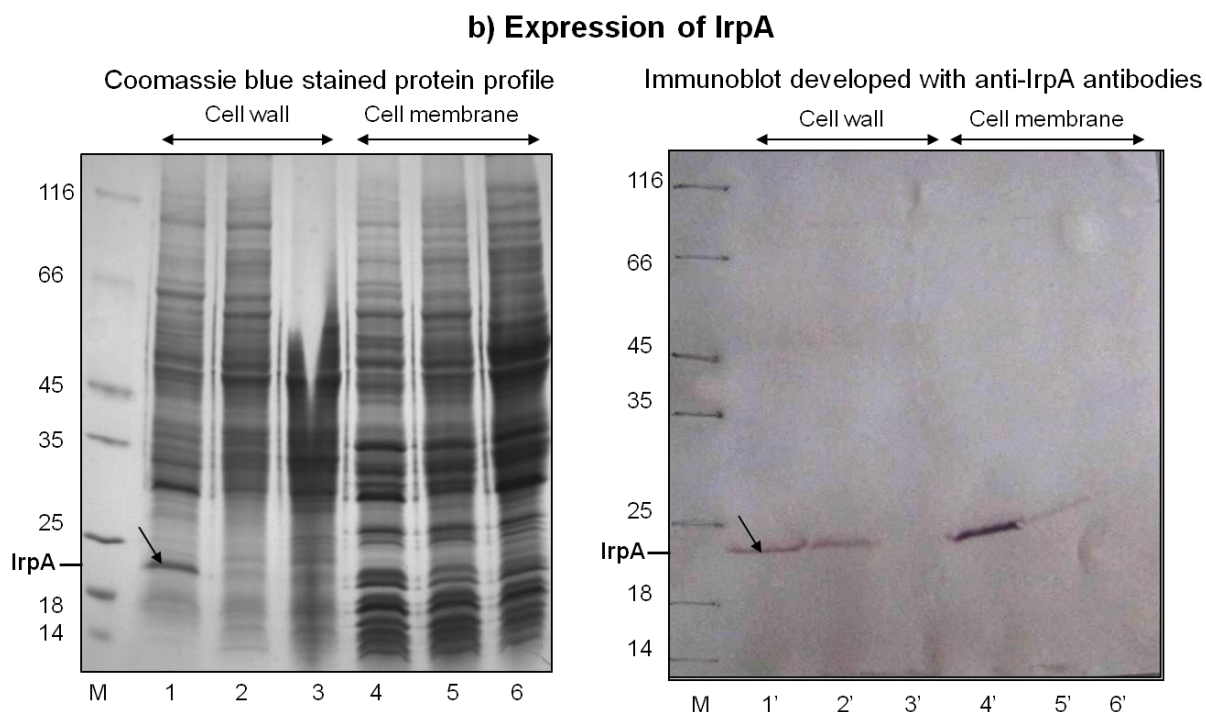
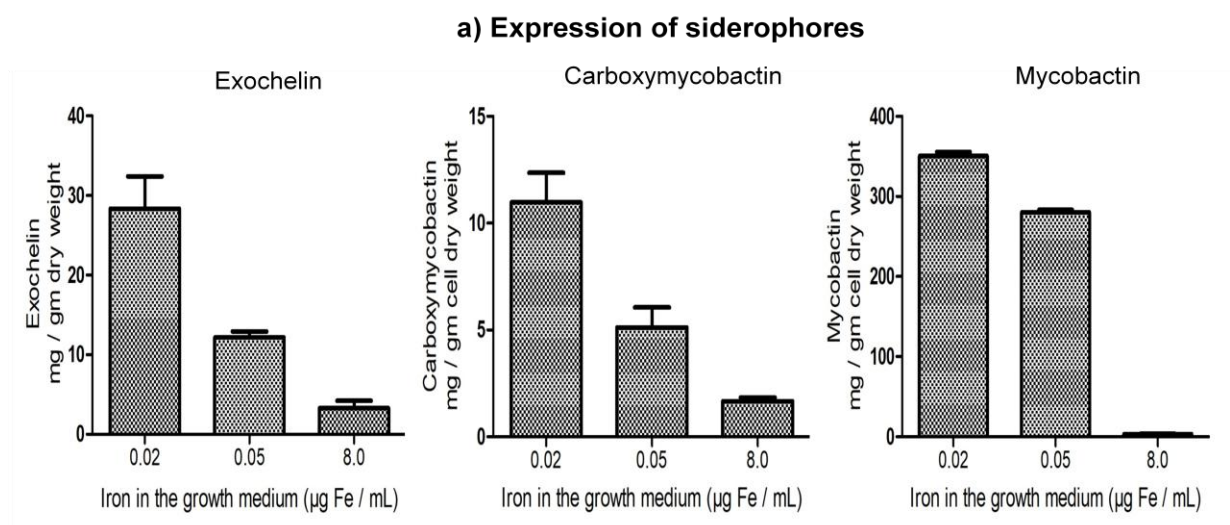


Fig. 3.18. Coordinated expression of IrpA and the siderophores: *M. smegmatis* was grown in medium containing 0.02, 0.05 and 8.0 $\mu\text{g Fe / mL}$ for 5 days. The figures shows the levels of the three siderophores exochelin, carboxymycobactin and mycobactin. SDS-PAGE separation of 50 μg of the respective cell wall and cell membrane proteins were visualised with Coomassie Blue and an identical set subjected to immunoblotting with anti-IrpA antibodies. Lanes 1 to 3 represent the cell wall proteins from organisms grown in the presence of 0.02, 0.05 and 8.0 $\mu\text{g Fe / mL}$ and lanes 4 to 6 represent the corresponding cell membrane proteins. The corresponding lanes in the immunoblot are labeled as 1' to 6'. M represents the protein molecular weight marker.

3.3.2.3. Time-course expression of IrpA

When *M. smegmatis*, inoculated into high (8.0 $\mu\text{g Fe / mL}$) and low (0.02 $\mu\text{g Fe / mL}$) iron media was grown for different days, the respective cell wall proteins showed that IrpA was expressed even on day 4, with high levels seen subsequently (Fig. 3.19). As growth was poor on day 2, the organisms were not processed for cell wall protein profiling.

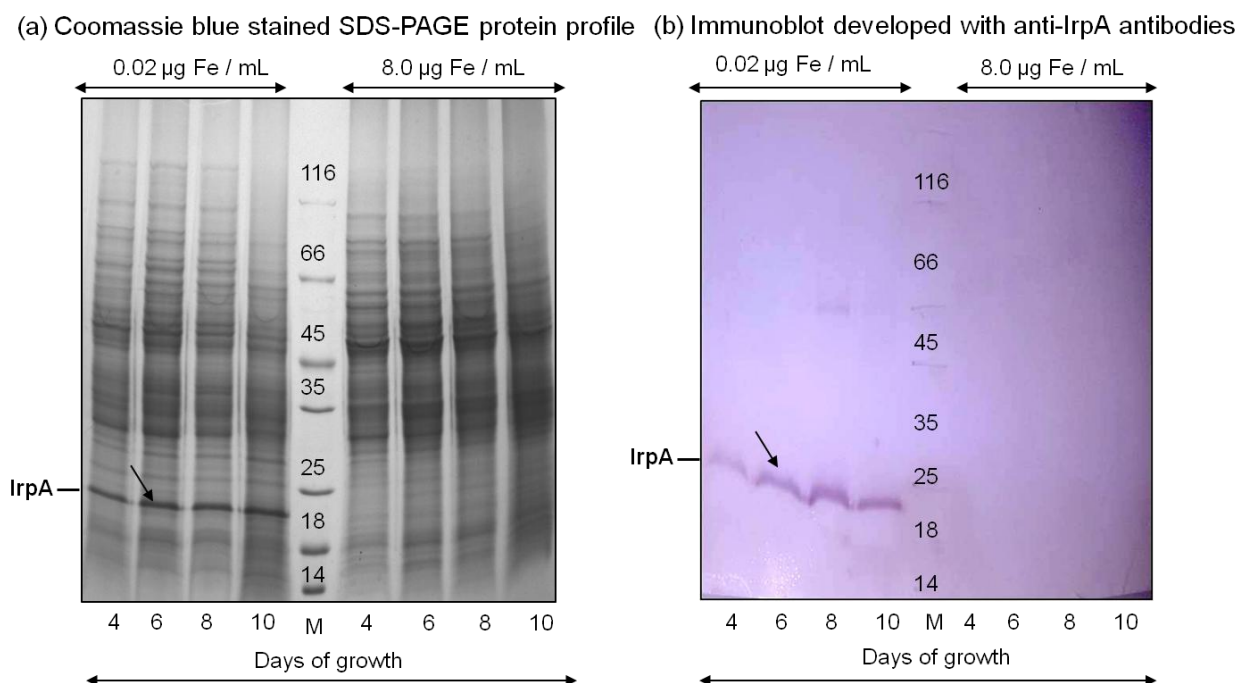


Fig. 3.19. Time-course expression of IrpA in *M. smegmatis*: *M. smegmatis* was grown in low (0.02 $\mu\text{g Fe / mL}$) and high (8.0 $\mu\text{g Fe / mL}$) iron media over a period of 10 days. The cells were

harvested at days 4, 6, 8 and 10 respectively. 50 μg of cell wall proteins were electrophoretically separated on 5-20% SDS-PAGE (Panel a), transferred onto nitrocellulose membrane and developed with anti-IrpA antibodies diluted 1:500 (Panel b). M: Molecular weight marker.

3.3.2.4. IrpA is absent in *M. bovis* BCG Pasteur

Anti-IrpA antibodies showed faint reactivity with a 26 kDa band in cell wall proteins of vaccine strain *M. bovis* BCG Pasteur, irrespective of the iron status of the organisms (Fig. 3.20). The positive control (lane 1 & 1') shows the reactivity of IrpA from *M. smegmatis*.

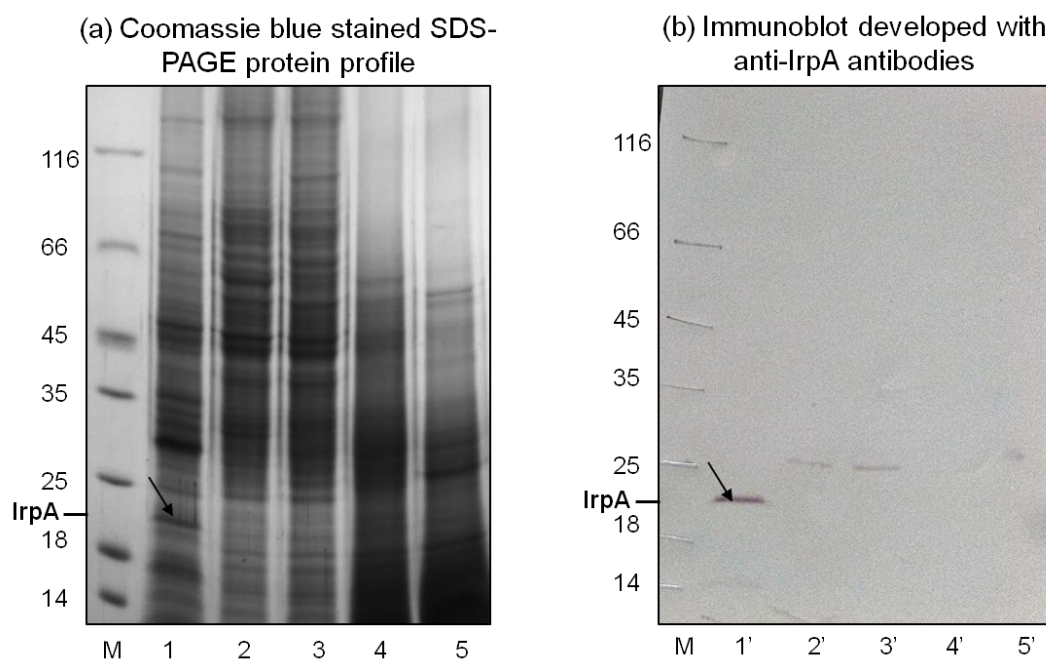
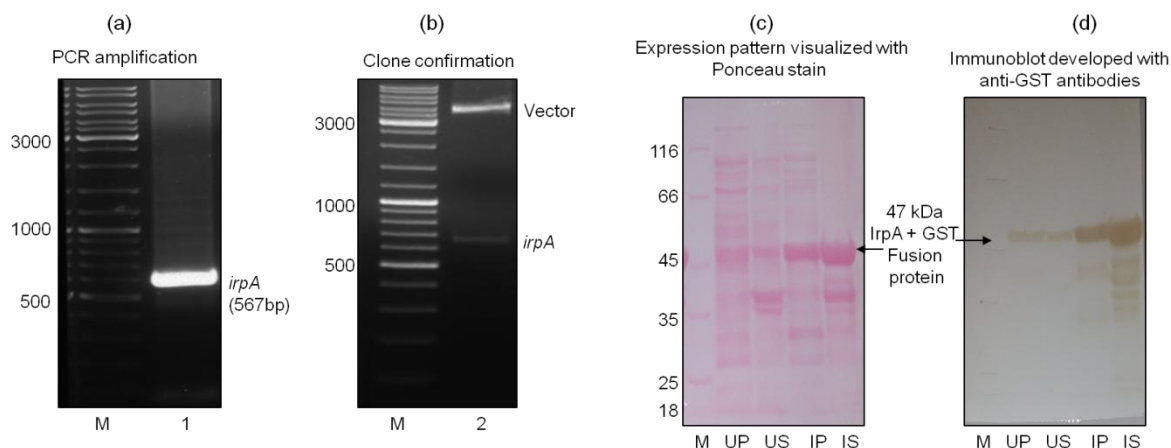


Fig. 3.20. Immunoblotting of cell wall and membrane proteins of *M. bovis* BCG Pasteur with anti-IrpA-antibodies: Cell wall proteins of *M. bovis* BCG Pasteur, grown in low (0.02 μg Fe / mL) and (8.0 μg Fe / mL) iron media were subjected to SDS-PAGE (Panel a) and immunoblotting with anti-IrpA antibodies diluted 1:500 (Panel b). Cell wall proteins of iron-limited *M. smegmatis* was loaded as a positive control (lane 1). The other lanes were loaded as follows: Lanes 2 & 3 – cell wall proteins of iron-deficient and iron replete BCG, lane 4 & 5 - cell membrane proteins of iron-deficient and iron replete BCG. The immunoblot represents the corresponding lanes as in Panel (a). M represents the protein molecular weight marker.

3.3.3. Cloning and expression of rIrpA

Fig. 3.21a, (Panel a) shows the full length *irpA* (567 bp) cloned into pGEX-4T-1; the insert was released upon double digestion of the recombinant plasmid with *EcoRI* & *NotI*. The recombinant clone, when induced with 1 mM IPTG at 37°C for 3 h (Fig. 3.21b) expressed IrpA-GST fusion protein as a 47 kDa protein that reacted strongly with anti-GST antibodies. This fusion was purified by glutathione affinity chromatography as a single band and when digested with thrombin yielded IrpA and GST (26 kDa) (Fig. 3.21c). The release of IrpA was confirmed with anti-IrpA antibodies (Fig. 3.21d). However, the protein could not be recovered upon rechromatography the digested products, in which only the GST protein was present (Fig. 3.21d). It is likely that IrpA was probably unstable and degraded.

In view of the above, *IrpA* was cloned in pET23b (+) vector (Fig. 3.22a). When expressed in *E. coli* BL21 (DE3), the protein was obtained as insoluble inclusion bodies (Fig. 3.22b). Different optimization procedures, including growth at low temperatures, induction with varying concentrations of IPTG and co-expression with chaperone proteins, using the Arctic expression system did not yield soluble rIrpA (Fig. 3.22c).



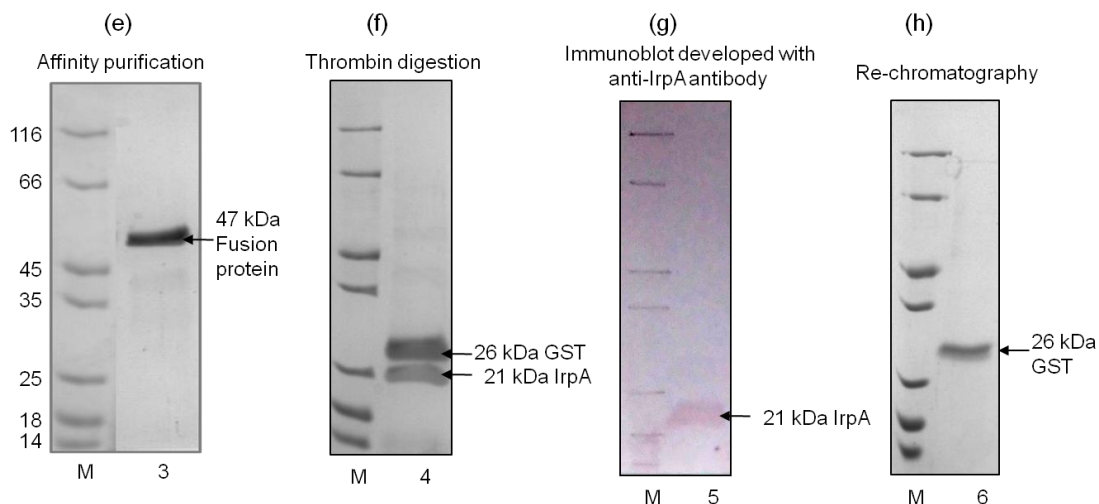


Fig. 3.21. Cloning, expression, and purification of rlrpA: The 567 bp amplicon (Panel a) was cloned into pGEX-4T-1 and a positive clone was verified by double digestion (Panel b). Panels c and d represent the nitrocellulose transferred proteins stained with Ponceau S and subjected to immunoblotting with anti-GST antibodies. The 47 kDa fusion protein was purified by affinity chromatography (Panel e) and cleaved with thrombin that yielded the 21 kDa rlrpA and 26 kDa GST proteins (Panel f). The rlrpA obtained was verified by immunoblot analysis with anti-rlrpA antibodies (Panel g). When the digested products were re-run after chromatographic separation (Panel h), only GST was recognised. M in Panel a and b represent 1 kb DNA ladder and in the other panels it represents protein molecular weight marker. US and UP represent un-induced supernatant and pellet while IS and IP represent IPTG-induced supernatant and pellet respectively.

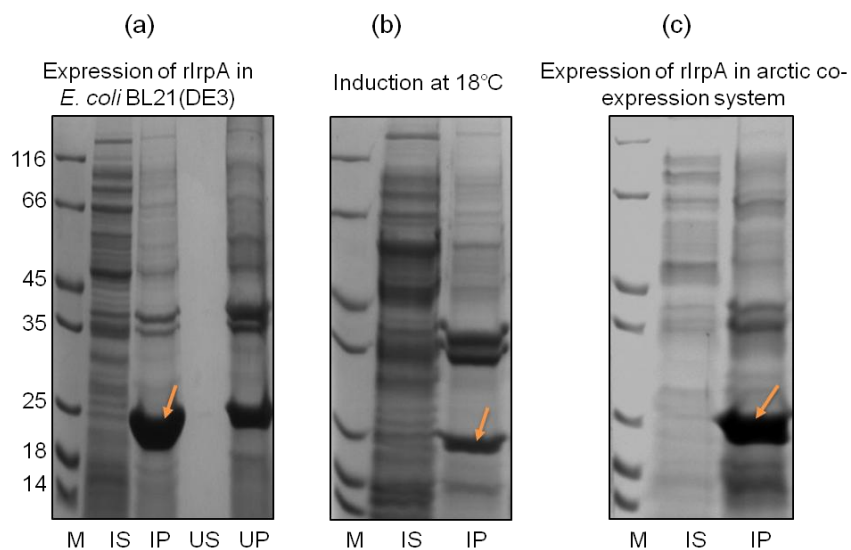


Fig. 3.22. Cloning and expression of rlrpA in *E. coli*: *irpA* was cloned into pET23b (+) vector. In Panel (a), the rlrpA induced by IPTG at 37°C was obtained as insoluble protein, as visualized with Coomassie Blue upon SDS-PAGE. Panels b and c represent the attempts made to obtain rlrpA as soluble protein by induction at 18°C and cloning using the Arctic co-expression system. M represents the protein molecular weight marker. US and UP represent un-induced supernatant and pellet while IS and IP represent IPTG-induced supernatant and pellet respectively. Arrow mark indicates the insoluble expression of rlrpA.

3.4. Functional characterisation of LrpA as a putative receptor for ferri-exochelin

3.4.1. *In silico* analysis: modeling and docking studies

3.4.1.1. Homology modeling of LrpA

Homology modeling requires a template to generate a model. Search for a homologous sequence by BLAST analysis against PDB database identified the N-terminal region of ClpC1 from *M. tuberculosis*. The latter shows 100% sequence similarity with the ClpC protein in *M. smegmatis*. Fig. 3.23a shows the alignment of LrpA, showing 34% with the N-terminal region of ClpC and ClpC1 (sequence coverage 97% and 34% identity with template). Using ClpC1 as template, tertiary structure of LrpA was modelled using Modeller version 9.17 (Fig. 3.23b). The secondary structure of the protein revealed that 9 alpha (α)-helices were present. The model, validated by Procheck was satisfactory as 82.6% of residues were present in the most favored region, with 13.8% of residues in additionally allowed regions and 3.6% residues in generously allowed regions; there were no residues in the disallowed regions.

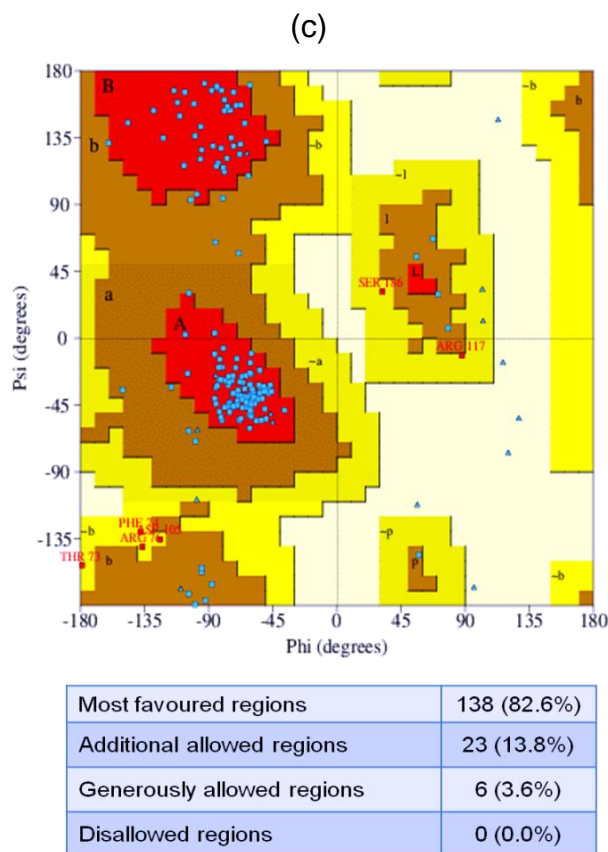


Fig. 3.23. *In silico* modeling of IrpA from *M. smegmatis*: Panel (a) shows the multiple sequence alignment (T-Coffee) of IrpA with ClpC and ClpC1 from *M. smegmatis* and *M. tuberculosis* respectively. Panel b shows the tertiary structure of IrpA generated by Modeller version 9.17 and Panel c represents the Ramachandran plot.

3.4.1.2. Docking of exochelin onto IrpA

The three-dimensional structure of ferri-exochelin MS was developed by using the ChemDraw 3D ultra (Version 10.0). Using AutoDock / Vina, 3D ferri-exochelin was docked onto the modelled IrpA. Three residues, namely two Arginine residues (R7 & R76) and a glutamic acid residue (D71) bound ferri-exochelin by non-covalent interactions (Fig. 3.24).

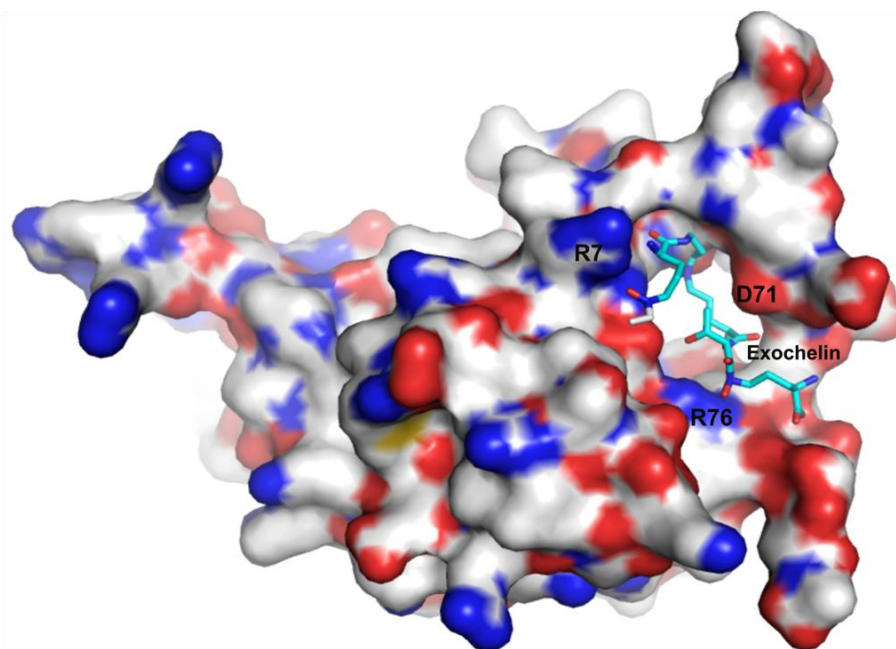


Fig. 3.24. Docking of ferri-exochelin to IrpA: The 3D-structure of ferri-exochelin was docked onto the modeled structure of IrpA using Autodock / Vina. The three interacting amino acid residues were identified as R7, R76 and D71 that interacted through non-covalent interactions with ferri-exochelin

3.4.2. Experimental studies to establish IrpA as ferri-exochelin receptor

In our efforts to establish IrpA as a potential ferri-exochelin receptor in *M. smegmatis*, uptake of radiolabeled ferri-exochelin by live organisms was done. The organisms, grown in low iron (0.02 $\mu\text{g Fe / mL}$) medium served as the test organisms as they expressed IrpA; the corresponding iron replete organisms (grown in the presence of 8.0 $\mu\text{g Fe / mL}$) served as control. Uptake of ferri-exochelin was studied in the above two sets of organisms, with pre-incubation of the organisms with specific anti-IrpA antibodies done in an identical set to study the role of IrpA in this uptake process. Further, the role of IrpA, if any, on the uptake of iron from ferri-carboxymycobactin was studied. In addition, uptake studies were done using liposomes prepared from cell wall proteins from iron-limited and iron replete organisms.

3.4.2.1. Uptake of ^{55}Fe -exochelin by *M. smegmatis*

Fig. 3.25a shows the enhanced uptake of ^{55}Fe -exochelin by iron-limited organisms, with a 4-fold accumulation of the radiolabel when compared to the iron replete organisms.

As the iron from the extracellular carboxymycobactin is transferred to the intracellular mycobactin in *M. tuberculosis* (Gobin & Horwitz, 1996; earlier findings in our lab that is under communication), we wished to see if a similar process occurred in *M. smegmatis*. Hence, mycobactin was extracted from organisms incubated with ^{55}Fe -exochelin. The radiolabel in the mycobactin fraction was almost negligible in *M. smegmatis* (Fig. 3.25b), unlike that seen in *M. tuberculosis*.

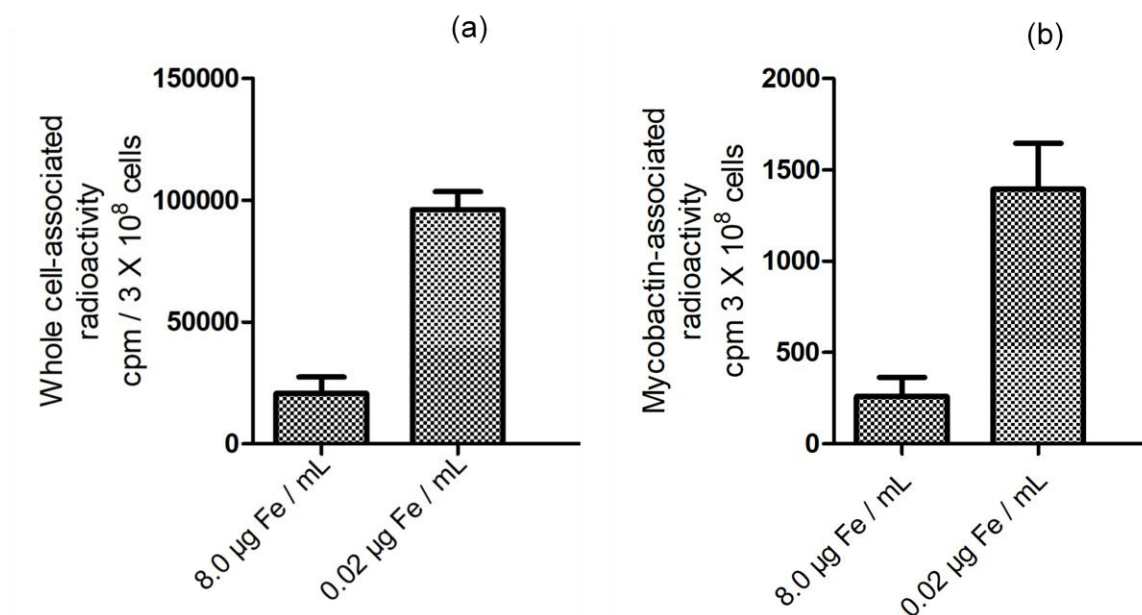


Fig. 3.25. Uptake of ^{55}Fe -exochelin by *M. smegmatis* and recovery of the label in mycobactin: Aliquots of 3×10^8 cells of iron-limited and iron replete *M. smegmatis* were incubated with 1×10^5 cpm of ^{55}Fe -exochelin and the radioactivity in the cells upon suitable washing was determined. An identical set of cells were processed for mycobactin and the radiolabel in the two sets were determined. The error bars represent the standard deviation from four values obtained from two identical experiments performed in duplicates.

3.4.2.2. Uptake of ^{55}Fe -carboxymycobactin by *M. smegmatis*

In order to see if the carboxymycobactin-mycobactin machinery operated in *M. smegmatis*, uptake of iron from ^{55}Fe -carboxymycobactin was studied. It was seen that there was poor uptake of this siderophore by whole cells, with poor recovery of the radiolabel in mycobactin (Fig. 3.26).

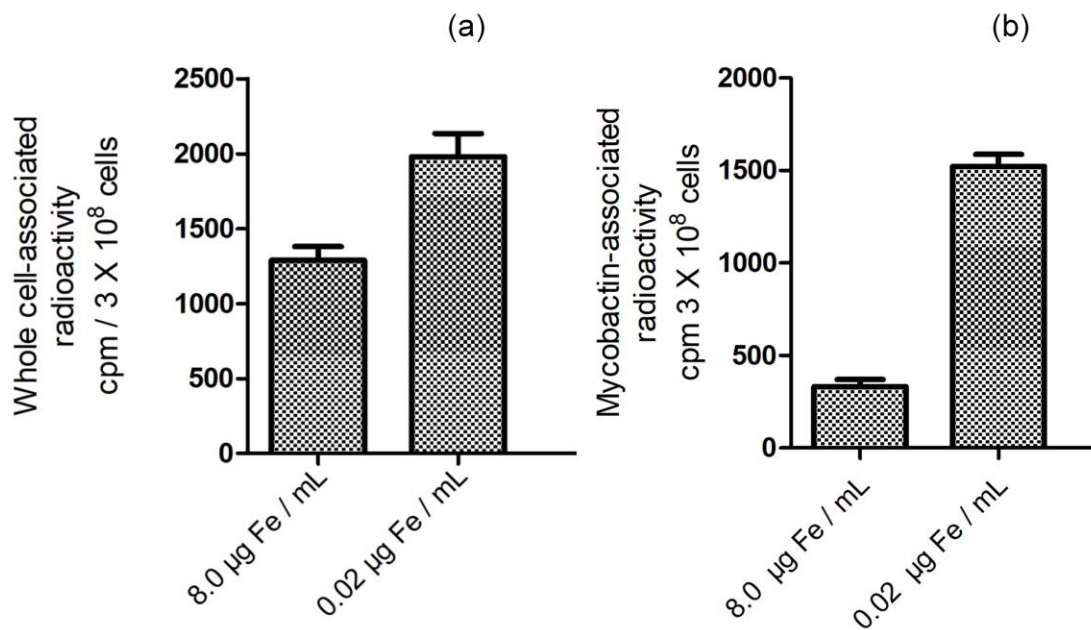


Fig. 3.26. Uptake of ⁵⁵Fe-carboxymycobactin by *M. smegmatis*: Aliquots of 3 X 10⁸ cells of iron-limited and iron replete *M. smegmatis* were incubated with 1 X 10⁵ cpm of ⁵⁵Fe-carboxymycobactin and the radioactivity in the cells upon suitable washing was determined. An identical set of cells were processed for mycobactin and the radiolabel in the two sets were determined. The error bars represent the standard deviation from four values obtained from two identical experiments performed in duplicates.

3.4.2.3. Uptake of ⁵⁵Fe-exochelin by *M. smegmatis* was inhibited by antibodies against IrpA

IrpA was predicted to function as a potential receptor for the ferri-exochelin by in silico modeling and docking studies. IrpA-positive iron-limited *M. smegmatis* (Fig. 3.25) showed higher uptake of ⁵⁵Fe-exochelin than organisms grown in high iron medium. In order to strengthen the role of IrpA in the uptake of this siderophore, the protein was blocked by incubating the organisms with specific anti-IrpA antibodies. From Fig. 3.27a, it is evident that the uptake of ⁵⁵Fe-exochelin was reduced 6-fold in organisms incubated with anti-IrpA antibodies when compared to untreated organisms or those incubated with pre-immune serum. (P value is P < 0.000, P value is less than 0.05 is statistically significant). Additionally, the uptake of ⁵⁵Fe-exochelin was demonstrated to

be unaffected by prior incubation of the organisms with anti-HupB antibodies (Fig. 3.28), implying that HupB may not be playing any role in the uptake of this siderophore.

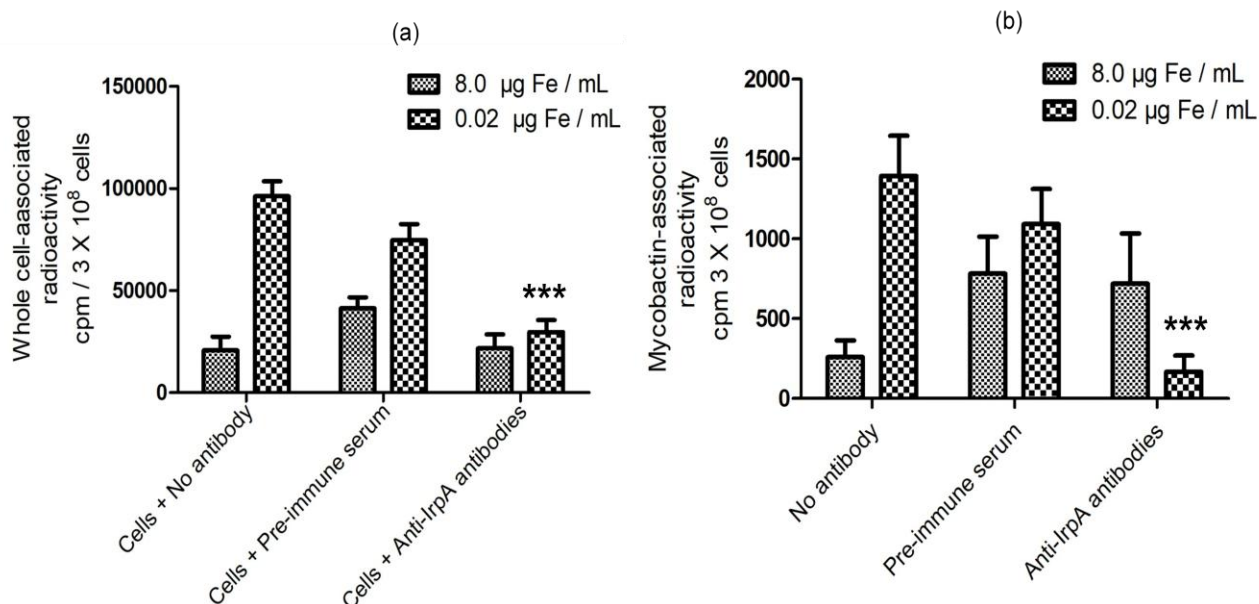


Fig. 3.27. Inhibition of uptake of ^{55}Fe -exochelin by anti-IrpA antibodies: *M. smegmatis*, grown in high and low iron media were pre-incubated with anti-IrpA antibodies and pre-immune serum as detailed in Methods; cells without any antibody served as the control. After appropriate washing to remove unbound antibodies, 1×10^5 cpm of ^{55}Fe -exochelin was added and incubated at 37°C for 2 h. The figure shows the radioactivity in whole cells and in the mycobactin fraction in all the three samples, with the error bars represent standard deviation calculated from four values obtained from two identical experiments performed in duplicates. * indicates it is statistically significant, with a value of $P < 0.0001$.

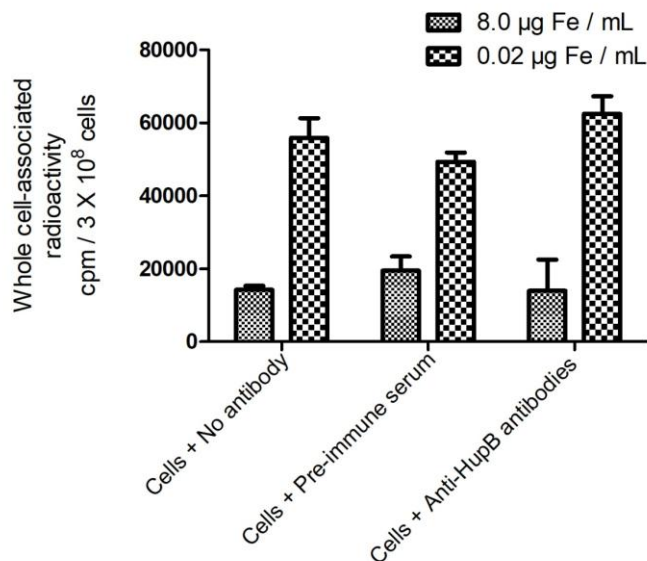
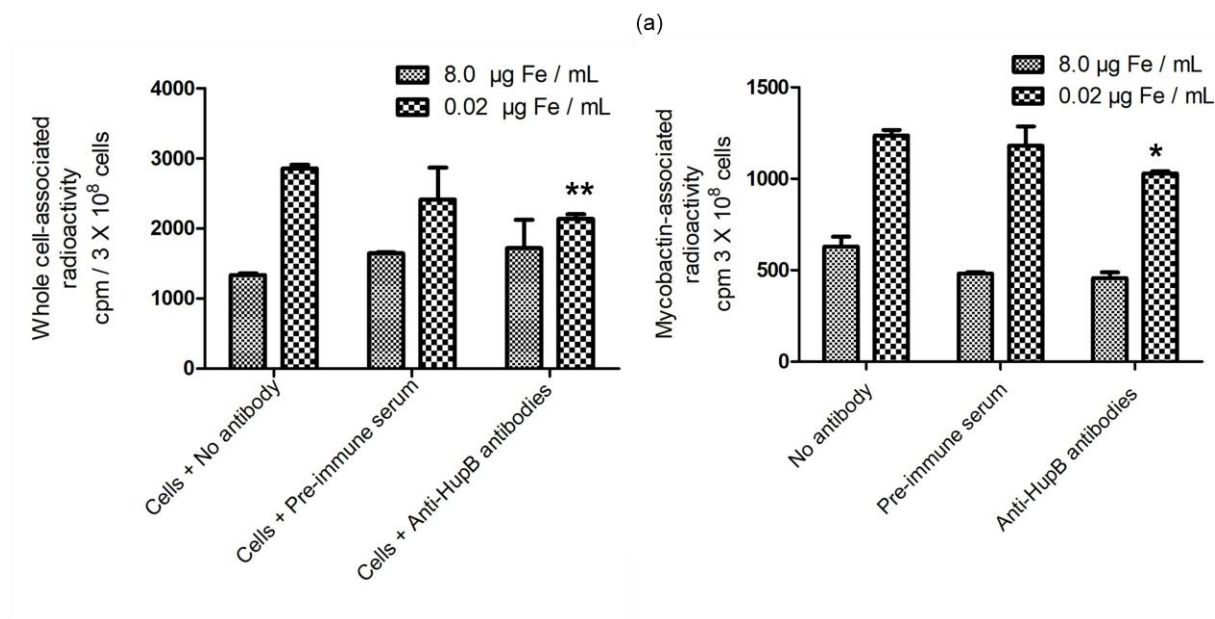


Fig. 3.28. Anti-HupB antibodies did not alter the uptake of ⁵⁵Fe-exochelin in *M. smegmatis*. The experiment was done identical to that indicated in Fig.3.27, except that anti-IrpA antibodies were replaced by anti-HupB antibodies.

Although uptake of iron from ⁵⁵Fe-crboxymycobactin was marginal in *M. smegmatis*, the role of HupB and IrpA were checked and Fig. 3.29a & b shows that neither of them had any influence on the uptake of this siderophore.



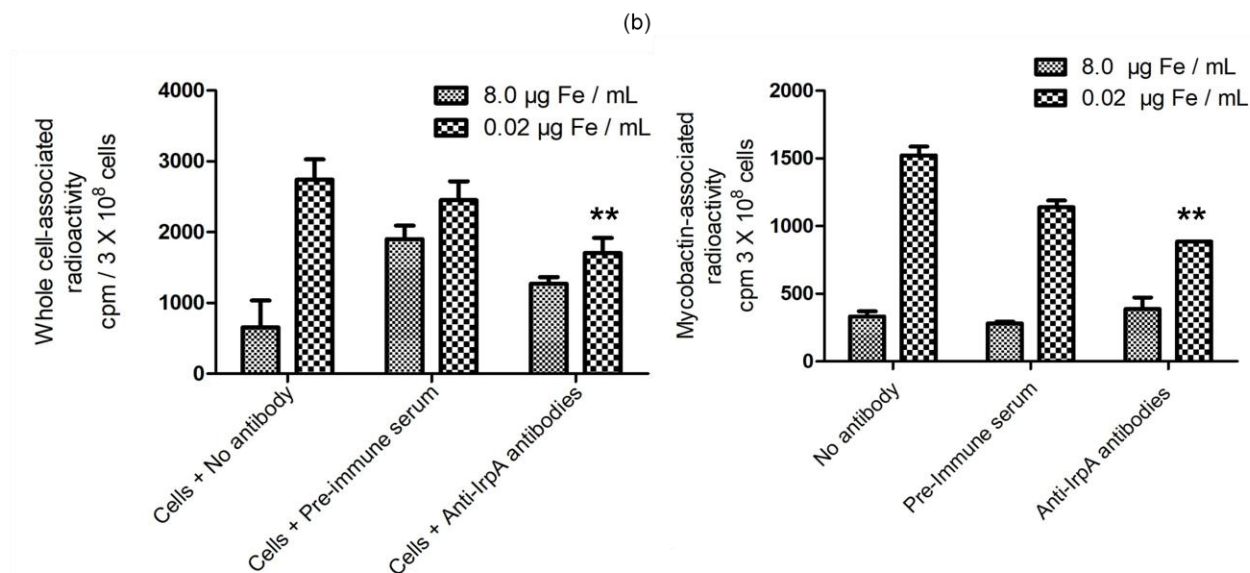


Fig. 3.29. Anti-HupB and anti-IrpA antibodies do not block the uptake of ⁵⁵Fe-CMb by *M. smegmatis*. The experiment was set up as detailed in Fig. 3.27. Panels (a) and (b) represent uptake studies conducted in the presence of anti-HupB and anti-IrpA antibodies respectively. * indicates it is statistically significant, with a value of < 0.0064.

3.4.2.4. Uptake of ⁵⁵Fe-exochelin by liposomes prepared with IrpA-containing cell wall proteins of *M. smegmatis*

Liposomes with only mycobactin incorporated into it served as control and there was no radioactivity associated with these liposomes upon incubating them with ⁵⁵Fe-exochelin. Marked uptake of the radiolabeled siderophore was seen with protoeo-liposomes prepared with cell wall proteins of iron-limited *M. smegmatis*. The role of IrpA in this uptake was evident in the 70% decrease in the uptake upon prior incubation of these liposomes with anti-IrpA antibodies (Fig. 3.30); this was found to be statistically significant (P<0.0001).

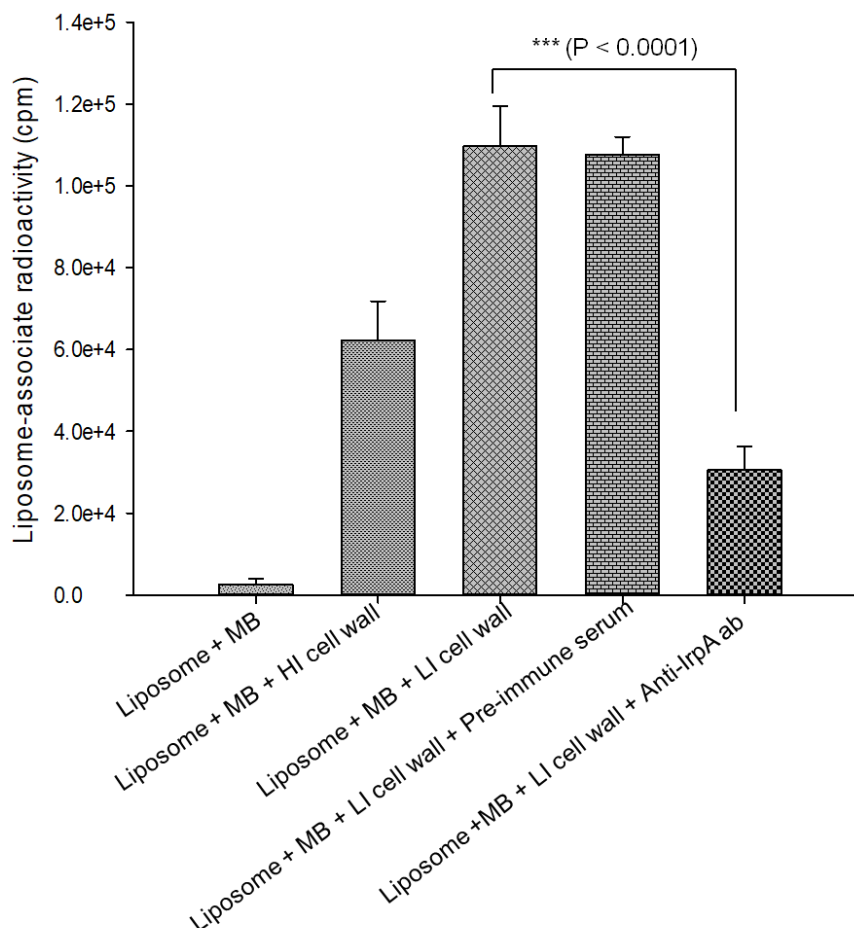


Fig. 3.30. Liposomal uptake of ^{55}Fe -exochelin: inhibition of uptake with anti-IrpA antibodies: Liposomes were prepared with desferri-Mb as detailed in Methodology. Proteo-liposomes were prepared by adding 100 μg of CHAPS-solubilized cell wall proteins from *M. smegmatis* grown in high and low iron media. The different liposomes were variously treated as indicated in the figure, followed by the addition of ^{55}Fe -exochelin. After suitable washes, the liposome-associated radioactivity was measured. The error bars represent standard deviation calculated from four values obtained from two identical experiments performed in duplicates. ‘**’ indicates p-values, which shows a significant value of $p = <0.001$ (T-test).

3.4.3. Immunoprecipitation of cell wall proteins of *M. smegmatis* with anti-IrpA antibodies: co-precipitation of IrpA and HupB

When CHAPS-solubilised cell wall proteins from iron-limited *M. smegmatis* was added to Protein A coated beads with anti-IrpA antibodies, it was seen that HupB co-

precipitated with IrpA (Fig. 3.31c). Both IrpA and HupB were detected using the respective antibodies. While there were several other bands seen, they were seen in the lane corresponding to precipitation with pre-immune serum also. Also, since no major band was seen, they were not analysed further. This is a preliminary finding and further studies will be needed to understand this co-precipitation pattern of IrpA and HupB.

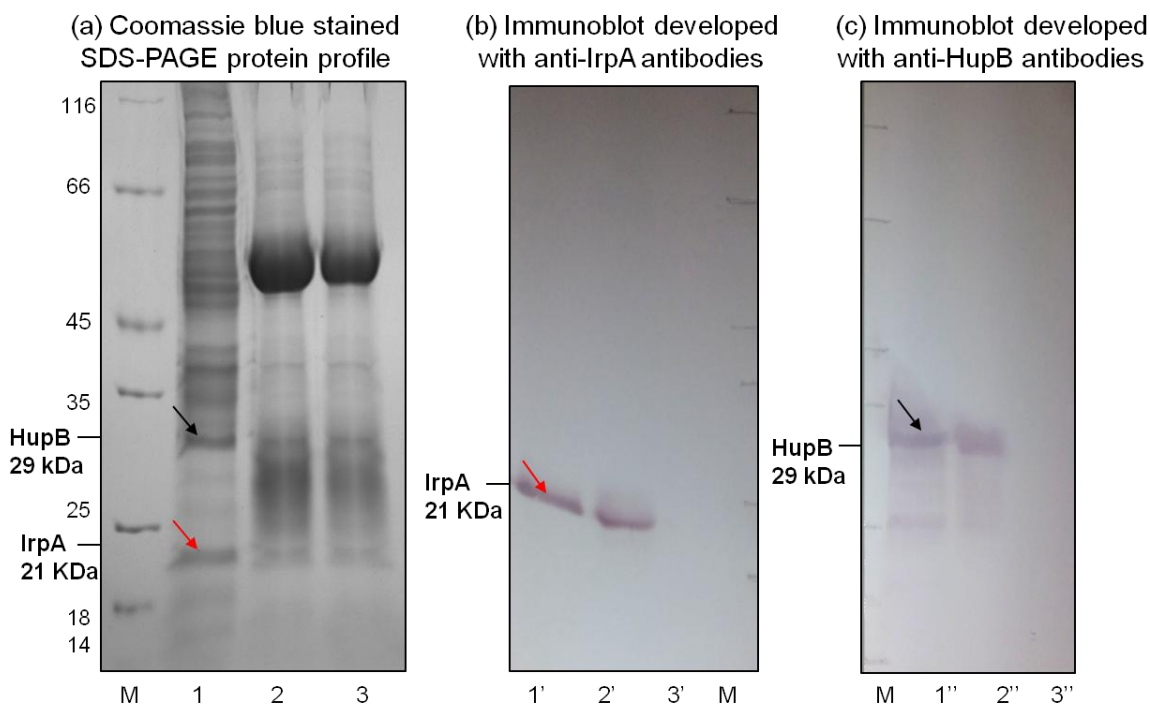


Fig. 3.31. Co-precipitation of IrpA and HupB with anti-IrpA antibodies. Immunoprecipitation of CHAPS-solubilized cell wall proteins from *M. smegmatis* grown in low iron media was done with anti-IrpA antibodies. Panel (a) shows the SDS-PAGE profile showing cell wall proteins (lane 1), Protein A beads-based immunoprecipitated profile with anti-IrpA antibodies (lane 2) and Protein A beads-based immunoprecipitated profile with pre-immune serum (lane a). Panels (b) and (c) show the corresponding immunoblots developed with anti-IrpA and anti-HupB antibodies respectively, with the lanes being loaded identical to that in Panel (a). M represents the protein molecular weight marker.

CHAPTER 4
DISCUSSION

Bacterial iron acquisition has been a subject of interest, not only with respect to the understanding of the regulation of the iron acquisition machineries but also the adaptation by pathogenic bacteria to the iron-limiting conditions imposed by the mammalian host. Unlike *E. coli* that is easily amenable to genetic manipulation and creation of genetic mutants, mycobacteria posed difficulties in the generation of knock out mutants. But, with the development of better vectors and techniques for the genetic manipulation of mycobacteria and the generation of mycobacterial KO mutants, various fields of mycobacterial research including iron acquisition have made considerable advances.

Despite the limitations, some aspects of mycobacterial iron acquisition are well explored. This includes the chemistry of the siderophores produced by different mycobacterial species. Mycobactins are produced by almost all mycobacteria, except *M. paratuberculosis* (Ratledge, 2004). As detailed in Review of Literature, mycobactins from different mycobacteria differ in specific side chains, while retaining the core nucleus, with these variations being so marked that they can be used as taxonomic markers (Sritharan, 2016). The credit for elucidation of the chemistry of these compounds goes to Snow and his group (Snow, 1970), who have meticulously characterised them in the 1970s. Unfortunately, the role of these compounds in the utilization of iron is far from complete. In *M. smegmatis*, it forms 10% of the cell dry weight under iron limiting conditions and it was proposed that they act as iron storage molecules (Ratledge, 2004 & Sritharan, 2000) In *M. tuberculosis*, mycobactin was proposed to function as an important partner in the uptake of iron from ferri-carboxymycobactin, the process mediated by the cell wall-associated protein HupB (Sritharan, 2016). Studies in our lab have provided the experimental evidence to establish our hypothesis (under communication).

The commonality of the intracellular siderophore in mycobacteria does not extend to the secreted molecule that chelates iron from the immediate environment. Carboxymycobactin, the non-acylated form of mycobactin is produced by pathogenic mycobacteria. This molecule, being more polar effectively chelates available iron from the aqueous environment prevailing within the mammalian host. It is well established that both mycobactin and carboxymycobactin form the predominant siderophores in *M.*

tuberculosis under iron limiting conditions of growth (Yeruva *et al.*, 2006). For a long time, it was thought that carboxymycobactins are produced only by the pathogenic mycobacteria. But, their presence in the spent growth medium of *M. smegmatis* albeit in small quantities (Ratledge & Ewing, 1996) cleared the notion that they were restricted to the pathogens. The contribution of carboxymycobactin to the extracellular pool of siderophores by *M. smegmatis* was small (~10%), with exochelin MS forming the major iron chelator (Lane *et al.*, 1998).

In this study, we studied the relative amounts of these two extracellular siderophores. It must be mentioned that iron-regulated growth of mycobacteria, standardized as 0.02 µg Fe / mL in the growth medium for iron-limited growth and 8 instead of 4 µg Fe / mL for iron sufficient growth for *M. tuberculosis* (Yeruva *et al.*, 2006) was adopted for *M. smegmatis* in this study. In low iron medium, *M. smegmatis* showed high expression of mycobactin and a 5-fold higher amount of exochelin compared to carboxymycobactin, all of which were negligible in organisms grown in medium containing 8 µg Fe / mL. While this is an expected finding, the time course of their expression of the two extracellular siderophores was interesting as it was observed that both of them were not expressed at the same time. In *M. smegmatis* grown in low iron medium, exochelin was the first to rise with peak levels observed on day 4; during this period, carboxymycobactin was negligible. With increase in the time of growth, exochelin levels dropped and carboxymycobactin began to rise, a feature noted till 10 days of growth. It was thus evident that exochelin was the first to rise, followed by carboxymycobactin that formed the major extracellular siderophore in the late log conditions when exochelin was considerably low. Interestingly, this trend was also seen in the extended growth of organisms in high iron medium, when the siderophores were detected due to onset of iron limitation because of nutrient depletion in the medium of growth. It must be reiterated that the culture conditions standardized in this study ensured log phase growth for the first 4 days and organisms grown in high iron medium do not show the presence of any siderophores during this phase. When the growth of such organisms were further extended, siderophore expression was seen. When the pattern of the two extracellular siderophores were analysed in cultures grown in high iron medium for 10 days, it was again evident that exochelin was the first to rise

followed by carboxymycobactin. It must be pointed out that the relative increase in these siderophores are being discussed and not their absolute amounts, which however was much less compared to that seen in organisms grown in low iron medium. The overall conclusion is that exochelin is the preferred siderophore of choice during active growth and carboxymycobactin is produced at later stages of growth. The implications of these observations and association of these two compounds with the intracellular mycobactin remains unclear.

A significant observation in this study was that the radiolabeled iron from ferri-exochelin was not recovered in mycobactin in whole cell uptake studies performed for 2 hours. This may be compared with that observed in *M. tuberculosis*. In the latter, transfer of iron from ferri-carboxymycobactin to the cell bound mycobactin was demonstrated by Horwitz and his group (Gobin & Horwitz, 1996) and our recent studies implicated the iron-regulated HupB to play an important role in mediating this transfer (under communication). The major points of difference between *M. smegmatis* and *M. tuberculosis*, based on the observations in this study in *M. smegmatis* are a) HupB is not an iron-regulated protein, b) iron from exochelin is not transferred to mycobactin within the first two hours upon uptake, c) carboxymycobactin is not the preferred siderophore for uptake by this non-pathogenic mycobacterium unlike *M. tuberculosis* and d) uptake of ferri-exochelin occurs via a 21 kDa iron-regulated protein that possibly functions as a receptor. Addressing the preferred extracellular siderophore in *M. smegmatis*, uptake studies by log phase live organisms of *M. smegmatis* pointed to ferri-exochelin as the siderophore of choice. When ^{55}Fe -exochelin was incubated with *M. smegmatis*, iron-limited organisms acquired iron, a feature not seen upon addition of ^{55}Fe -carboxymycobactin. While this may indicate that exochelin is the preferred extracellular siderophore, it is possible that the uptake machinery for carboxymycobactin is not expressed in log phase organisms. It is hypothesized that since carboxymycobactin is expressed by *M. smegmatis* only later, the uptake machinery for its uptake is also expressed later. These may be answered if uptake studies are done with organisms harvested after 4 days. Such a study will show if ^{55}Fe -carboxymycobactin is preferentially taken up and if so, whether the iron is transferred to

mycobactin. In the current study, iron from ^{55}Fe -exochelin is not recovered in mycobactin, implicating an alternative mechanism for its internalization.

The HupB homologue in *M. smegmatis* detected with antibodies against HupB of *M. tuberculosis* was expressed constitutively, irrespective of the amount of iron in the medium of growth. This was confirmed by studying the effect of varying concentrations of iron on HupB expression. While we presumed earlier that this protein is the 29 kDa IREP first reported in *M. smegmatis* (Hall *et al.*, 1987) and shown to be a putative receptor for ferri-exochelin, our findings in this study show the need to sequence the 29 kDa band to check if it is the HupB homologue. Since a 21 kDa band, named as IrpA was the major IREP identified under the conditions used in this study, with complete repression seen in organisms exposed to 8.0 $\mu\text{g Fe / mL}$, it formed the major focus of this study. IrpA showed iron-dependent expression, reflected by the corresponding levels of the siderophores. Though three IREPs IrpA, IrpB and IrpC were selected based on their relative expression in iron-limited organisms vs iron replete cells, IrpA was chosen as it was present in the genome of *M. smegmatis* and was absent in *M. tuberculosis*. Sequencing identified IrpA as Clp protease subunit and it was one among the 8 Clp proteases in the genome of *M. smegmatis*. Interestingly, while seven of the Clp proteases show the corresponding ortholog in the genome of *M. tuberculosis*, the latter did not show the IrpA homologue. Surprisingly, in the modeling of this protein, the PDB database selected ClpC1, one of the Clp proteases of *M. tuberculosis* as the reference sequence for modeling; it was seen that there was high level of similarity of IrpA with the N-terminal region of ClpC1 present in both *M. tuberculosis* and *M. smegmatis* (referred to as ClpC). However, the possibility of IrpA (188 aa) as a cleavage product of ClpC (encoded by MSMEG_6091; 848 aa) does not arise as it is encoded by MSMEG_3761 that is well separated in the genome.

IrpA is regulated by iron and co-expressed with exochelin and mycobactin. Hence, presuming that the protein may have a role in iron acquisition, *in silico* studies were performed to study IrpA as a potential receptor for ferri-exochelin. As mentioned above, ClpC1 was chosen as the template sequence for homology modeling. The model filled the criteria for a stable protein, as deduced from the Ramachandran plot. The probable association of IrpA with ferri-exochelin at the arginine residues at

positions 7 and 76 and glutamate at position 71, revealed by docking studies requires experimental validation to study their significance in the active binding site. IrpA is suggested as a putative ferri-exochelin receptor as blocking of the protein with anti-IrpA antibodies resulted in a 6-fold decrease in the uptake of ferri-exochelin. The specificity of this observation stems from the inability of the pre-immune serum to effect such an inhibition. The low uptake of ferri-exochelin by iron replete organisms can be attributed to the negligible expression of IrpA in these organisms. While a similar strategy was employed to demonstrate HupB as a ferri-carboxymycobactin receptor in *M. tuberculosis* (under communication; Choudhury *et al.*, 2017), the latter study was strengthened by studies performed with a *hupB* KO mutant of *M. tuberculosis* that showed results identical to organisms incubated with anti-HupB antibodies. Additionally, and of greater significance was the direct demonstration of the interaction of ferri-carboxymycobactin with purified HupB, reflective of receptor-ligand interaction. Here, our efforts to obtain rIrpA as a soluble protein was not successful. Cloning of *irpA* into pET 23b (+), though successful resulted in the expression of insoluble rIrpA that was not easily amenable to re-folding upon removal of the urea used to solubilize it. Unfortunately, our alternate efforts to obtain it as GST-fusion though successful did not yield sufficient amounts of intact protein upon cleavage of the GST tag. Thus, it was not possible to perform ligand binding studies as done successfully for HupB. The latter was shown to interact specifically with the ferri-exochelin and not the desferri form using spectrofluorimetry and CD spectral analysis.

Till date, the exochelin machinery in *M. smegmatis* is not completely understood, with fragmented information provided from three reports (Fiss *et al.*, 1994; Yu *et al.*, 1998; Zhu *et al.*, 1998). These studies included random mutagenesis using UV light and transposons, with screening of the mutants on CAS agar plates to identify mutants defective in exochelin production. The first study (Fiss *et al.*, 1994) reported the identification of *fxuA*, *fxuB* and *fxuC* genes; they were designated as cytoplasmic membrane permeases based merely on their homology with *fepG*, *fepC* and *fepD* genes in *E. coli*, in which the translated products of these genes mediated internalization of ferric-enterobactin. In addition, *fxbA* encoding a formylase, catalyzing the addition of a formyl group in exochelin biosynthesis was identified. Subsequent

study (Yu *et al.*, 1998) by this group and another independent report (Zhu *et al.*, 1998) identified the genes *fxbB* and *fxbC*, whose translated products, by virtue of their similarity to known non-ribosomal peptidases were suggested to mediate biosynthesis of exochelin by the non-ribosomal pathway. ExiT was proposed to function as an exporter of exochelin to the outside of the cell. Based on the above information and the identification of porins facilitating iron transport under high iron conditions, Niederweiss and his group proposed a model (Fig. 4.1) for iron transport under iron-sufficient and iron-limiting conditions (Jones & Niederweiss, 2010), implicating a ferri-exochelin receptor in the outer membrane for mediating the internalization of the ferri-exochelin.

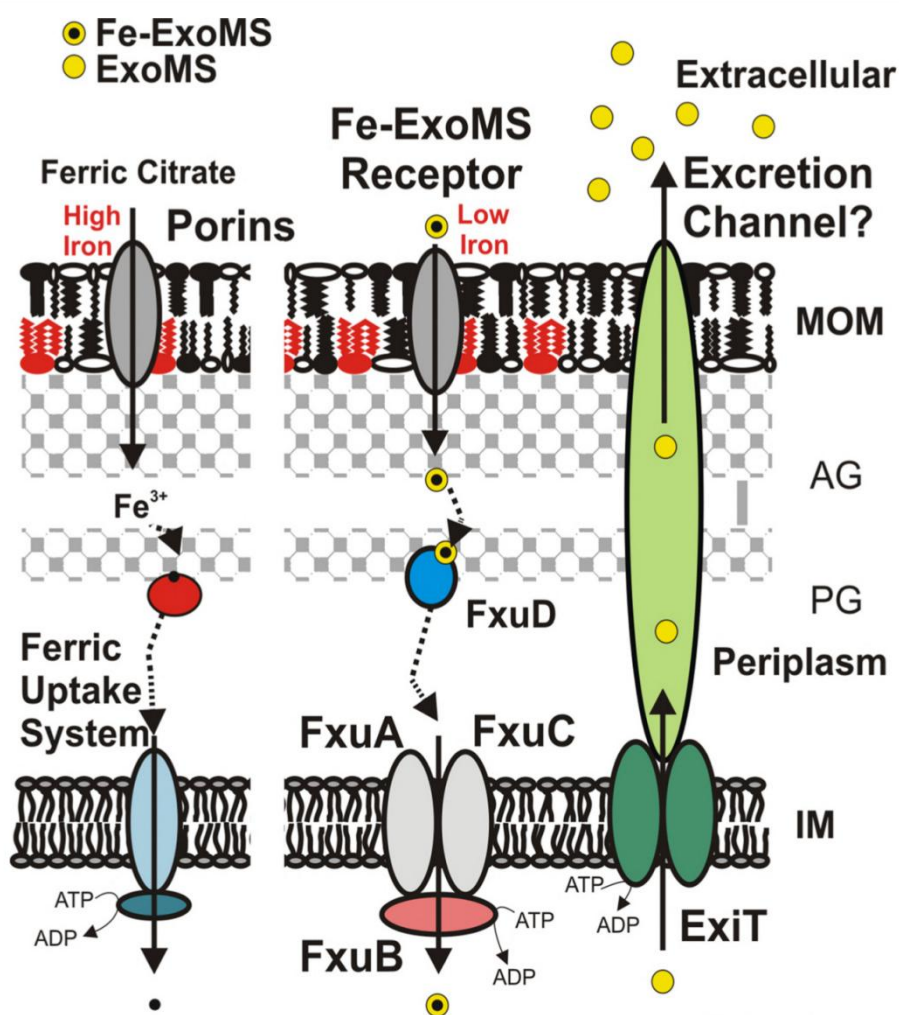


Fig. 4.1. Transport of iron in *M. smegmatis*. The model, presented by Jones and Niederweiss (2010) shows transport of the metal ion, in the ferric state through porins, operating in high iron conditions. Ferri-exochelin (yellow with black dots) is thought to be taken up by a receptor.

Internalisation across the inner membrane is presumed to be mediated by the FxuABC system. ExiT is implicated as the exporter of the exochelin to the outside.

Based on our findings in this study, we propose that IrpA, identified as a cell wall associated protein functions as the receptor for ferri-exochelin (Fig. 4.2). This was also evident in the uptake of ferri-exochelin by liposomes prepared with the cell wall proteins. Conclusive evidence however needs to be produced by demonstrating direct interaction of the purified protein with the ferri-exochelin. The role of HupB, not influenced by iron in *M. smegmatis* remains to be understood. Its co-precipitation along with IrpA upon incubating CHAPS-solubilised cell wall proteins suggests a possible association of the protein with IrpA, the nature of which requires further studies.

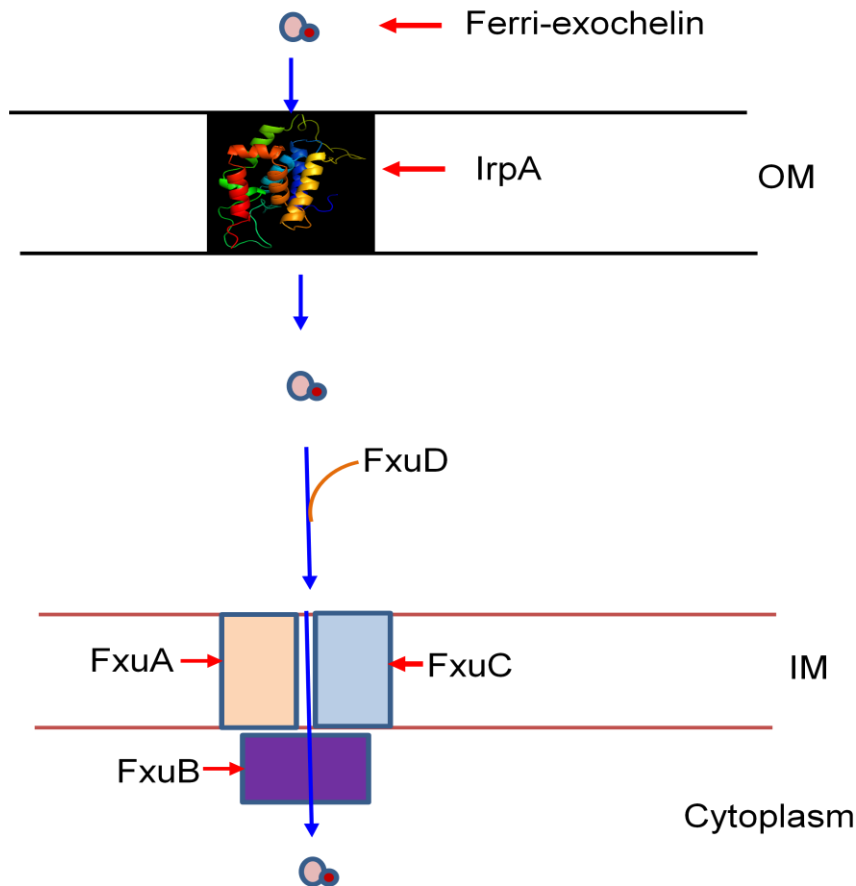


Fig. 4.2. Schematic representation of IrpA as a ferri-exochelin receptor in *M. smegmatis*: IrpA is presented as the receptor for ferri-exochelin in the model for transport of iron under iron-limiting conditions

In conclusion, we observed that exochelin is the first extracellular siderophore to be expressed upon sensing iron-limiting conditions. Ferri-exochelin is the preferred siderophore for uptake of iron, with carboxymycobactin not taken up by log phase cells. The significance of exochelin in *M. smegmatis* was highlighted in the study of biofilm formation by this mycobacterium; the study demonstrated that the inability to express iron resulted in the failure to form biofilm (Ojha & Hatfull, 2007). Ferri-exochelin is taken up by IrpA, a protein seen to be present only in *M. smegmatis* and absent in *M. tuberculosis*. The latter, lacking the exochelin biosynthetic machinery possibly does not require this protein, explaining its absence at the genome level. This study, therefore has helped to further understand iron acquisition in the non-pathogenic *M. smegmatis*.

CHAPTER 5
SUMMARY

Mycobacterium smegmatis produces three siderophores, namely mycobactin that is cell-bound due to its hydrophobicity and the secreted water soluble exochelin and carboxymycobactin, with the latter expressed at considerably lower levels. A 29 kDa protein was reported to be an iron-regulated protein in a study in which the growth conditions included 4.0 $\mu\text{g Fe / mL}$ as sufficient medium. In this study, it was increased to 8.0 $\mu\text{g Fe / mL}$, as established in our lab for all mycobacteria, including *M. tuberculosis*. Under these conditions, the predominant iron-regulated protein was a 21 kDa protein. The focus of the study was therefore the identification and characterization of this protein. With the 28 kDa HupB protein of *M. tuberculosis* being extensively studied in our lab, the corresponding homologue, identified by immunoblot analysis with antibodies against HupB from *M. tuberculosis* was also studied.

- 1. Influence of iron levels on the expression of HupB from *M. smegmatis*:** The cell wall proteins of *M. smegmatis* grown in low (0.02 $\mu\text{g Fe / mL}$) and high (8.0 $\mu\text{g Fe / mL}$) medium, when analysed with antibodies against HupB from *M. tuberculosis*, showed the presence of the HupB homologue, a 29 kDa protein in both the samples. The expression of the protein, irrespective of the iron levels in the medium of growth was confirmed by immunoblot analysis of the cell wall preparations from organisms grown in varying iron concentrations, ranging from 0.02 to 12.0 $\mu\text{g Fe / mL}$. The constitutive expression of HupB was also seen in the vaccine strain *M. bovis* BCG.
- 2. Identification of novel iron-regulated envelope proteins in *M. smegmatis*:** Three iron-regulated envelope proteins were up-regulated in *M. smegmatis* grown in low iron medium. These proteins, with approximate molecular masses of 21, 109 and 145 kDa were co-expressed with the siderophores and all of them were repressed when grown in high iron medium. These proteins are named as IrpA, IrpB and IrpC. They were purified from the cell wall fractions and identified by MALDI-TOF MS / MS analysis as Clp protease subunit, putative membrane protein and FtsK/SpolIIE family protein (ESX conserved component eccC3) respectively. Comparative genome analysis revealed that IrpA was present in *M. smegmatis* and other non-pathogenic mycobacteria. The other two proteins IrpB and IrpC were identified in all

mycobacterial species. The association of IrpC with iron metabolism was reported in *M. tuberculosis*, in which it was shown to play a role in mycobactin-mediated uptake.

- 3. Iron-dependent expression of IrpA:** IrpA expression was regulated by iron levels, with maximal expression in low iron conditions and complete repression seen in high iron medium. This was established by immunoblotting with rabbit anti-IrpA antibodies raised against the purified protein. There was good correlation of the protein expressed with the levels of the siderophores.
- 4. IrpA is present only in *M. smegmatis* and other non-pathogenic mycobacteria:** IrpA is a 21 kDa protein consisting of 188 amino acids with a pI of 6.5. It is annotated as Clp protease subunit (Accession No. gi|118470816; locus tag MSMEG_3761) in the genome of *M. smegmatis* strain mc²155. STRING software revealed several neighborhood proteins, including ClpS (ATP-dependent Clp protease adaptor protein), molecular chaperones and several hypothetical proteins with unknown functions. The *irpA* gene was present only in *M. smegmatis* and was absent in the genome of *M. tuberculosis*. In addition to this protein annotated as Clp proteases, seven additional Clp proteases were identified in the genome of *M. smegmatis*, with the corresponding gene present in *M. tuberculosis*. It was thus highly likely that IrpA played a specific role in the non-pathogenic *M. smegmatis* that was not required in *M. tuberculosis*. It was also absent in *M. bovis* BCG but was seen in several non-pathogenic mycobacterial species.
- 5. Modeling of IrpA and docking of ferri-exochelin:** Homology modeling of IrpA was done using Modeller version 9.17. Interestingly, since there was homology of IrpA with the N-terminal region of ClpC and the corresponding ClpC1 protein from *M. tuberculosis*, the software identified the latter as the template for modeling IrpA. The ferri-exochelin was then docked on to the protein using AutoDock / Vina that identified the interaction of the siderophore with two arginine residues (R7 & R76) and a glutamic acid residue (D71) in IrpA.

6. Experimental studies to establish IrpA as ferri-exochelin receptor: In order to establish IrpA as ferri-exochelin receptor, uptake of ^{55}Fe -exochelin by *M. smegmatis* grown in low and high iron conditions were performed. There was a four-fold increase in the uptake of ^{55}Fe -exochelin by iron-limited vs iron replete organisms. A notable observation was the poor recovery of the label in mycobactin. This was unlike the finding in *M. tuberculosis* in our earlier studies, when most of the label from the extracellular siderophore was recovered in the cell-bound mycobactin. In order to study if ^{55}Fe -carboxymycobactin was utilised by *M. smegmatis* and observe any transfer to mycobactin as in the pathogen, uptake was performed with ^{55}Fe -carboxymycobactin. We observed poor uptake by whole cells and negligible label in mycobactin.

The specificity of IrpA in uptake of ^{55}Fe -exochelin uptake was demonstrated by performing uptake studies upon prior incubation of the organisms with anti-IrpA antibodies. A six-fold decrease in the uptake of the radiolabel was noted in the presence of anti-IrpA antibodies, with no notable decrease in the control organisms incubated with pre-immune serum. Further, anti-HupB antibodies did not influence uptake of ^{55}Fe -exochelin, indicating the specific role of IrpA in *M. smegmatis*. This was further confirmed using liposomes prepared with cell wall proteins from *M. smegmatis* grown in high and low iron medium. There was 70% decrease in the liposomal uptake of ^{55}Fe -exochelin in the presence of anti-IrpA antibodies.

In conclusion, this study has identified IrpA as a putative ferri-exochelin receptor. Additional studies are however needed to demonstrate direct interaction of purified protein with ferri-exochelin. It also remains to be seen if the 29 kDa ferri-exochelin receptor identified earlier has any association with this protein or if it is the HupB homologue. It would be interesting to see if there is any interaction of IrpA with HupB, as our study showed that HupB was co-precipitated with IrpA from the cell wall proteins treated with anti-IrpA antibodies.

**CHAPTER 6
BIBLIOGRAPHY**

- Abraham, M. J., Murtola, T., Schulz, R., S., Smith, J. C., Hess, B. & Lindahl, E. (2015).** Gromacs: High performance molecular simulations through multi-level parallelism from laptops to supercomputers. *SoftwareX* 1–2, 19–25.
- Barclay, R., Ewing, D. F. & Ratledge, C. (1985).** Isolation, identification, and structural analysis of the mycobactins of *Mycobacterium avium*, *Mycobacterium intracellulare*, *Mycobacterium scrofulaceum*, and *Mycobacterium paratuberculosis*. *J Bacteriol* 164, 896–903.
- Bimboim, H. C. & Doly, J. (1979).** A rapid alkaline extraction procedure for screening recombinant plasmid DNA. *Nucleic Acids Res* 7, 1513–1523.
- Brennan, P. J. & Crick, D. C. (2007).** The cell-wall core of *Mycobacterium tuberculosis* in the context of drug discovery. *Curr Top Med Chem* 7, 475–488.
- Brennan, P. J. & Nikaido, H. (1995).** The Envelope of Mycobacteria. *Annu Rev Biochem* 64, 29–63.
- Bullen, J J, E. G. (1999).** Iron and infection Molecular physiological and clinical aspects. Johan Wiley & Sons Inc.
- Canueto-Quintero, J., Caballero-Granado, F. J., Herrero-Romero, M., Dominguez-Castellano, a, Martin-Rico, P., Verdu, E. V, Santamaria, D. S., Cerquera, R. C., Torres-Tortosa, M. & Grp Andaluz Estudio, E. (2003).** Epidemiological, clinical, and prognostic differences between the diseases caused by *Mycobacterium kansasii* and *Mycobacterium tuberculosis* in patients infected with human immunodeficiency virus: A multicenter study. *Clin Infect Dis* 37, 584–590.
- Chan, E. D. & Iseman, M. D. (2013).** Underlying Host Risk Factors for Nontuberculous Mycobacterial Lung Disease 1.
- Chavadi, S. S., Stirrett, K. L., Edupuganti, U. R., Vergnolle, O., Sadhanandan, G., Marchiano, E., Martin, C., Qiu, W. G., Soll, C. E. & Quadri, L. E. N. (2011).** Mutational and phylogenetic analyses of the mycobacterial mbt gene cluster. *J Bacteriol* 193, 5905–5913.
- Chipperfield, J. R. & Ratledge, C. (2000).** Salicylic acid is not a bacterial siderophore: A theoretical study. *BioMetals* 13, 165–168.

- Choudhury, M., Koduru, N Tejaswi., Beni, S, Sasan., Kumar, N., Nagu, P Prakash. & Sritharan, M. (2017).** Functional role of the iron-regulated protein HupB in the siderophore-mediated iron uptake machinery in *Mycobacterium tuberculosis*. *Scientific Reports (In press)*
- Cohavy, O., Harth, G., Horwitz, M., Eggena, M., Landers, C., Sutton, C., Targan, S. R. & Braun, J. (1999).** Identification of a novel mycobacterial histone H1 homologue (HupB) as an antigenic target of pANCA monoclonal antibody and serum immunoglobulin A from patients with Crohn's disease. *Infect Immun* **67**, 6510–6517.
- Cole, S. T., Brosch, R., Parkhill, J., Garnier, T., Churcher, C., Harris, D., Gordon, S. V, Eiglmeier, K., Gas, S. & other authors. (1998).** Deciphering the biology of *Mycobacterium tuberculosis* from the complete genome sequence. *Nature* **393**, 537–544.
- Dover, L. G. & Ratledge, C. (1996).** Identification of a 29 kDa protein in the envelope of *Mycobacterium smegmatis* as a putative ferri-exochelate receptor.
- Dover, L. G. & Ratledge, C. (1996).** Identification of a 29 kDa protein in the envelope of *Mycobacterium smegmatis* as a putative ferri-exochelate receptor. *Microbiology* **142**, 1521–1530.
- Dussurget, O., Timm, J., Gomez, M., Gold, B., Yu, S., Sabol, S. Z., Holmes, R. K., Jacobs, W. R. & Smith, I. (1999).** Transcriptional control of the iron-responsive *fbxA* gene by the mycobacterial regulator IdeR. *J Bacteriol* **181**, 3402–3408.
- Eswar, N., Webb, B., Marti-Renom, M. A., Madhusudhan, M. S., Eramian, D., Shen, M.-Y., Pieper, U. & Sali, A. (2006).** *Comparative protein structure modeling using Modeller. Curr Protoc Bioinforma.*
- Faller, M. (2004).** The Structure of a Mycobacterial Outer-Membrane Channel. *Science (80-)* **303**, 1189–1192.
- Feese, M. D., Ingason, B. P., Goranson-Siekierke, J., Holmes, R. K. & Hol, W. G. J. (2001).** Crystal Structure of the Iron-dependent Regulator from *Mycobacterium tuberculosis* at 2.0-Å Resolution Reveals the Src Homology Domain 3-like Fold and Metal Binding Function of the Third Domain. *J Biol Chem* **276**, 5959–5966.

- Fiser, A. & Sali, A. (2003).** ModLoop: Automated modeling of loops in protein structures. *Bioinformatics* **19**, 2500–2501.
- Fiss, E. H., Yu, S. & Jacobs, W. R. (1994).** Identification of genes involved in the sequestration of iron in mycobacteria: The ferric exochelin biosynthetic and uptake pathways. *Mol Microbiol* **14**, 557–569.
- Gobin, B. J. & Horwitz, M. A. (1996).** Exochelins of *Mycobacterium tuberculosis* Remove Iron from Human Iron - binding Proteins and Donate Iron to Mycobactins in the M . tuberculosis Cell Wall. *J Exp Med* **183**.
- Gobin, J., Moore, C. H., Reeve Jr., J. R., Wong, D. K., Gibson, B. W. & Horwitz, M. A. (1995).** Iron acquisition by *Mycobacterium tuberculosis*: isolation and characterization of a family of iron-binding exochelins. *Proc Natl Acad Sci U S A* **92**, 5189–5193.
- Gobin, J., Wong, D. K., Gibson, B. W. & Horwitz, M. A. (1999).** Characterization of exochelins of the *Mycobacterium bovis* type strain and BCG substrains. *Infect Immun* **67**, 2035–2039.
- Gold, B., Marcela Rodriguez, G., Marras, S. A. E., Pentecost, M. & Smith, I. (2001).** The *Mycobacterium tuberculosis* *ideR* is a dual functional regulator that controls transcription of genes involved in iron acquisition, iron storage and survival in macrophages. *Mol Microbiol* **42**, 851–865.
- Goren, M. B. (1972).** Mycobacterial lipids: selected topics. *Bacteriol Rev* **36**, 33–64.
- Gutacker, M. M., Smoot, J. C., Migliaccio, C. A. L., Ricklefs, S. M., Hua, S., Cousins, D. V, Graviss, E. A., Shashkina, E., Kreiswirth, B. M. & Musser, J. M. (2002).** Genome-wide analysis of synonymymous single nucleotide polymorphisms in *Mycobacterium tuberculosis* complex organisms: resolution of genetic relationships among closely related microbial strains. *Genetics* **162**, 1533–1543.
- Hall, R. M. & Ratledge, C. (1984).** Mycobactins as chemotaxonomic characters for some rapidly growing mycobacteria. *J Gen Microbiol* **130**, 1883–92.
- Hall, R. M., Wheeler, P. R. & Ratledge, C. (1983).** Exochelin-mediated iron uptake into *Mycobacterium leprae*. *Int J Lepr Other Mycobact Dis* **51**, 490–4.
- Hall, R. M. & Ratledge, ;manjula Sritharan; ANN J. Messenger and Colin. (1987).**

- Iron Transport in *Mycobacterium smegmatis*: Occurrence of Iron-regulated Envelope Proteins as Potential Receptors for Iron Uptake. *J Gen Microbiol* **133**, 2107–2114.
- Huang, F. & He, Z. G. (2010).** Characterization of an interplay between a *Mycobacterium tuberculosis* MazF homolog, Rv1495 and its sole DNA topoisomerase i. *Nucleic Acids Res* **38**, 8219–8230.
- Hughes, A. L., Friedman, R. & Murray, M. (2002).** Genomewide Pattern of Synonymous Nucleotide Substitution in Two Complete Genomes of *Mycobacterium tuberculosis*. *Emerging Infect Dis* **8**.
- Inoue, H., Nojima, H. & Okayama, H. (1990).** High efficiency transformation of *Escherichia coli* with plasmids. *Gene* **96**, 23–28.
- Jones, C. M. & Niederweis, M. (2010).** Role of porins in iron uptake by *Mycobacterium smegmatis*. *J Bacteriol* **192**, 6411–6417.
- Kieser, K. J. & Rubin, E. J. (2014).** How sisters grow apart: mycobacterial growth and division. *Nat Rev Microbiol* **12**, 550–562. Nature Publishing Group.
- Kochan, I. (1976).** Role of iron in the regulation of nutritional immunity. *Bioorg Chem* **2**, 55–57.
- Krithika, R., Marathe, U., Saxena, P., Ansari, M. Z., Mohanty, D. & Gokhale, R. S. (2006).** A genetic locus required for iron acquisition in *Mycobacterium tuberculosis*. *Proc Natl Acad Sci U S A* **103**, 2069–74.
- Kumar, M., Khan, F. G., Sharma, S., Kumar, R., Faujdar, J., Sharma, R., Chauhan, D. S., Singh, R., Magotra, S. K. & Khan, I. a. (2011).** Identification of *Mycobacterium tuberculosis* genes preferentially expressed during human infection. *Microb Pathog* **50**, 31–38. Elsevier Ltd.
- L. P. Macham and C. Ratledge. (1975).** A New Group of Water-soluble Iron-binding Compounds from Mycobacteria : The Exochelins. *J Gen Microbiol* **89**, 379–382.
- Laemmli, U. K. (1970).** Cleavage of structural proteins during the assembly of the head of bacteriophage T4. *Nature* **227**, 680–685.
- Lane, S. J., Marshall, P. S., Upton, R. J., Road, G. W., Ratledge, C. & Ewing, M. (1995).** Novel Extracellular Mycobactins, the Carboxymycobactins from

- Mycobacterium avium*. *Tetrahedron Lett* **36**, 4129–4132.
- Lane, S. J., Marshall, P. S., Upton, R. J. & Ratledge, C. (1998)**. Isolation and characterization of carboxymycobactins as the second extracellular siderophores in *Mycobacterium smegmatis*. *BioMetals* **11**, 13–20.
- Laskowski, R. A., MacArthur, M. W., Moss, D. S. & Thornton, J. M. (1993)**. PROCHECK: a program to check the stereochemical quality of protein structures. *J Appl Crystallogr* **26**, 283–291. International Union of Crystallography.
- Lee, B. H., Murugasu-Oei, B. & Dick, T. (1998)**. Upregulation of a histone-like protein in dormant *Mycobacterium smegmatis*. *Mol Gen Genet* **260**, 475–479.
- Lionel P . MACHAM, M. C. . S. A. C. R. (1977)**. Iron Transport in *Mycobacterium smegmatis*: The Isolation , Purification and Function of Exochelin MS. *J Gen Microbiol* **101**, 41–49.
- Macham, L. P., Ratledge, C. & Nocton, J. C. (1975)**. Extracellular iron acquisition by mycobacteria: role of the exochelins and evidence against the participation of mycobactin. *Infect Immun* **12**, 1242–1251.
- Matsumoto, S., Furugen, M., Yukitake, H. & Yamada, T. (2000)**. The gene encoding mycobacterial DNA-binding protein I (MDPI) transformed rapidly growing bacteria to slowly growing bacteria. *FEMS Microbiol Lett* **182**, 297–301.
- Mendelsohn, L. D. (2004)**. ChemDraw 8 ultra, windows and macintosh versions. *J Chem Inf Comput Sci* **44**, 2225–2226.
- Niki, M., Niki, M., Tateishi, Y., Ozeki, Y., Kirikae, T., Lewin, A., Inoue, Y., Matsumoto, M., Dahl, J. L. & other authors. (2012)**. A novel mechanism of growth phase-dependent tolerance to isoniazid in mycobacteria. *J Biol Chem* **287**, 27743–27752.
- Ojha, A. & Hatfull, G. F. (2007)**. The role of iron in *Mycobacterium smegmatis* biofilm formation: The exochelin siderophore is essential in limiting iron conditions for biofilm formation but not for planktonic growth. *Mol Microbiol* **66**, 468–483.
- Pandey, S. D., Choudhury, M. & Sritharan, M. (2014a)**. Transcriptional regulation of *Mycobacterium tuberculosis* hupB gene expression. *Microbiology* **160**, 1637–1647.

- Pandey, S. D., Choudhury, M., Yousuf, S., Wheeler, P. R., Gordon, S. V., Ranjan, A. & Sritharan, M. (2014b).** Iron-regulated protein HupB of *Mycobacterium tuberculosis* positively regulates siderophore biosynthesis and is essential for growth in macrophages. *J Bacteriol* **196**, 1853–1865. American Society for Microbiology.
- Prabhakar, S., Annapurna, P. S., Jain, N. K., Dey, a B., Tyagi, J. S. & Prasad, H. K. (1998).** Identification of an immunogenic histone-like protein (HLPMt) of *Mycobacterium tuberculosis*. *Tuber Lung Dis* **79**, 43–53.
- Prabhakar, S., Mishra, A., Singhal, A., Katoch, V. M., Tyagi, J. S. & Prasad, H. K. (2004).** Use of the hupB Gene Encoding a Histone-Like Protein of *Mycobacterium tuberculosis* as a Target for Detection and Differentiation of *M. tuberculosis* and *M. bovis* Use of the hupB Gene Encoding a Histone-Like Protein of *Mycobacterium tuberculosis* as a Targ.
- Pym, A. S., Domenech, P., Honoré, N., Song, J., Deretic, V. & Cole, S. T. (2001).** Regulation of catalase-peroxidase (KatG) expression, isoniazid sensitivity and virulence by furA of *Mycobacterium tuberculosis*. *Mol Microbiol* **40**, 879–889.
- Quadri, L. E., Sello, J., Keating, T. A., Weinreb, P. H. & Walsh, C. T. (1998).** Identification of a *Mycobacterium tuberculosis* gene cluster encoding the biosynthetic enzymes for assembly of the virulence-conferring siderophore mycobactin. *Chem Biol* **5**, 631–645.
- Ratledge, C. (2004).** Iron, mycobacteria and tuberculosis. *Tuberculosis* **84**, 110–130.
- Ratledge, C. & Dover, L. G. (2000a).** Iron Metabolism In Pathogenic Bacteria. *Annu Rev Microbiol* **54**, 881–941.
- Ratledge, C. & Ewing, M. (1996).** The occurrence of carboxymycobactin, the siderophore of pathogenic mycobacteria, as a second extracellular siderophore in *Mycobacterium smegmatis*. *Microbiology* **142**, 2207–2212.
- Richard M. Hall, Manjula Sritharan, A. J. M. and C. R. (1987).** Iron Transport in *Mycobacterium smegmatis*: Occurrence of Iron-regulated Envelope Proteins as Potential Receptors for Iron Uptake. *J Gen Microbiol* **133**, 2107–2114.
- Runyon, E. H. (1959).** Anonymous mycobacteria in pulmonary disease. *Med Clin North Am* **43**, 273–90. Elsevier.

- Russell, D. G. (2007).** Who puts the tubercle in tuberculosis? *Nat Rev Microbiol* **5**, 39–47.
- Ryndak, M. B., Wang, S., Smith, I. & Rodriguez, G. M. (2010).** The *Mycobacterium tuberculosis* high-affinity iron importer, IrtA, contains an FAD-binding domain. *J Bacteriol* **192**, 861–869.
- Sala, C., Forti, F., Di Florio, E., Canneva, F., Milano, A., Riccardi, G. & Ghisotti, D. (2003).** *Mycobacterium tuberculosis* fura autoregulates its own expression. *J Bacteriol* **185**, 5357–5362.
- Schmitt, M. P., Predich, M., Doukhan, L., Smith, I. & Holmes, R. K. (1995).** Characterization of an iron-dependent regulatory protein (IdeR) of *Mycobacterium tuberculosis* as a functional homolog of the diphtheria toxin repressor (DtxR) from *Corynebacterium diphtheriae*. *Infect Immun* **63**, 4284–4289.
- Sharadamma, N., Khan, K., Kumar, S., Neelakanteshwar Patil, K., Hasnain, S. E. & Muniyappa, K. (2011).** Synergy between the N-terminal and C-terminal domains of *Mycobacterium tuberculosis* HupB is essential for high-affinity binding, DNA supercoiling and inhibition of RecA-promoted strand exchange. *FEBS J* **278**, 3447–3462.
- Sharman, G. J., Williams, D. H., Ewing, D. F. & Ratledge, C. (1995a).** Isolation, purification and structure of exochelin MS, the extracellular siderophore from *Mycobacterium smegmatis*. *Biochem J* **305**, 187–196.
- Sharman, G. J., Williams, D. H., Ewing, D. F. & Ratledge, C. (1995b).** Determination of the structure of exochelin MN, the extracellular siderophore from *Mycobacterium neoaurum*. *Chem Biol* **2**, 553–561.
- Shimoji, Y., Ng, V., Matsumura, K., Fischetti, V. a & Rambukkana, a. (1999).** A 21-kDa surface protein of *Mycobacterium leprae* binds peripheral nerve laminin-2 and mediates Schwann cell invasion. *Proc Natl Acad Sci U S A* **96**, 9857–62.
- Shires, K. & Steyn, L. (2001).** The cold-shock stress response in *Mycobacterium smegmatis* induces the expression of a histone-like protein. *Mol Microbiol* **39**, 994–1009.
- Sivakolundu, S., Mannela, U. D., Jain, S., Srikantam, A., Peri, S., Deo Pandey, S. & Sritharan, M. (2013).** Serum iron profile and ELISA-based detection of antibodies

- against the iron-regulated protein HupB of *Mycobacterium tuberculosis* in TB patients and household contacts in Hyderabad (Andhra Pradesh), India. *Trans R Soc Trop Med Hyg* **107**, 43–50.
- Snow, G. A. (1970).** Mycobactins: iron-chelating growth factors from mycobacteria. *Bacteriol Rev* **34**, 99–125.
- Sritharan, M. (2000).** Iron as a candidate in virulence and pathogenesis in mycobacteria and other microorganisms. *World J Microbiol Biotechnol* **16**, 769–780.
- Sritharan, M. (2016).** Iron Homeostasis in *Mycobacterium tuberculosis*: Mechanistic Insights into Siderophore-Mediated Iron Uptake. *J Bacteriol* **198**, 2399–2409.
- Sritharan, M. & Ratledge, C. (1989).** Co-ordinated expression of the components of iron transport (mycobactin, exochelin and envelope proteins) in *Mycobacterium neoaurum*. *FEMS Microbiol Lett* **60**, 183–185.
- Sritharan, M. & Ratledge, C. (1990).** Iron-regulated envelope proteins of mycobacteria grown in vitro and their occurrence in *Mycobacterium avium* and *Mycobacterium leprae* grown in vivo. *Bio Met* **2**, 203–208.
- Sritharan, N., Choudhury, M., Sivakolundu, S., Chaurasia, R., Chouhan, N., Rao, P. P. & Sritharan, M. (2014).** Highly immunoreactive antibodies against the rHup-F2 fragment (aa 63-161) of the iron-regulated HupB protein of *Mycobacterium tuberculosis* and its potential for the serodiagnosis of extrapulmonary and recurrent tuberculosis. *Eur J Clin Microbiol Infect Dis* **34**, 33–40. Springer Verlag.
- Stahl, C., Kubetzko, S., Kaps, I., Seeber, S., Engelhardt, H. & Niederweis, M. (2001).** MspA provides the main hydrophilic pathway through the cell wall of *Mycobacterium smegmatis*. *Mol Microbiol* **40**, 451–464.
- Stephenson, M. C. & Ratledge, C. (1979).** Iron transport in *Mycobacterium smegmatis*: Uptake of iron from ferric citrate. *J Gen Microbiol* **149**, 131–135.
- Stephenson, M. C. & Ratledge, C. (1980).** Specificity of Exochelins for Iron Transport in Three Species of Mycobacteria the other type is extractable from the medium as its ferric complex into chloroform and has. *J Gen Microbiol* **116**, 521–523.
- Takatsuka, M., Osada-Oka, M., Satoh, E. F., Kitadokoro, K., Nishiuchi, Y., Niki, M.,**

- Inoue, M., Iwai, K., Arakawa, T. & other authors. (2011).** A histone-like protein of mycobacteria possesses ferritin superfamily protein-like activity and protects against DNA damage by Fenton reaction. *PLoS One* **6**, e20985 (S. Bereswill, Ed.).
- Tortoli, E. (2003).** Impact of genotypic studies on mycobacterial taxonomy: The new mycobacteria of the 1990s. *Clin Microbiol Rev* **16**, 319–354.
- Towbin, H., Staehelin, T. & Gordon, J. (1979).** Electrophoretic transfer of proteins from polyacrylamide gels to nitrocellulose sheets: procedure and some applications. *Proc Natl Acad Sci U S A* **76**, 4350–4.
- Trias, J., Jarlier, V. & Benz, R. (1992).** Porins in the cell wall of mycobacteria. *Science* **258**, 1479–1481.
- Trott, O. & Olson, A. (2010).** AutoDock Vina: improving the speed and accuracy of docking with a new scoring function, efficient optimization and multithreading. *J Comput Chem* **31**, 455–461.
- Voss, J. J. De, Rutter, K., Schroeder, B. G., Iii, C. E. B. & Voss, J. J. D. E. (1999).** Iron Acquisition and Metabolism by Iron Acquisition and Metabolism by Mycobacteria. *J Bacteriol* **181**, 4443–4451.
- Walls, D. & Loughran, S. T. (2011).** Protein Chromatography. *Methods Mol Biol* **681**, 151–175.
- Wells, R. M., Jones, C. M., Xi, Z., Speer, A., Danilchanka, O., Doornbos, K. S., Sun, P., Wu, F., Tian, C. & Niederweis, M. (2013).** Discovery of a Siderophore Export System Essential for Virulence of *Mycobacterium tuberculosis*. *PLoS Pathog* **9**.
- Yeruva, V. C., Duggirala, S., Lakshmi, V., Kolarich, D., Altmann, F. & Sritharan, M. (2006).** Identification and characterization of a major cell wall-associated iron-regulated envelope protein (Irep-28) in *Mycobacterium tuberculosis*. *Clin Vaccine Immunol* **13**, 1137–1142.
- Yu, S.; Fiss, E.H.; Jacobs, W. . (1998).** Analysis of the Exochelin Locus in *Mycobacterium smegmatis*: Biosynthesis Genes Have Homology with Gen. *J Bacteriol* **180**, 4676–4685.
- Zahrt, T. C., Song, J., Siple, J. & Deretic, V. (2001).** Mycobacterial FurA is a negative regulator of catalase-peroxidase gene katG. *Mol Microbiol* **39**, 1174–1185.

Zhu, W., Arceneaux, J. E. L., Beggs, M. L., Byers, B. R., Eisenach, K. D. & Lundrigan, M. D. (1998). Exochelin genes in *Mycobacterium smegmatis*: Identification of an ABC transporter and two non-ribosomal peptide synthetase genes. *Mol Microbiol* **29**, 629–639.

CHAPTER 7
APPENDIX

Publications

Sritharan, N., Choudhury, M., Sivakolundu, S., Chaurasia, R., Chouhan, N., Rao, P. P. & Sritharan, M. (2014). Highly immunoreactive antibodies against the rHup-F2 fragment (aa 63-161) of the iron-regulated HupB protein of *Mycobacterium tuberculosis* and its potential for the serodiagnosis of extrapulmonary and recurrent tuberculosis. *Eur J Clin Microbiol Infect Dis* **34**, 33–40. Springer Verlag.

Under Preparation

1. HupB is constitutively expressed in the non-pathogenic *Mycobacterium smegmatis* and the vaccine strain *M. bovis* BCG
2. IrpA is a putative ferri-exochelin receptor in *Mycobacterium smegmatis*